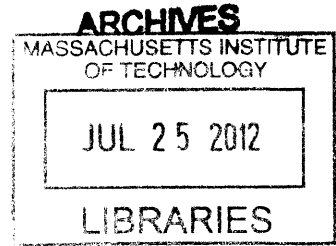


Reactor Protection System Design Alternatives for Sodium Fast Reactors

by

Jacob D. DeWitte
B.S., Nuclear Engineering (2008)
University of Florida



SUBMITTED TO THE DEPARTMENT OF NUCLEAR SCIENCE AND ENGINEERING

IN PARTIAL FULFILLMENT OF THE REQUIREMENTS FOR THE DEGREE OF
MASTER OF SCIENCE IN NUCLEAR SCIENCE AND ENGINEERING

AT THE

MASSACHUSETTS INSTITUTE OF TECHNOLOGY

JANUARY 28, 2011

Copyright © Massachusetts Institute of Technology. All rights reserved.

A handwritten signature in black ink, appearing to read "Jacob D. DeWitte".

Author.....
Department of Nuclear Science and Engineering
January 28, 2011

Certified by.....
Professor Emeritus Neil E. Todreas
Thesis Supervisor

Certified by.....
Professor Emeritus Michael J. Driscoll
Thesis Co-Supervisor

Certified by.....
Professor Mujid Kazimi
TEPCO Professor of Nuclear Engineering
Chair, Department Committee on Graduate Students

Reactor Protection System Design Alternatives for Sodium Fast Reactors

by

Jacob D. DeWitte

Submitted to the Department of Nuclear Science and Engineering in partial fulfillment of the requirements for the Degree of

Master of Science in Nuclear Science and Engineering

at the Massachusetts Institute of Technology

Abstract

Historically, unprotected transients have been viewed as design basis events that can significantly challenge sodium-cooled fast reactors. The perceived potential consequences of a severe unprotected transient in a sodium-cooled fast reactor include an energetic core disruptive accident, vessel failure, and a large early release. These consequences can be avoided if unprotected transients are properly defended against, potentially improving the economics of sodium fast reactors.

One way to defend against such accidents is to include a highly reliable reactor protection system. The perceived undesirability of the consequences arising from an unprotected transient has led some sodium fast reactor designers to consider incorporating several design modifications to the reactor protection system, including: self-actuated shutdown systems, articulated control rods, and seismic anticipatory scram systems. This study investigates the performance of these systems in sodium fast reactors.

To analyze the impact of these proposed design alternatives, a model to analyze plant performance that incorporates uncertainty analysis is developed using RELAP5-3D and the ABR-1000 as the reference design. The performance of the proposed alternatives is analyzed during unprotected loss of flow and unprotected transient overpower scenarios, each exacerbated by a loss of heat sink. The recently developed Technology Neutral Framework is used to contextually rate performance of the proposed alternatives. Ultimately, this thesis offers a methodology for a designer to analyze reactor protection system design efficacy.

The principle results of this thesis suggest that when using the Technology Neutral Framework as a licensing framework for a sodium-cooled fast reactor, the two independent scram systems of the ABR-1000's reactor protection system perform well enough to screen unprotected transients from the design basis. While a regulator may still require consideration of accidents involving the failure of the reactor protection system, these events will not drive the design of the system. However, self-actuated shutdown systems may be called for to diversify the reactor protection system. Of these, the Curie point latch marginally reduces the conditional cladding damage probability for metal cores because of their rapid inherent feedback effects, but is more effective for the more sluggish oxide cores given reasonably long pump coastdown times. Flow levitated absorbers are highly effective

at mitigating unprotected loss of flow events for both fuel types, but are limited in response during unprotected transient overpower events. When considered from a risk-informed perspective, a clear rationale and objective is needed to justify the inclusion of an additional feature such as self-actuated shutdown systems. The use of articulated safety rods as one of the diverse means of reactivity insertion and the implementation of an anticipatory seismic scram system may be the most cost-effective alternatives to provide defense in depth in light of the sodium fast reactor's susceptibility to seismic events.

Acknowledgements

Thank you to my family for their unending support, love, and encouragement. Thank you to my friends for listening, for providing feedback, and helping me to stay focused. Thank you especially to Matthew Denman and Koroush Shirvan for their help and guidance with RELAP, and thank you to Caroline Cochran for her support and advice. Finally, thank you Professor Todreas and Professor Driscoll for your patience, wisdom, and guidance, all of which was invaluable. This work was supported by the Rickover Fellowship and a DOE NERI grant (contract DE-FG07-07ID14888).

Table of Contents

Abstract.....	3
Acknowledgements.....	5
List of Figures.....	9
List of Tables.....	11
Acronyms.....	12
1 Introduction, Motivation, and Background.....	14
1.1 Introduction and Motivation.....	14
1.2 Background.....	15
1.3 Technology Neutral Framework.....	19
1.4 Application of the Technology Neutral Framework to the Sodium Fast Reactor.....	26
1.5 Objectives and Organization.....	27
2 Plant Modeling Methodology.....	29
2.1 Introduction.....	29
2.2 MCNP Model.....	29
2.3 RELAP5-3D Model.....	30
2.4 Uncertainty Analysis.....	31
2.5 Summary.....	35
3 Reactor Protection System Design Description.....	36
3.1 Introduction.....	36
3.2 General Design Criteria for the RPS.....	36
3.3 Reactor Protection System Design in Sodium Fast Reactors.....	40
3.4 Rod Worth Calculations.....	43
3.5 Summary.....	45
4 Sodium Fast Reactor Transient Performance.....	46
4.1 Introduction.....	46
4.2 Unprotected Loss of Flow Events.....	46
4.3 Unprotected Transient Overpower Events.....	49
4.4 Impact of Reactor Protection System Reliability on Plant Safety.....	52
4.5 Three Independent Scram Systems versus Two Independent Scram Systems.....	52
4.6 Summary.....	53
5 Self-Actuated Shutdown System Selection.....	54

5.1	Introduction	54
5.2	Self-Actuated Shutdown Systems Considered	55
5.3	Ranking Methodology	58
5.4	Summary	63
6	Curie Point Latch Performance Analysis	64
6.1	Introduction	64
6.2	System Design Description	65
6.3	Curie Temperature Selection	67
6.4	Unprotected Loss of Flow Performance for a Metal Core	68
6.5	Unprotected Loss of Flow Performance for an Oxide Core	73
6.6	Unprotected Transient Overpower Performance for a Metal Core	78
6.7	Unprotected Transient Overpower Performance for an Oxide Core	79
6.8	Potential Design Improvements	80
6.9	Impact on Reactor Operations	84
6.10	Economic Analysis and Results	85
6.11	Summary	85
7	Flow Levitated Absorber Performance	87
7.1	Introduction	87
7.2	System Design Description	88
7.3	Unprotected Loss of Flow Performance for a Metal Core	88
7.4	Unprotected Loss of Flow Performance for an Oxide Core	93
7.5	Unprotected Transient Overpower Performance	97
7.6	Impact on Reactor Operations	98
7.7	Economic Analysis and Results	100
7.8	Summary	101
8	Seismic Considerations for Reactor Protection Systems	102
8.1	Introduction	102
8.2	Seismic Impacts on Sodium Fast Reactors	102
8.3	Reactor Protection System Design Alternatives	103
8.4	Articulated Control Rods	103
8.5	Seismic Anticipatory Scram System	104
8.6	Summary	104
9	Summary, Conclusions, and Recommendations for Future Work	106

9.1	Summary	106
9.2	Conclusions	106
9.3	Future Work	108
	References	110
	Appendix A – MCNP Model	113
	Appendix B – RELAP5-3D Inputs	130
	Appendix C – Matlab Wrapper	148

List of Figures

FIGURE 1-1: LOOP TYPE SFR DESIGN (4).	16
FIGURE 1-2: POOL TYPE SFR DESIGN (4).	16
FIGURE 1-3: THE FREQUENCY-CONSEQUENCE CURVE (2).	24
FIGURE 3-1: PRIMARY CONTROL ASSEMBLY BANK INTEGRAL WORTH CURVE FOR A METAL CORE.	43
FIGURE 3-2: SECONDARY CONTROL ASSEMBLY BANK INTEGRAL WORTH CURVE FOR A METAL CORE.	44
FIGURE 3-3: PRIMARY CONTROL ASSEMBLY BANK INTEGRAL WORTH CURVE FOR AN OXIDE CORE.	44
FIGURE 3-4: SECONDARY CONTROL ASSEMBLY BANK INTEGRAL WORTH CURVE FOR AN OXIDE CORE.	45
FIGURE 4-1: BLOCK DIAGRAM OF ULOF PROGRESSION.	48
FIGURE 4-2: PEAK CLADDING TEMPERATURE DURING A ULOF IN A METAL CORE.	49
FIGURE 4-3: PEAK CLADDING TEMPERATURE DURING A ULOF IN AN OXIDE CORE.	49
FIGURE 4-4: BLOCK DIAGRAM OF UTOP PROGRESSION.	50
FIGURE 4-5: PEAK CLADDING TEMPERATURE DURING A UTOP IN A METAL CORE.	51
FIGURE 4-6: PEAK CLADDING TEMPERATURE DURING A UTOP IN AN OXIDE CORE.	51
FIGURE 6-1: ILLUSTRATION OF MAGNETIC MOMENTS OF FERROMAGNETIC AND PARAMAGNETIC MATERIALS.	65
FIGURE 6-2: POSSIBLE CPL DESIGN.	66
FIGURE 6-3: SCHEMATIC OF A CPL IN A LATCHED AND A DE-LATCHED STATE (43).	66
FIGURE 6-4: METAL FUEL ULOF ASSEMBLY OUTLET TEMPERATURES.	67
FIGURE 6-5: METAL FUEL UTOP ASSEMBLY OUTLET TEMPERATURES.	68
FIGURE 6-6: CPL PERFORMANCE FOR A ULOF WITH INSTANTANEOUS FLOW SEIZURE (METAL CORE).	71
FIGURE 6-7: CPL PERFORMANCE FOR A ULOF WITH A 3 SECOND FLOW-HALVING TIME (METAL CORE).	71
FIGURE 6-8: CPL PERFORMANCE FOR A ULOF WITH A 5 SECOND FLOW-HALVING TIME (METAL CORE).	72
FIGURE 6-9: CPL PERFORMANCE FOR A ULOF WITH AN 8 SECOND FLOW-HALVING TIME (METAL CORE).	72
FIGURE 6-10: CPL PERFORMANCE FOR A ULOF WITH INSTANTANEOUS FLOW SEIZURE (OXIDE CORE).	75
FIGURE 6-11: CPL PERFORMANCE FOR A ULOF WITH A 5 SECOND FLOW-HALVING TIME (OXIDE CORE).	76
FIGURE 6-12: CPL PERFORMANCE FOR A ULOF WITH A 10 SECOND FLOW-HALVING TIME (OXIDE CORE).	76
FIGURE 6-13: CPL PERFORMANCE FOR A ULOF WITH A 20 SECOND FLOW-HALVING TIME (OXIDE CORE).	77
FIGURE 6-14: CPL PERFORMANCE FOR A UTOP (METAL FUEL).	79
FIGURE 6-15: CPL PERFORMANCE FOR A UTOP (OXIDE CORE).	80
FIGURE 6-16: PROPOSED CPL PLACEMENT IN CORE OUTLET PATH.	81
FIGURE 6-17: MODIFIED CPL PERFORMANCE DURING A ULOF (METAL CORE).	82
FIGURE 6-18: MODIFIED CPL PERFORMANCE DURING A ULOF (OXIDE CORE).	82
FIGURE 6-19: MODIFIED CPL PERFORMANCE DURING A UTOP (METAL CORE).	83
FIGURE 6-20: MODIFIED CPL PERFORMANCE DURING A UTOP (OXIDE CORE).	83
FIGURE 7-1: SIMPLIFIED SCHEMATIC OF AN FLA.	87

FIGURE 7-2: FLA PERFORMANCE FOR A ULOF WITH INSTANTANEOUS FLOW SEIZURE (METAL CORE)	90
FIGURE 7-3: FLA PERFORMANCE FOR A ULOF WITH A 3 SECOND FLOW-HALVING TIME (METAL CORE)	91
FIGURE 7-4: FLA PERFORMANCE FOR A ULOF WITH A 5 SECOND FLOW-HALVING TIME (METAL CORE)	91
FIGURE 7-5: FLA PERFORMANCE FOR A ULOF WITH AN 8 SECOND FLOW-HALVING TIME (METAL CORE)	92
FIGURE 7-6: FLA PERFORMANCE FOR A ULOF WITH INSTANTANEOUS FLOW SEIZURE (OXIDE CORE)	95
FIGURE 7-7: FLA PERFORMANCE FOR A ULOF WITH A 5 SECOND FLOW-HALVING TIME (OXIDE CORE).....	95
FIGURE 7-8: FLA PERFORMANCE FOR A ULOF WITH A 10 SECOND FLOW-HALVING TIME (OXIDE CORE).....	96
FIGURE 7-9: FLA PERFORMANCE FOR A ULOF WITH A 20 SECOND FLOW-HALVING TIME (OXIDE CORE).....	96
FIGURE 7-10: PROPOSED FLA-TRADITIONAL CR DRIVELINE DESIGN.....	100
FIGURE B-0-1: RELAP5 MODEL OF THE ABR-1000 PRIMARY SYSTEM.....	130
FIGURE B-0-2: RELAP5 MODEL OF THE ABR-1000 INTERMEDIATE HEAT TRANSPORT SYSTEM.....	131
FIGURE B-0-3: RELAP5 MODEL OF THE ABR-1000 DECAY HEAT REMOVAL SYSTEM.	131
FIGURE C-0-1: MATLAB WRAPPER CODE SUITE FLOW PATH.....	148

List of Tables

TABLE 1-1: RISK CONTRIBUTORS FOR DIFFERENT SFRS (5) (9) (10).	25
TABLE 2-1: MEAN FEEDBACK COEFFICIENTS FOR THE ABR-1000 (8).....	34
TABLE 3-1: RPS DESIGN SPACE SUMMARY PER 10 CFR 50, APPENDIX A.....	41
TABLE 3-2: EFFECTS OF REDUNDANCY ON SYSTEM RELIABILITY (22).....	41
TABLE 4-1: LOF SCENARIOS FOR THE ALMR (5).....	47
TABLE 4-2: ALMR TOP REACTIVITY INSERTION DISTRIBUTIONS (5).....	50
TABLE 5-1: PRIMARY DESIGN CHARACTERISTICS OF SASS (32).....	55
TABLE 5-2: FIRST ROUND RANKING OF SASS.....	60
TABLE 5-3: SECOND ROUND RANKING OF SASS.....	62
TABLE 6-1: TIME-DEPENDENT REACTIVITY INSERTION FOLLOWING CURIE POINT ACTIVATION FOR A METAL CORE.	69
TABLE 6-2: FLOW-HALVING TIMES FOR A METAL CORE.....	70
TABLE 6-3: CPL ULOF RESULTS FOR A METAL CORE.....	73
TABLE 6-4: TIME-DEPENDENT REACTIVITY INSERTION FOLLOWING CURIE POINT ACTIVATION FOR AN OXIDE CORE.	74
TABLE 6-5: FLOW-HALVING TIMES FOR AN OXIDE CORE (33) (34) (14).....	75
TABLE 6-6: CPL ULOF RESULTS FOR AN OXIDE CORE.....	78
TABLE 6-7: CPL DESIGN MODIFICATION PERFORMANCE RESULTS.....	84
TABLE 7-1: FLA REACTIVITY INSERTION TABLE FOR A METAL CORE.....	89
TABLE 7-2: FLOW-HALVING TIMES FOR A METAL CORE.....	89
TABLE 7-3: FLA REACTIVITY INSERTION FOR AN OXIDE CORE.....	94
TABLE 7-4: FLOW-HALVING TIMES FOR AN OXIDE CORE.....	94

Acronyms

AEC – Atomic energy commission

ALMR – Advanced liquid metal reactor

AOO – Anticipated operational occurrence

BOEC - Beginning of equilibrium cycle

CDF – Core damage frequency

CFR – Code of federal regulations

CPL – Curie point latch

CRBR – Clinch river breeder reactor

CRDL – Control rode driveline

DBA – Design Basis Accident

DOE – Department of Energy

DRACS – Direct removal air cooling system

EBR-II – Experimental breeder reactor II

ECDA – Energetic core disruptive accident

EPA – Environmental protection agency

FCC – Frequency consequence curve

FFTF – Fast flux test facility

FLA – Flow levitated absorber

GDC – General Design Criteria

GE – General Electric

GEM – Gas expansion module

HFP – Hot full power

HZP – Hot zero power

HTGR – High Temperature Gas Reactor

IHTS – Intermediate heat transport system

LBE – Licensing basis event

LOCA – Loss of coolant accident

LOF – Loss of flow
LWR – Light water reactor
NRC – Nuclear Regulatory Commission
NGNP – Next generation nuclear plant
OBE – Operating basis earthquake
PCS – Plant control system
PGA – Peak ground acceleration
PRA – Probabilistic risk assessment
PRISM – Power reactor innovative small module
PSER – Pre-application safety evaluation report
PSID – Preliminary safety information document
PWR – Pressurized water reactor
RPS – Reactor protection system
RVACS – Reactor vessel air cooling system
SASS – Self-actuated shutdown system
SBO – Station blackout
SFR – Sodium-cooled fast reactor
SSE – Safe shutdown earthquake
TNF – Technology neutral framework (NUREG-1860)
TOP – Transient overpower
QHOs – Quantitative health objective
ULOF – Unprotected loss of flow
USBO – Unprotected station blackout
UTOP – Unprotected transient overpower

1 Introduction, Motivation, and Background

1.1 Introduction and Motivation

Sodium fast reactors (SFRs) have gained renewed interest for commercial deployment. Once touted for their ability to breed fissile fuel to power a nuclear-driven society that was faced with limited uranium supplies, SFRs are now being considered for their waste consumption attributes, and scalability characteristics as small modular reactors. Furthermore, recent studies and developments suggest innovative SFR designs could start on low enriched uranium (LEU), contrary to the presumption that SFRs needed a full core loading of plutonium recovered from the light water reactor (LWR) fleet (1). These developments may accelerate SFR deployment. However economic challenges remain that are inherent to the technology and current regulatory practices.

In general, there is no technological barrier to SFR deployment, and a number of demonstration reactors have been constructed, but SFRs are often considered more expensive to construct than competitive LWRs. One of the historical cost drivers for SFRs includes designing against energetic core disruptive accidents (ECDA), which are postulated as able to arise because the fuel is not arranged in the most reactive configuration in a fast reactor core, and because coolant void reactivity is typically positive over a large region of the core meaning some events could rearrange the fuel into a more reactive configuration. ECDAs typically lead to increased regulatory scrutiny and in the extreme may result in the inclusion of core catchers, fuel streaming channels, and/or heightened containment requirements into the plant design. If the risk of ECDAs is shown to be small enough, especially under the scope of the Technology Neutral Framework (TNF) (2), then the additional costs of designing against ECDAs can be eliminated.

One method of reducing the risk of ECDA is the inclusion of a highly reliable reactor protection system (RPS). Most modern SFR designs possess two independent and diversely-sourced control rod insertion – or scram – systems as part of the RPS (note that throughout this thesis the terms: “control rod insertion system,” “scram system,” and “reactivity control system” refer to the same subsystem that is part of the RPS). These systems are typically solid absorber assemblies occupying dedicated positions within the core that are driven by electric drive motors and control systems. They are designed to be both mechanically and electrically robust, and automatically insert in response to actuating signals from the plant’s instrumentation system. However, the undesirability of the consequences arising from an ECDA has led some SFR designers to consider incorporating a third independent scram system, as well as engineering enhanced diversity into the RPS. This thesis investigates: 1) the need for three scram systems; 2) potential design alternatives to increase the diversity of an SFR’s RPS through passive systems; and 3) potential designs that improve RPS performance during seismic events; all to ensure SFR RPS reliability at a level that precludes ECDA from the design basis without excessive cost add-ons.

1.2 Background

SFRs are a fast-spectrum reactor, and typically employ a closed fuel recycle system. A range of plant size options is available for the SFR, ranging from modular systems of tens of MWe to large monolithic reactors of about 1800 MWe (3). SFR core outlet temperatures range from 500-575 °C (3).

The primary coolant system in a SFR can either be arranged in a pool layout or a loop layout. For both options, the primary sodium has a relatively large thermal inertia. The two concepts are shown in Figure 1-1 and Figure 1-2 respectively. SFRs maintain safety margins via designed features and inherent characteristics, such as operation at atmospheric

pressure. Furthermore, a clean (non-radioactive) secondary sodium loop provides a buffer between radioactive sodium in the primary loop and the power conversion cycle.

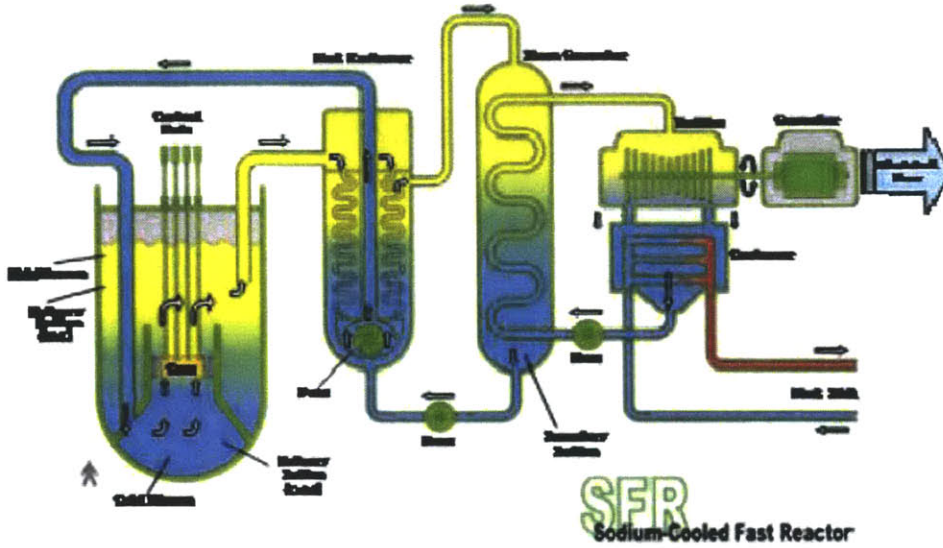


FIGURE 1-1: LOOP TYPE SFR DESIGN (4).

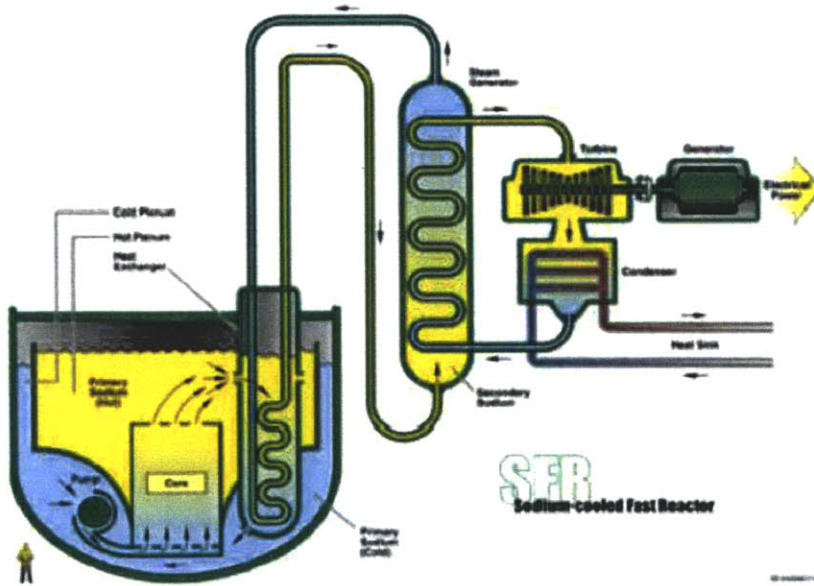


FIGURE 1-2: POOL TYPE SFR DESIGN (4).

Two fuel forms have been traditionally considered for SFRs: metallic fuel (U-Pu-Zr); and mixed oxide fuel (PuO₂-UO₂). However, advanced fuel forms such as UC and UN are also being investigated for future deployment.

The US effort to develop a commercial SFR started with the Clinch River Breeder Reactor (CRBR), which was loop-type SFR with oxide fuel. After CRBR was canceled due to cost overruns, licensing delays, and political opposition, the DOE initiated the Integral Fast Reactor (IFR) program. This program emphasized a pool type reactor concept that would avoid some of the regulatory hurdles which impeded CRBR. An initial design competition selected General Electric's (GE) PRISM reactor as the flagship design of the IFR program. After its selection as the focus of the IFR program, the PRISM design was renamed the Advanced Liquid Metal Reactor (ALMR), while the core maintained the PRISM designation. Following the cancellation of the IFR program, GE reverted to its original designation – PRISM. In the 1990s, GE proceeded to increase the thermal power of PRISM to 1000 MW_{th} and named the new design S-PRISM. GE halted work on S-PRISM in 2003, but resumed work in 2005, changing the name of the reactor back to PRISM. Therefore, any reference to PRISM, ALMR, or IFR refers to the same fundamental pool type design which served as the basis for the ABR-1000 design developed by ANL in 2005.

ECDAs have historically been regarded as limiting events for SFRs that significantly alter the safety profile of SFRs due to the potential severity of ECDAs. However, the uncertainty surrounding the initiation, sequence, and consequences of ECDAs has led designers and regulators to inconsistently treat ECDAs in SFR safety evaluations. Such treatment ranges from very little consideration of ECDAs due to their low probability of occurrence (demonstrated by adequate component reliability, shutdown systems, and heat removal systems), to inclusion of ECDAs as design-basis accidents (DBAs) in the classical

sense. These extremes lead one to conclude that a more fundamental approach to analyze ECDAs in a safety space would be favorable.

There are typically three classes of initial conditions that can lead to fuel melting and relocation (5):

1. Events leading to high reactivity insertion rates that negate RPS response.
Such events include: gas-bubble intake; failure of the core support system; and failure of the core restraint system.
2. Malfunctions within the design basis of the RPS combined with failure of a plant protection component. These sequences include loss of flow and transient overpower events.
3. Malfunctions leading to the interruption of heat removal, including post-shutdown decay heat removal. These events can be categorized as loss of heat sink events.

This thesis focuses on the effects of the events in categories 2 and 3 above on plant performance with respect to RPS performance, and these events will be discussed more thoroughly in Chapter 4.

One of the dominant sources of uncertainty for the deployment of SFRs has been the characterization of the licensing framework to which a new SFR design must comply. The existing licensing framework is heavily-oriented toward LWR plant characteristics. The NRC and the nuclear industry have engaged in various activities to identify those aspects of the regulations that require reinterpretation or change to accommodate the different characteristics of SFR designs, but whether design-specific regulations will be developed for SFRs or whether the existing regulations will be transformed into generic requirements that are independent of design type has yet to be determined. It is also possible that a hybrid of the two regulatory concepts will be required in which there are primarily generic, technology

neutral regulations, but also some design-specific requirements. The Technology Neutral Framework (TNF) described in NUREG-1860 is one possible approach to technology neutral regulations that are risk-informed (2).

1.3 Technology Neutral Framework

Existing nuclear power plants were licensed under Part 50 of Title 10 of the Code of Federal Regulations (CFR), Domestic Licensing of Production and Utilization Facilities (6). This was a two-step process in which the applicant first obtained a construction permit based on the regulatory review of information provided in a preliminary safety analysis report (PSAR), and subsequently obtained an operating license based on the regulatory review of information in a final safety analysis report (FSAR). General Design Criteria (GDC) are provided in Appendix A to Part 50. Based on experience obtained by regulatory staff in the evaluation of a number of applications, the NRC has issued Regulatory Guides that indicate to the applicant those practices that have been found to be acceptable in the past. In addition, the NRC has developed Standard Review Plans as guidance to its own regulatory staff as to what is expected in different sections of the application. Applicants are not required to follow either the Regulatory Guides or the Standard Review Plans, as long as they prove to the regulatory staff that they have satisfied the requirements of the applicable sections of the CFR. In practice, however, the applicant uses both Regulatory Guides and Standard Review Plans as guidelines for preparing application materials, because it minimizes the likelihood of regulatory delay.

The review of license applications is a very lengthy and expensive process for both the applicant and for the NRC that introduces significant uncertainties into the construction process, and is a primary source of concern for investors. This is one of the reasons why debt for new nuclear projects costs a premium compared to non-nuclear projects. To both address this uncertainty and prepare for a future round of new applications, changes have been made

to streamline the regulatory process. Each of the 104 nuclear power plants operating in the U.S. in 2011 are in some respect unique. The standardization of plant designs can substantially decrease the licensing effort for a class of plant designs. Part 52 of Title 10 of the CFR enables the certification of a standardized plant design. Once the standardized design has been approved, the regulatory review of a specific application referencing that design can be limited to the unique features associated with that particular plant, such as site characteristics. Part 52 has two other new regulatory features that can streamline the licensing process: it changes the two-step process of a construction permit and operating license into a one-step combined construction and operating license; and, for new sites, a utility can obtain an Early Site Permit (ESP) separate from a specific application. All of the new applications submitted by utilities use the new Part 52 approach of design certification in combination with the regulatory framework established under Part 50. This approach should reduce the licensing efforts, and thus costs, for advanced light water reactors.

Licensing designs other than LWRs poses a set of special problems that have not been addressed by Part 52. The existing body of reactor regulations and regulatory guidance is very LWR specific. Either the regulatory and licensing framework must be specially tailored for each new design concept (e.g. HTGRs or SFRs), or a technology neutral approach to regulation must be developed. Part 53 of Title 10 of the CFR has been reserved for such an approach. NUREG-1860 was an attempt to explore technology neutral approaches for licensing nuclear power plants.

The current US SFR licensing knowledge has come about from NRC interactions with the Clinch River Breeder Reactor (CRBR) and the Advanced Liquid Metal Reactor (ALMR) programs. In the 1970s through the early 1980s, the Department of Energy (DOE) attempted to license CRBR but Congress cut funding before a construction permit was issued by the NRC. While ECDAAs were not considered as part of the design basis for CRBR, accidents

which could lead to ECDA's, including unprotected accidents and large break loss of coolant accidents, required significant regulatory attention which prolonged the licensing process. Although a construction permit was not issued for CRBR, the CRBR licensing process did produce a Safety Evaluation Report (SER) in 1983, NUREG-0968. In order to avoid repeating the CRBR project's experience, the ALMR design incorporated more passive safety measures into the PRISM design. Under the ALMR program, the DOE submitted a Preliminary Safety Information Document (PSID) to the NRC in 1986 and the NRC in turn issued a Preliminary Safety Evaluation Report (PSER) in 1994. While the incorporation of passive safety features succeeded in reducing some of the regulatory concern with ECDA's, to satisfy defense-in-depth the NRC still forced changes to the PRISM reactor including the addition of an ultimate shutdown system, gas expansion modules (GEMs), and a containment dome (7).

The NRC staff used a risk-informed approach for accident selection for the ALMR. They divided accident sequences into four Event Categories (EC I through EC IV) based on the initiating frequency of each sequence. Each EC's requirements were then generally related to requirements assigned to LWR accident classifications. For example, sequences in EC I had initiating frequencies greater than $10^{-2}/\text{yr}$ and their requirements corresponded to Anticipated Operational Occurrences (AOO) in LWRs. Accidents categorized in EC II had initiating frequencies ranging between $10^{-2}/\text{yr}$ to $10^{-4}/\text{yr}$ and defined the design basis for the reactor. These accidents were analyzed with conservative assumptions, (e.g., all parameters at their 2-sigma values) and any components used in the analysis were held to safety grade standards. The primary performance requirement for EC II accidents was to avoid core damage, typically by setting conservative limits for failure metrics (e.g., cladding damage fractions must remain less than 0.2, coolant temperatures must remain below their boiling point, etc.). Accidents in EC III extend over the subsequent two orders of magnitude,

between $10^{-4}/\text{yr}$ to $10^{-6}/\text{yr}$, and constituted the Beyond Design Basis Accidents. Core damage was allowed for EC III sequences but radioactive materials had to be contained. EC IV sequences constituted all accidents having a frequency of less than $10^{-6}/\text{yr}$ and had no direct parallel with LWR accident groupings, but were used to define containment requirements (7). For example, an ECDA which produced a break in the reactor vessel head was used to determine the S-PRISM containment pressure requirements.

While the NRC attempted to align accidents with their ECs using initiating frequencies, there was also a deterministic classification scheme that occasionally conflicted with the frequency classification. For example, unprotected accidents, or accidents where the Reactor Protection System (RPS) failed, were classified as EC III, because the deterministic definition for EC III was the failure of two major safety systems (8). This classification conflicted with the frequency definition for EC III, between $10^{-4}/\text{yr}$ to $10^{-6}/\text{yr}$, because the RPS had a point estimate unreliability of $10^{-7}/\text{demand}$ (5). Major safety systems should have an unreliability of less than $10^{-2}/\text{yr}$, theoretically pushing all unprotected accidents into EC IV. These discrepancies were not resolved when funding was cut to the ALMR program in 1994, and are an example of the challenges encountered while attempting to combine deterministic and probabilistic safety analysis methods.

To continue advancing the work on technology neutral licensing frameworks, the NRC Office of Research has published NUREG-1860. NUREG-1860 is a study on the feasibility of a risk-informed and performance-based licensing framework, that is often referred to as the TNF. It is important to note that it is not a regulation and will almost certainly be changed before final implementation (if formally adopted), but it provides an example of what 10 CFR 53 could look like. The HTGR vendors working on the Next Generation Nuclear Plant (NGNP) have proposed a risk-informed and performance-based

licensing strategy to the NRC, though not specifically following NUREG-1860. The NRC has deferred any rulemaking until the pre-application reaches a more complete level of detail.

In the TNF, probabilistic risk assessment (PRA) methods play a central role in determining licensing basis events (LBEs) which replace traditional DBAs. Within the TNF approach, accident sequences are grouped according to similar phenomenology and consequences. The limits set in NUREG-1860 are on a per-LBE basis, shown in Figure 1-3. LBEs with a high frequency of occurrence must have low consequences to be acceptable. LBEs with a low frequency are allowed to have higher consequences. All LBEs must lie below the frequency-consequence curve (FCC). This curve has been developed to be commensurate with or more conservative than current NRC and EPA regulations. Appendix H of the TNF describes which portions of 10 CFR 50 are applicable within the framework.

To maintain conservative margins, the LBE representing a group of sequences is assigned the 95th percentile frequency of the most likely sequence in the group and the 95th percentile consequence from the most severe (or most challenging) consequence sequence in the group. The systems whose performance is required to keep the LBEs below the F-C curve are categorized as safety grade and must conform to the special treatment requirements of such safety-related systems.

The lowest frequency considered, as seen in Figure 1-3, is $10^{-7}/\text{yr}$. NUREG-1860 specifies that LBEs with a mean frequency less than $10^{-7}/\text{yr}$ are precluded from categorization as LBEs.

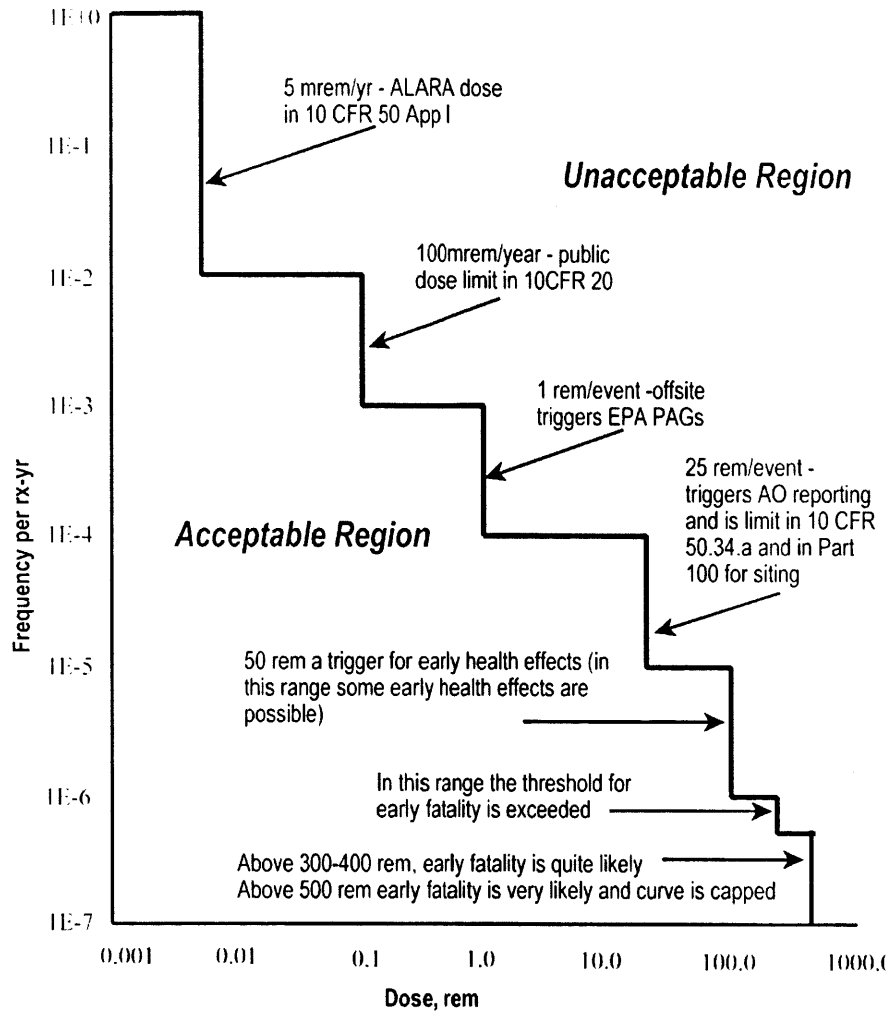


FIGURE 1-3: THE FREQUENCY-CONSEQUENCE CURVE (2).

The TNF also includes deterministic requirements for the probabilistically selected LBEs. One example from these requirements is that a certain number of barriers remaining to fission product release must remain intact depending on the frequency of the sequence. For more frequent sequences, more barriers must stay intact, thus preserving defense-in-depth principles. Another example is that the core must maintain a coolable geometry for all sequences with frequencies greater than $10^{-5}/\text{yr}$.

Another requirement is that a deterministic LBE must be negotiated between the licensee and the regulator that represents “a serious challenge to fission product retention in the fuel and coolant system.” Finally, there are defense-in-depth guidelines regarding

protective systems, operation stability, barrier integrity, and protective actions. These guidelines should lead to a balanced design with a high level of safety that is applicable to a variety of technologies.

Of all the changes proposed in the TNF, arguably the most impactful from a severe accident standpoint is that LBEs (which are actual sequences determined for each plant design) replace postulated, and often unphysical DBAs. These DBAs are accidents that do not take frequencies into account so they often represent extremely low ($<10^{-7}/\text{yr}$) event sequences, which would fall below the FCC threshold. This is an important point for SFRs since a designer may argue that ECDAs lie far below this cutoff, which could potentially prevent excessive regulatory attention to these rare events.

Using the TNF requires the availability of a PRA. The available PRAs for sodium reactors are for PRISM, EBR-II, and ALMR. ALMR and PRISM are both pool type reactors that are less than 1000 MW thermal. The PRAs for PRISM and ALMR were performed by GE staff. The lack of detail of these documents reflects the fact that these designs are in the conceptual phase. The PRISM PRA is Level 3 while the ALMR PRA is only Level 1. The PRA for EBR-II is thorough and similar to other modern Level 1 PRAs. All of the PRAs include seismic initiators with only EBR-II including fire initiators. There are some features that all of the PRAs share in common. All of the reactors are assessed to have internally initiated core damage frequencies below typical GEN-II PWRs. Additionally, the risk for each of these designs is dominated by seismic initiators. This information is summarized in Table 1-1. Finally all of the PRAs include only point estimates for all events.

TABLE 1-1: RISK CONTRIBUTORS FOR DIFFERENT SFRS (5) (9) (10).

Design	Internal CDF (per year)	Seismic Contribution to CDF (per year)
EBR-II	2×10^{-6}	2×10^{-5}
PRISM	1×10^{-8}	5×10^{-8}
ALMR	1×10^{-10}	3×10^{-6}

1.4 Application of the Technology Neutral Framework to the Sodium Fast Reactor

To investigate the coupled safety-economic challenges associated with SFR design, and perhaps identify areas of opportunity for cost reductions, the DOE issued a multi-university Nuclear Energy Research Initiative Project (NERI) research grant – Project # 08-020. The project team is made up of members from the Massachusetts Institute of Technology, Ohio State University, and Idaho State University. The main goal of the overall project is to propose a methodology using risk-based methods to improve the reference SFR and to develop and describe tools that support this methodology. Rather than applying traditional deterministic regulatory requirements to the design of SFRs, the newly developed TNF is used to identify LBEs which will be used to characterize plant safety. Within this framework, certain event sequences have a very low probability of causing significant consequences. By studying these events, opportunities for design simplification and cost reduction can be made without compromising safety. This approach may present opportunities to improve reactor design by revealing systems or components that are possibly overdesigned to compensate for requirements imposed by deterministic licensing requirements.

Under the TNF, if the mean frequency of radioactivity release can be shown to be under $10^{-7}/\text{yr}$, then the accident is not considered to be part of the design basis for the reactor. While the regulator reserves the right to require additional analysis of any two event sequences regardless of frequency, it can generally be assumed that event sequences below this frequency cutoff will not require additional mitigating systems to be added to the plant design.

1.5 Objectives and Organization

The overarching objective of this thesis is to characterize a level of RPS reliability that precludes ECDAAs from the design basis while maintaining defense-in-depth principles.

This objective is achieved via a three pronged approach:

- Analyze RPS performance during two design basis events: a loss of flow (LOF) accident and a transient overpower (TOP) accident.
- Characterize the performance of self-actuated shutdown systems (SASS) during unprotected transients as a means to increasing RPS diversity.
- Investigate RPS design modifications that may improve RPS performance during seismic events.

The framework of how this approach is executed throughout this thesis follows:

- Chapter 2 presents the methodology employed to model plant performance.
- Chapter 3 describes the RPS, and identifies a reference design for this thesis.
- Chapter 4 describes SFR transient performance in two scenarios: a loss of flow event and a transient overpower event. The impact of RPS reliability on plant performance is analyzed for these two scenarios.
- Chapter 5 introduces SASS and discusses the SASS ranking process. The methodology employed and results obtained are also described.
- Chapter 6 investigates the performance of a Curie point latch during a ULOF and a UTOP. A design description is offered as well as implications on steady state operations.
- Chapter 7 follows suit from chapter 6, analyzing the performance of flow levitated absorbers in an SFR.

- Chapter 8 discusses seismic considerations for the RPS in an SFR. Two design modifications are presented and summarily analyzed: articulated control rods and a seismic anticipatory scram system.
- Chapter 9 concludes the thesis by presenting a summary of the work completed, followed by the conclusions of the analysis. Finally, recommendations for future work based on the completed work are offered.

2 Plant Modeling Methodology

2.1 Introduction

This chapter provides an overview of the computer tools used for this work, and a general description of the models used. The codes used were: MCNP5 and RELAP5-3D. MCNP5 was used to calculate the reactivity worth curves for the control assemblies in the reference design. RELAP5-3D was used to model plant performance during LOF, TOP, ULOF, and UTOP events. A Matlab code was also developed to handle the uncertainty analysis for the RELAP5-3D model.

The ABR-1000 plant from Argonne National Laboratory (ANL) was selected as the reference design from both a core and plant perspective, the ALMR was used for supplemental information if it was missing in the ABR-1000 documentation.

2.2 MCNP Model

The MCNP5 code was used for the reactor physics calculations performed in this thesis. MCNP5 is a general particle transport code developed and maintained by Los Alamos National Laboratory and distributed through the Radiation Safety Information Computational Center (RSICC) in Oak Ridge, Tennessee (11). The calculations were performed in parallel on an eight-core desktop workstation. The supporting nuclear data was generated from the JENDL-3.3 database using NJOY 99.0 (12).

A reference MCNP model of the ABR-1000 core was developed per the parameters described by ANL (13) (14). An example input is provided in Appendix A. The ABR-1000 describes a recycle core (conversion ratio < 1.0) where the control assemblies have a higher worth at the beginning of equilibrium cycle (BOEC) (13) (14). Therefore all calculations were performed assuming BOEC isotopics. The core was modeled with one-third of a reflected core according to one-third polar symmetry to save computational time.

2.3 RELAP5-3D Model

The full-plant design parameters for the SFR model are based upon the ABR-1000. The full-plant model was constructed using RELAP5-3D, based upon a previous RELAP5-3D input deck created by Memmott (15). This model consists of five separate components that were created individually and then combined to create the full-plant model (16). These components are:

- The Core
- The Primary System
- The Secondary Loop
- The Power Conversion System (PCS) Boundary
- The DRACS

There are two major contributing factors that need to be included in the SFR full-plant model in order to accurately portray the physics involved in the steady state operation of the full-plant. The first factor is the geometry and thermal-hydraulic characteristics. This broad category includes the assembly parameters, the core layout, the drag coefficients for both laminar and turbulent regimes (which are used by RELAP5-3D to evaluate the friction factors), and the bypass flow characteristics. The heat transfer coefficients are calculated by the RELAP5-3D code based upon geometric and hydraulic characteristics of the model. The RELAP5-3D model of the SFR core was created by Dustin Langewisch by scaling up the RELAP5-3D core model developed for a smaller SFR design, the Advanced Burner Test Reactor (ABTR) (15). The second contributing factor of complete SFR core design is the neutronic characteristics. This includes both axial and core-wide power profiles, reactivity feedback mechanisms, and neutronic properties. The design parameters for both aspects of the SFR core model were adopted from the ABR-1000 concept. Reference input decks are provided in Appendix B.

2.4 Uncertainty Analysis

The need to analyze low-probability, high-consequence accidents in the nuclear industry has led to the development of complicated analytical methods and models that require a significant number of Monte Carlo simulations to approximate plant failure probabilities (17). Since Monte Carlo simulations are often computationally expensive, numerous approaches have been developed to simplify these problems. Meta-models such as response surfaces have been created to approximate the response of the complex systems without the drawback of long run times. Advanced numerical techniques such as importance sampling and Latin hypercube sampling also enable the modeling of complex system response with orders of magnitude fewer simulations than required by traditional Monte Carlo sampling. While each of these approaches has its drawbacks, meta-models may miss some details in the underlying analysis codes or may be excessively mathematically complex. Therefore, importance sampling was employed to quantify plant performance by randomly simulating uncertainties in feedback coefficients and scram actuation signals.

Small pool type sodium reactors are designed to survive most unprotected transients without cladding rupture. In order to avoid running a prohibitively large number of RELAP5-3D simulations, the sampling should be biased in a way to force selecting the reactivity coefficient values from the more challenging tails of their underlying epistemic distributions while maintaining an unbiased estimate of the failure probabilities. By employing importance sampling, each simulation is assigned a different weight when calculating failure probabilities and small failure probabilities can be calculated with fewer simulations (18) (19).

Mathematically, this can be represented starting with Equations 1 and 2 where $F(t)$ is the conditional cladding failure probability distribution and $w(\lambda)$ is the weighting factor (20).

$$F(t) = \int F(t|\lambda) I(\lambda) w(\lambda) d\lambda \quad (1)$$

$$w(\lambda) = \frac{\pi(\lambda)}{I(\lambda)} \quad (2)$$

Because $I(\lambda)$ is the desired sampling distribution for the Monte Carlo approximation of $F(t)$, every draw of $I(\lambda)$ is weighted by the ratio of the original, $\pi(\lambda)$, and the desired, $I(\lambda)$, sampling distribution (20).

In Monte Carlo space, Equation 1 is approximated by a summation of evaluations of $F(t|\lambda)$ for values of λ sampled from $I(\lambda)$ and weighted by $w(\lambda)$. This is mathematically expressed in Equation 3.

$$F(t) \cong \frac{1}{\sum_{i=1}^N w(\lambda_i)} \sum_{i=1}^N w(\lambda_i) F(t|\lambda_i) \quad (3)$$

One limitation of importance sampling is that the optimal sampling scheme used cannot be known beforehand. However, it is known that sampling from the extreme tails of the distributions will lead to shorter failure times. Therefore the following importance sampling scheme was employed (19):

- 50% of the samples selected above the 95th percentile
- 45% of the samples selected between the 50th and 95 percentiles
- 5% of the samples selected below the 50th percentile

The importance functions used for linear and normal distributions using the sampling scheme above are represented in Equations 4 and 5 respectively.

$$I(\rho) = \left\{ \begin{array}{l} \frac{1}{(\rho'' - \rho')} \frac{0.2}{0.5}, \\ \rho' < \rho < \rho' + (\rho'' - \rho') * .5 \\ \frac{1}{(\rho'' - \rho')} \frac{0.3}{0.45}, \\ \rho' + (\rho'' - \rho') * .5 < \rho < \rho' + (\rho'' - \rho') * .95 \\ \frac{1}{(\rho'' - \rho')} \frac{0.5}{0.05}, \\ \rho' + (\rho'' - \rho') * .95 < \rho < \rho'' \end{array} \right\} \quad (4)$$

$$I(\alpha) = \left\{ \begin{array}{l} N(\mu, \sigma) \frac{0.2}{0.5}, \quad -\infty < \frac{\alpha - \mu}{\sigma} < 0 \\ N(\mu, \sigma) \frac{0.3}{0.45}, \quad 0 < \frac{\alpha - \mu}{\sigma} < 1.65 \\ N(\mu, \sigma) \frac{0.5}{0.05}, \quad 1.65 < \frac{\alpha - \mu}{\sigma} < \infty \end{array} \right\} \quad (5)$$

Hence from the definition of $w(\lambda)$ from Equation 2, the weighting functions $w(\rho)$ and $w(\alpha)$ can be calculated using Equations 6 and 7 respectively.

$$w(\rho) = \left\{ \begin{array}{l} \frac{1}{\frac{(\rho'' - \rho')}{1} \frac{0.2}{0.5}} = 2.5, \\ \rho' < \rho < \rho' + (\rho'' - \rho') * .5 \\ \frac{1}{\frac{(\rho'' - \rho')}{1} \frac{0.3}{0.45}} = 1.5, \\ \rho' + (\rho'' - \rho') * .5 < \rho < \rho' + (\rho'' - \rho') * .95 \\ \frac{1}{\frac{(\rho'' - \rho')}{1} \frac{0.5}{0.05}} = 0.1, \\ \rho' + (\rho'' - \rho') * .95 < \rho < \rho'' \end{array} \right\} \quad (6)$$

$$w(\alpha) = \left\{ \begin{array}{l} \frac{N(\mu, \sigma)}{N(\mu, \sigma) \frac{0.2}{0.5}} = 2.5, \quad -\infty < \frac{\alpha - \mu}{\sigma} < 0 \\ \frac{N(\mu, \sigma)}{N(\mu, \sigma) \frac{0.3}{0.45}} = 1.5, \quad 0 < \frac{\alpha - \mu}{\sigma} < 1.65 \\ \frac{N(\mu, \sigma)}{N(\mu, \sigma) \frac{0.5}{0.05}} = 0.1, \quad 1.65 < \frac{\alpha - \mu}{\sigma} < \infty \end{array} \right\} \quad (7)$$

Equation 3 can now be applied to the practical case discussed in this thesis by inserting the feedback coefficients considered.

For both TOP and LOF events, ANL studied the epistemic reactivity coefficient uncertainties for SFR cores. ANL reports the epistemic uncertainties as normal distributions with the following standard deviations (8) (21):

- Doppler ($\sigma_{Doppler} = 20\% \alpha_{Doppler}$)
- Sodium density ($\sigma_{Na} = 20\% \alpha_{Na}$)
- Axial expansion ($\sigma_{AE} = 30\% \alpha_{AE}$)
- Core radial expansion ($\sigma_{CRE} = 20\% \alpha_{CRE}$)
- Control rod drive line expansion ($\sigma_{CRDL} = 20\% \alpha_{CRDL}$)

where α is the respective feedback coefficient. Table 2-1 lists the reference values for the feedback coefficients for the ABR-1000.

TABLE 2-1: MEAN FEEDBACK COEFFICIENTS FOR THE ABR-1000 (8).

Reactivity Coefficient	Metal		Oxide	
	BOEC	EOEC	BOEC	EOEC
Sodium Density ($^{\circ}\text{C}/^{\circ}\text{C}$)	0.1	0.12	0.1	0.12
Doppler ($^{\circ}\text{C}/^{\circ}\text{C}$)	-0.1	-0.1	-0.12	-0.12
Axial Expansion ($^{\circ}\text{C}/^{\circ}\text{C}$)	-0.06	-0.06	-0.05	-0.05
Core Radial Expansion ($^{\circ}\text{C}/^{\circ}\text{C}$)	-0.38	-0.38	-0.31	-0.3
Control Rod Drive Line Expansion ($^{\circ}\text{C}/\text{cm}$)	-49	-51	-26	-28

The following quantities were modeled as point estimates, so no uncertainties were considered or propagated. Conservative values for these variables were assumed, as documented in (15) (19).

- Pump coast down flow rate
- Reactivity insertion rate
- Heat transfer properties of fuel

- Heat transfer properties of clad
- Fluid transport and heat transfer properties of sodium coolant
- Creep and eutectic formation rate
- Power peaking factor

This methodology was implemented via a modified Matlab “wrapper” code for RELAP5-3D that was adapted from work done by Denman (19). The Matlab code package is provided in Appendix C.

2.5 Summary

MCNP5, RELAP5-3D, and a Matlab pre-/post-processor were used to perform the analyses conducted in this thesis. MCNP5 was used to calculate the control rod worth curves used in the RELAP5-3D plant simulations. RELAP5-3D was employed to analyze plant performance during LOF, TOP, ULOF, and UTOP events, and the performance of the two proposed SASS.

3 Reactor Protection System Design Description

3.1 Introduction

The RPS' primary function is to control reactivity in the reactor core. This is achieved by inserting and removing negative reactivity typically by introducing absorbing material. The RPS is used to control reactivity, and thus power in all stages of reactor operation; from start up to steady-state to shutdown. The RPS must subsequently have enough negative reactivity to accomplish these objectives. This chapter discusses RPS design in SFRs.

3.2 General Design Criteria for the RPS

The Nuclear Regulatory Commission (NRC) provides general design requirements for use in designing commercial nuclear power plants in Title 10, Chapters 50 and 52 of the CFR. Per the NRC (6):

These General Design Criteria (GDC) establish the necessary design, fabrication, construction, testing, and performance requirements for structures, systems, and components important to safety; that is, structures, systems, and components that provide reasonable assurance that the facility can be operated without undue risk to the health and safety of the public.

Criteria 20-29 in Appendix A of 10 CFR 50 pertain to the RPS (6):

Criterion 20--Protection system functions. The protection system shall be designed (1) to initiate automatically the operation of appropriate systems including the reactivity control systems, to assure that specified acceptable fuel design limits are not exceeded as a result of anticipated operational

occurrences and (2) to sense accident conditions and to initiate the operation of systems and components important to safety.

Criterion 21--Protection system reliability and testability. The protection system shall be designed for high functional reliability and inservice testability commensurate with the safety functions to be performed. Redundancy and independence designed into the protection system shall be sufficient to assure that (1) no single failure results in loss of the protection function and (2) removal from service of any component or channel does not result in loss of the required minimum redundancy unless the acceptable reliability of operation of the protection system can be otherwise demonstrated. The protection system shall be designed to permit periodic testing of its functioning when the reactor is in operation, including a capability to test channels independently to determine failures and losses of redundancy that may have occurred.

Criterion 22--Protection system independence. The protection system shall be designed to assure that the effects of natural phenomena, and of normal operating, maintenance, testing, and postulated accident conditions on redundant channels do not result in loss of the protection function, or shall be demonstrated to be acceptable on some other defined basis. Design techniques, such as functional diversity or diversity in component design and principles of operation, shall be used to the extent practical to prevent loss of the protection function.

Criterion 23--Protection system failure modes. The protection system shall be designed to fail into a safe state or into a state demonstrated to be acceptable

on some other defined basis if conditions such as disconnection of the system, loss of energy (e.g., electric power, instrument air), or postulated adverse environments (e.g., extreme heat or cold, fire, pressure, steam, water, and radiation) are experienced.

Criterion 24--Separation of protection and control systems. The protection system shall be separated from control systems to the extent that failure of any single control system component or channel, or failure or removal from service of any single protection system component or channel which is common to the control and protection systems leaves intact a system satisfying all reliability, redundancy, and independence requirements of the protection system. Interconnection of the protection and control systems shall be limited so as to assure that safety is not significantly impaired.

Criterion 25--Protection system requirements for reactivity control malfunctions. The protection system shall be designed to assure that specified acceptable fuel design limits are not exceeded for any single malfunction of the reactivity control systems, such as accidental withdrawal (not ejection or dropout) of control rods.

Criterion 26--Reactivity control system redundancy and capability. Two independent reactivity control systems of different design principles shall be provided. One of the systems shall use control rods, preferably including a positive means for inserting the rods, and shall be capable of reliably controlling reactivity changes to assure that under conditions of normal operation, including anticipated operational occurrences, and with appropriate margin for malfunctions such as stuck rods, specified acceptable

fuel design limits are not exceeded. The second reactivity control system shall be capable of reliably controlling the rate of reactivity changes resulting from planned, normal power changes (including xenon burnout) to assure acceptable fuel design limits are not exceeded. One of the systems shall be capable of holding the reactor core subcritical under cold conditions.

Criterion 27--Combined reactivity control systems capability. The reactivity control systems shall be designed to have a combined capability, in conjunction with poison addition by the emergency core cooling system, of reliably controlling reactivity changes to assure that under postulated accident conditions and with appropriate margin for stuck rods the capability to cool the core is maintained.

Criterion 28--Reactivity limits. The reactivity control systems shall be designed with appropriate limits on the potential amount and rate of reactivity increase to assure that the effects of postulated reactivity accidents can neither (1) result in damage to the reactor coolant pressure boundary greater than limited local yielding nor (2) sufficiently disturb the core, its support structures or other reactor pressure vessel internals to impair significantly the capability to cool the core. These postulated reactivity accidents shall include consideration of rod ejection (unless prevented by positive means), rod dropout, steam line rupture, changes in reactor coolant temperature and pressure, and cold water addition.

Criterion 29--Protection against anticipated operational occurrences. The protection and reactivity control systems shall be designed to assure an

extremely high probability of accomplishing their safety functions in the event of anticipated operational occurrences.

Therefore, an SFR must possess a diverse and redundant RPS with multiple reactivity control systems (or scram systems) of which one must be capable of shutting the reactor down from hot full power (HFP) to hot zero power (HZP).

3.3 Reactor Protection System Design in Sodium Fast Reactors

These requirements frame the design space for an SFR RPS, and designers have taken several approaches to meet these goals. Table 3-1 summarizes the practical design space for SFR RPS. Of the GDCs for the RPS, the requirement for diversity is arguably the most vague, yet most constraining criterion for SFRs. LWRs meet this requirement with control rod banks and liquid boron control since operators are able to dissolve boric acid in the primary coolant of an LWR. An operator cannot dissolve an absorber in sodium without encountering more limiting consequences. Therefore SFR designers typically meet diversity and redundancy requirements by incorporating two independent control rod banks with differing rod designs, different manufacturers, independent and diverse electronics, and different operational purposes – shutdown and power trimming (although both systems can shut the reactor down individually). The general effects of multiple redundant subsystems on overall system reliability are shown in Table 3-2.

TABLE 3-1: RPS DESIGN SPACE SUMMARY PER 10 CFR 50, APPENDIX A.

Function	Design Options
Reactivity Control	<ul style="list-style-type: none"> • Absorber insertion • Fuel removal • Leakage enhancement
Control Material	<ul style="list-style-type: none"> • Fuel • Boron carbide • Tantalum • Europium • Void/low density gas
Insertion Trigger	<ul style="list-style-type: none"> • Operator Action • Active Instrumentation • Passive Actuation
Driving Force	<ul style="list-style-type: none"> • Electronic Motor • Gravity • Spring • Explosive
Redundancy and Diversity	<ul style="list-style-type: none"> • Multiple Systems • Diverse Materials • Different Manufacturers • Varied Trip Signals

TABLE 3-2: EFFECTS OF REDUNDANCY ON SYSTEM RELIABILITY (22).

Number of Parallel Systems	Number Which Must Fail to Cause System Failure	Failure Probability
1	1	1.00E-03
2	2	1.00E-06
3	3	1.00E-09
4	4	1.00E-12
5	5	1.00E-15

For example, the ABR-1000 design incorporates two independent safety-grade reactivity control systems (8) (23). The primary system is required to have sufficient reactivity worth to bring the reactor from any operating condition to cold sub-critical at the refueling temperature with the most reactive control assembly stuck at the full power operating position. The reactivity associated with uncertainties in criticality and fissile loading is also accommodated by the primary control system. The secondary control system

is required to shut the reactor down from any operating condition to cold shutdown, also with the most reactive assembly inoperative. The oxide fuel version of the ABR-1000 includes a self-actuated shutdown system using a Curie point latch (described in more detail in Chapters 5 and 6) as another way of actuating a reactor scram, although the details of which rod bank this latch is included in are not provided since it could be included on the primary or secondary bank, or both.

The ALMR incorporates ten control assemblies loaded with natural boron carbide (13) (24) (25). The control rods provide startup control, power control, burnup compensation, and rapid shutdown. Each rod is designed with three different insertion mechanisms: gravity-driven free-fall, fast run-in by an irreversible electric motor, and slow drive-in using the shim motor. The ALMR also has six Gas Expansion Modules (GEMs) to enhance leakage during a loss of flow, thus aiding in reactor shutdown. Finally, the ALMR incorporates three Ultimate Shutdown Assemblies which are control assemblies loaded with enriched boron carbide. Each assembly provides enough negative reactivity to shut the reactor down. These assemblies make up the second reactivity control system and are only used to shut the reactor down. They are parked above the core during operation, and can be inserted either by gravity or fast run-in motors. It should be noted that the ALMR designers also considered using spheres loaded with enriched boron carbide that would be allowed to fall into the core upon actuating a gate above the core instead of the rod-assembly design for the shutdown system (13) (26) (27).

The European Fast Reactor (EFR) preliminarily includes a tertiary scram system (28) (29), while the designers of the Japanese Sodium Fast Reactor (JSFR) are also considering adding a tertiary scram system (30) (31). Both designs suggest the inclusion of passive shutdown systems incorporated into the RPS.

As seen from the above examples, there are several paths a designer can choose to address the GDC requirements on the RPS. For consistency, the RPS described in the ABR-1000 metal core is employed as the reference design for this thesis. Similarities between the active banks of the ABR-1000 and ALMR allow the use of the more detailed ALMR RPS operating characteristics.

3.4 Rod Worth Calculations

To calculate the worth of the control assemblies, an MCNP5 model was developed, as described in Chapter 2 and Appendix A. The cumulative worth of all the assemblies in the primary bank were calculated by performing MCNP5 calculations at varying axial positions from full insertion to full withdrawal at BOEC. The same procedure was performed to calculate the worth of the secondary bank assemblies. Finally the calculations were repeated using an oxide core model. The resulting integral worth curves are shown in Figure 3-1 through Figure 3-4.

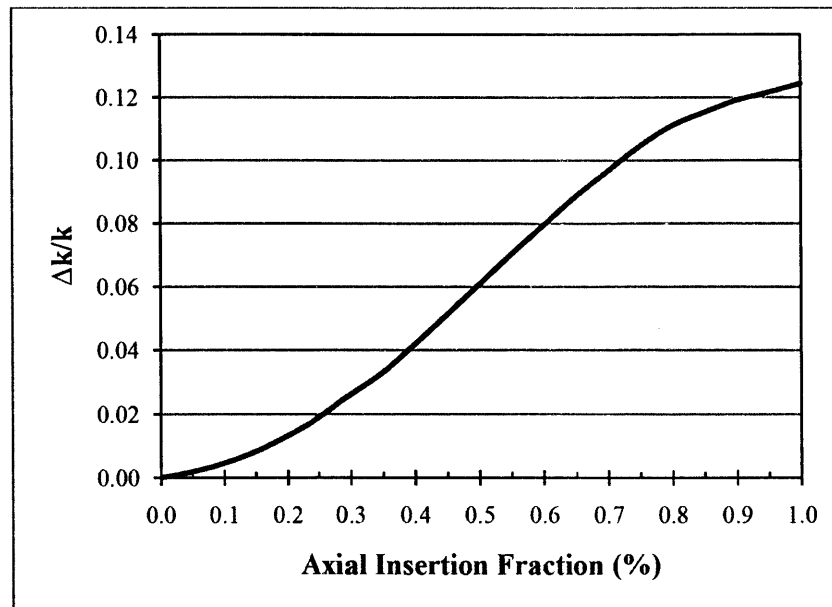


FIGURE 3-1: PRIMARY CONTROL ASSEMBLY BANK INTEGRAL WORTH CURVE FOR A METAL CORE.

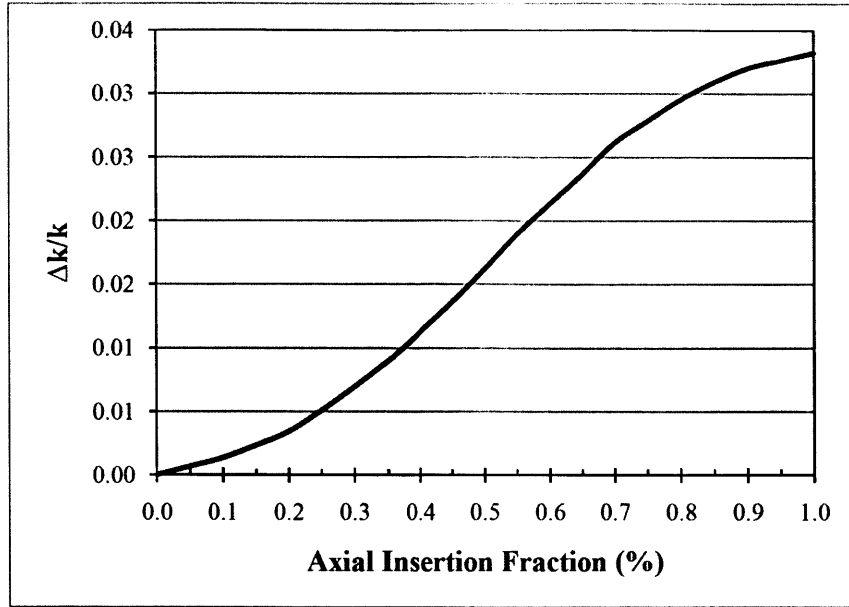


FIGURE 3-2: SECONDARY CONTROL ASSEMBLY BANK INTEGRAL WORTH CURVE FOR A METAL CORE.

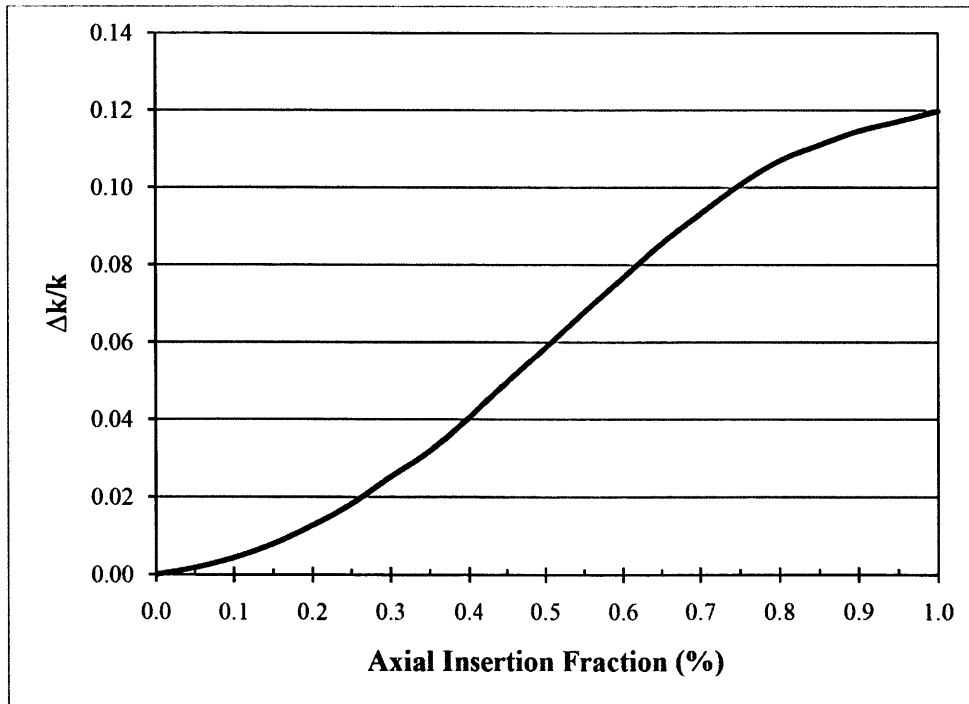


FIGURE 3-3: PRIMARY CONTROL ASSEMBLY BANK INTEGRAL WORTH CURVE FOR AN OXIDE CORE.

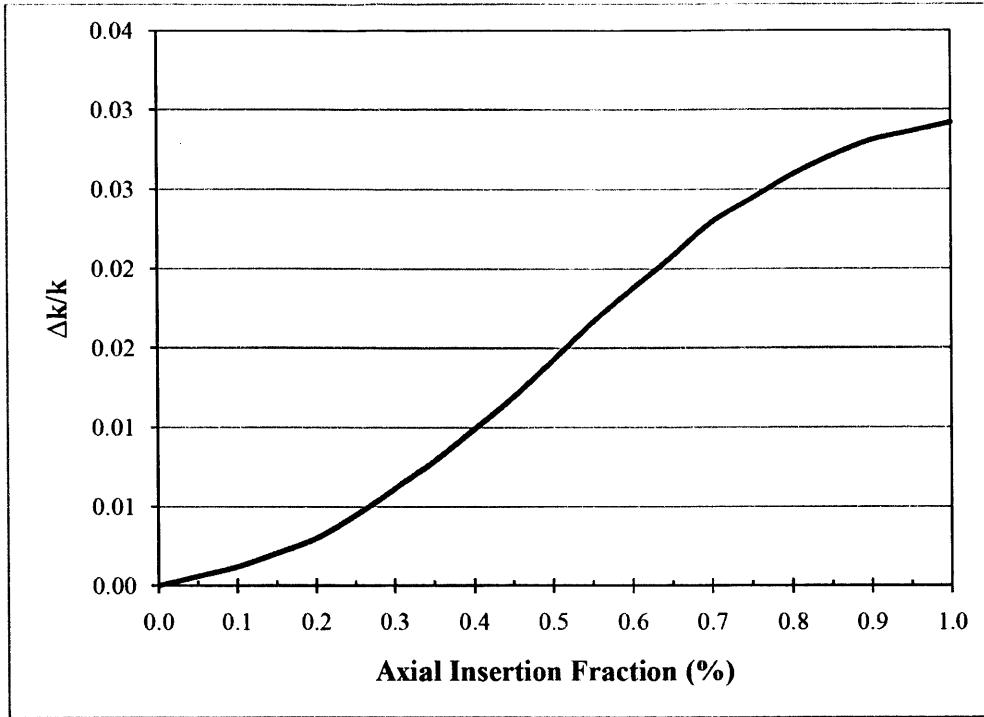


FIGURE 3-4: SECONDARY CONTROL ASSEMBLY BANK INTEGRAL WORTH CURVE FOR AN OXIDE CORE.

3.5 Summary

The NRC requires the RPS to be a system designed with diversity, redundancy, and independence that is capable of shutting a reactor down from HFP to HZP. These requirements, combined with an SFR's inherent characteristics lead to different RPS configurations for SFRs than those found in LWRs. For the purpose of this thesis, the ABR-1000 RPS was selected as the reference design. The ABR-1000 RPS is made of two independent control assembly banks. The primary bank is used for reactivity control during all operations and contains 15 assemblies loaded with natural boron carbide pins; while the secondary bank is held in reserve to shut the reactor down and contains 4 assemblies loaded with enriched boron carbide pins.

4 Sodium Fast Reactor Transient Performance

4.1 Introduction

There are three general transient categories for SFRs that can challenge the integrity of the plant:

- Transient Overpower (TOP)
- Loss of Flow (LOF)
- Loss of Heat Sink (LOHS)

To be consistent with TNF guidelines, this thesis will only take credit for safety grade components, and since the primary heat sink is not safety grade, all transients will be considered as LOHS. Therefore only TOPs and LOFs will be analyzed.

This chapter presents SFR plant transient performance for ULOF events and UTOP events. The impacts of RPS reliability on plant performance with respect to the safety goals outlined by the TNF are subsequently discussed. Finally the marginal increase in RPS reliability by the addition of a tertiary scram system compared to the reference two-scram system RPS is analyzed.

4.2 Unprotected Loss of Flow Events

LOF events can occur in a variety of ways. The dominant sequences as outlined in the ALMR PRA considered for this thesis are listed in Table 4-1. Note that only LOFs with an initiating frequency above the FCC ($10^{-7}/\text{yr}$) are considered.

TABLE 4-1: LOF SCENARIOS FOR THE ALMR (5).

Event	Initiating Frequency (yr ⁻¹)*
Station Blackout	0.007
Station Blackout w/o 2 Coastdown Motors	9.1 x10 ⁻⁹
SBO w/o 4 Coastdown Motors	4.73 x10 ⁻¹⁰

* *Initiating Frequency refers to the frequency of pump failures, station blackout events (SBO), and coastdown (CD) Motor failures.*

According to the ALMR PRA, the most frequent and severe initiating event is the station blackout (SBO). The SBO transient is a loss of electrical power accident. It is assumed that all electrical power to the plant is lost and that emergency backup power fails. Under these conditions, the heat sink via the Power Conversion System (PCS) is lost, the pumps stop working, and the fail-open valves of the DRACS open. For the station blackout transients performed here, the PCS is lost instantly upon accident initiation, while the coastdown motors keep the pumps operating at progressively decreasing speeds for a period of time. This gradual decrease in pump speed after accident initiation is called the pump coastdown. Since we are analyzing RPS performance, RPS failure is also assumed, making this an unprotected station blackout (USBO).

There are four separate phases of a USBO transient (32). The first phase of a USBO transient reflects rapidly increasing core temperatures while the pumps trip and slow down. Since an unprotected transient is being considered, the RPS fails to initiate as well. The net negative reactivity coefficients do reduce the reactor power as the core heats up, but the core power remains higher than the energy removed by coolant flow through the core, causing an increase in coolant temperature until the core power drops below the coolant's heat removal capability. The second phase of an USBO is a decrease in core temperatures (clad, fuel, and coolant) as the reactor power continues to decrease. The third phase of an USBO transient begins when the pump completely stops and natural circulation flow is established. The

natural circulation flow rate carries heat from the core to the DRACS exchanger, where the heat is rejected, and then returns to the core inlet. The heat removed from the DRACS is less than the decay heat produced by the core, so the coolant, clad, and fuel temperatures slowly increase. A second peak is seen after a long time lapse after the initiation of the transient. At this point, the decay heat produced by the core matches the decay heat removed by the DRACS systems. The fourth and final phase is a gradual cool down as the DRACS effectively cools the pool by removing more heat than is produced by the core. This transient sequence is illustrated in Figure 4-1.

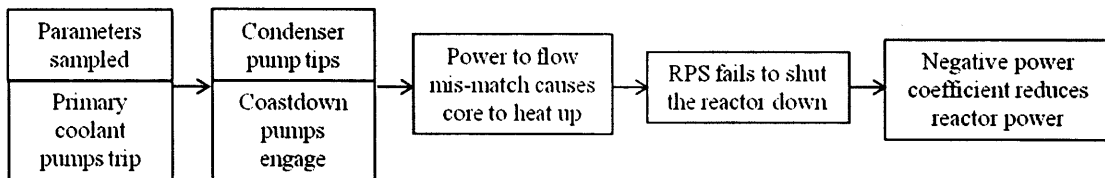


FIGURE 4-1: BLOCK DIAGRAM OF ULOF PROGRESSION.

Per Denman’s work (19), analyzing the most severe ULOF (with a coastdown halving-time of 5 seconds (33) (34) (21)) for a metal core yielded a conditional cladding failure probability of 0.0016 given a ULOF. Recalling that the RPS failure frequency during a LOF is $1.0 \times 10^{-7}/\text{yr}$, the initiating frequency for a ULOF is $7.0 \times 10^{-10}/\text{yr}$, so the frequency of cladding damage in a metal core is calculated to be $(0.0016 \times 7.0 \times 10^{-10})$ or $1.1 \times 10^{-12}/\text{yr}$, which is much less than the TNF FCC lower bound of 1.0×10^{-7} . The results of these simulations are shown in Figure 4-2.

Performing the same analysis for an oxide core (with a coastdown halving-time of 10 seconds (33) (34) (14)) resulted in a conditional cladding failure probability of 0.4071 given a ULOF. This yields a frequency of cladding damage in an oxide core of 2.8×10^{-10} , which is also less than the FCC, but two orders of magnitude greater than the value for a metal fuel core. The results of these simulations are shown in Figure 4-3.

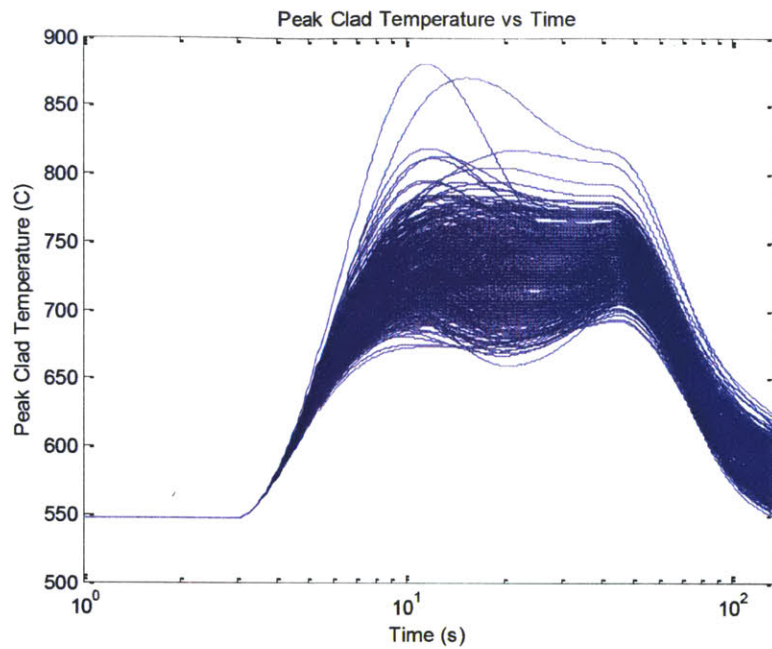


FIGURE 4-2: PEAK CLADDING TEMPERATURE DURING A ULOF IN A METAL CORE.

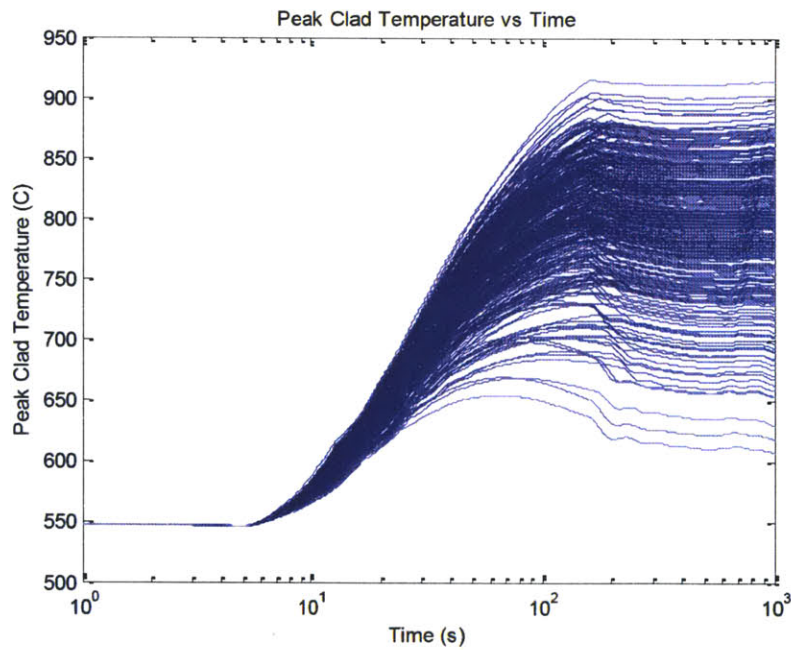


FIGURE 4-3: PEAK CLADDING TEMPERATURE DURING A ULOF IN AN OXIDE CORE.

4.3 Unprotected Transient Overpower Events

A UTOP represents the insertion of reactivity due to the removal of a control rod with the highest worth followed by a failure to scram (32). This can occur as a result of a

misalignment of the control rod stops. The total reactivity inserted, insertion rates, and accompanying frequencies for the ALMR design are provided in Table 4-2. The positive reactivity insertion produces an upward ramp of the core power until the negative feedbacks push the core power back down. The core power eventually reaches an equilibrium value that is higher than operational core power (>100%). Eventually the bulk coolant temperature increases to 535 °C, which trips the EM pumps to prevent them from overheating. The pump trip effectively creates a ULOF as well. This transient sequence is illustrated in Figure 4-4.

TABLE 4-2: ALMR TOP REACTIVITY INSERTION DISTRIBUTIONS (5).

Frequency of TOPs	Reactivity Insertions	Reactivity Insertion Rate
$3 \times 10^{-5}/\text{yr}$	\$0.3-0.5	\$0.03/s
$2 \times 10^{-6}/\text{yr}$	\$0.5-0.7	\$0.03/s
$1 \times 10^{-7}/\text{yr}$	\$0.7-0.9	\$0.03/s

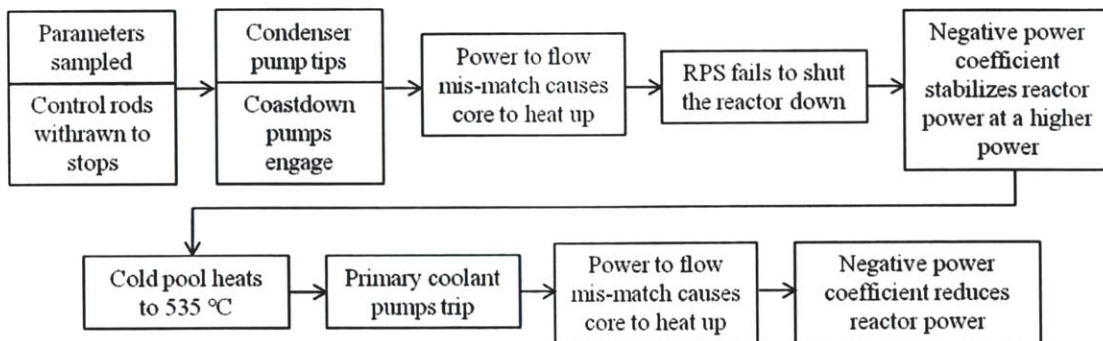


FIGURE 4-4: BLOCK DIAGRAM OF UTOP PROGRESSION.

Analyzing the most severe UTOP yielded a conditional cladding failure probability of 0.0082 for a metal core given a UTOP (19). Considering the initiating frequency for such a UTOP is $1.0 \times 10^{-14}/\text{yr}$, the frequency of cladding damage is $8.2 \times 10^{-17}/\text{yr}$ given a severe UTOP, much less than the TNF FCC lower bound of 1.0×10^{-7} . The same analysis for an oxide core produced a conditional cladding failure probability of approximately 1.0 given a UTOP (19). This yields a cladding damage frequency of 1.0×10^{-14} , also less than the FCC,

but three orders of magnitude greater than the cladding damage frequency for a metal fuel core. The results of both simulations are shown in Figure 4-5 and Figure 4-6.

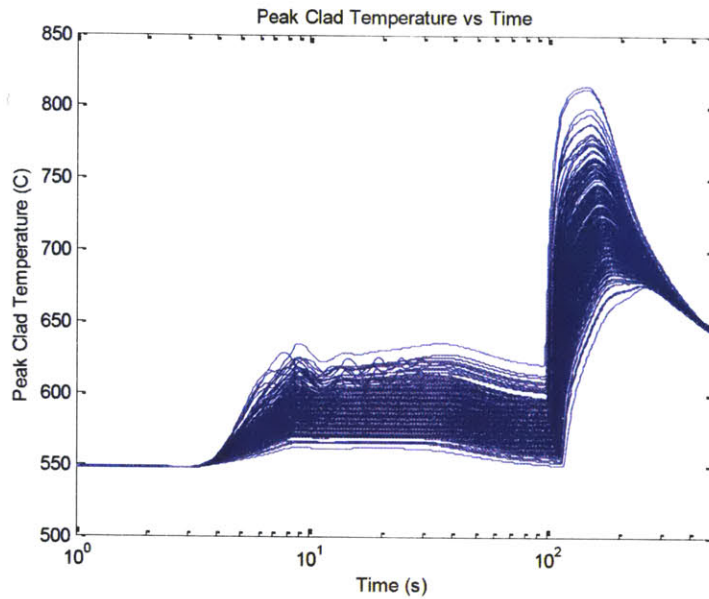


FIGURE 4-5: PEAK CLADDING TEMPERATURE DURING A UTOP IN A METAL CORE.

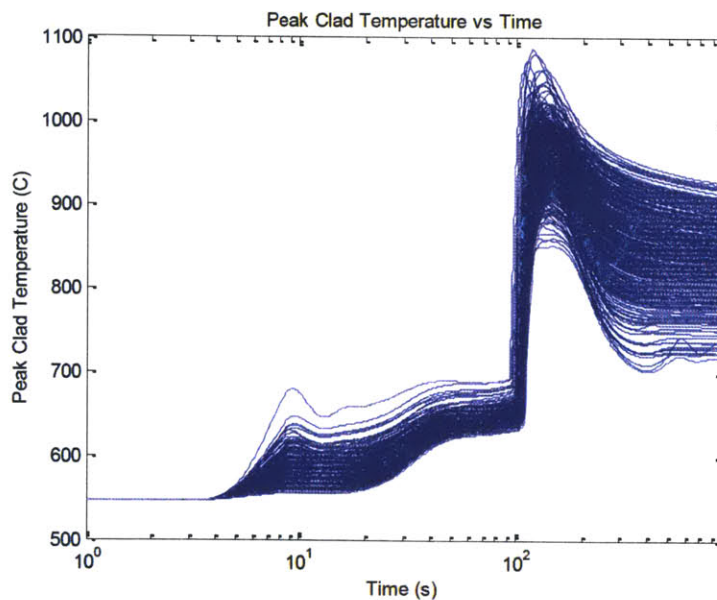


FIGURE 4-6: PEAK CLADDING TEMPERATURE DURING A UTOP IN AN OXIDE CORE.

For both a ULOF and a UTOP, the metal core modeled in this thesis outperforms the oxide core. While this difference will appear throughout this thesis, it should be noted that

the reference design has been optimized for metal fuel characteristics, not oxide fuel characteristics. Therefore these results should not be interpreted as an endorsement for metal fuel, and a designer considering an oxide fuel core would need to analyze these transients for an optimized oxide core. This is true for all analysis performed in this thesis. More information on metal and oxide core performance can be found in Denman's thesis (19).

4.4 Impact of Reactor Protection System Reliability on Plant Safety

Based on the initiating frequencies of LOF and TOP events from the ALMR PRA (Table 4-1 and Table 4-2), a designer would need to design an RPS with a failure frequency no greater than 1.4×10^{-5} /demand in order to exclude ULOFs and UTOPs from the design basis per the TNF FCC. This requirement is quite achievable since the ALMR PRA suggests the ALMR's RPS is an extremely robust system with a probability of failure during a TOP of 3.0×10^{-5} /demand and 1.0×10^{-7} /demand for all other transients (5). Considering the TNF recommends a lower frequency of radiation release cutoff at 1.0×10^{-7} /yr, clearly all unprotected transients in the ALMR PRA are automatically excluded as licensing basis events. Therefore, the ALMR's RPS is designed with significant extra margin.

4.5 Three Independent Scram Systems versus Two Independent Scram Systems

The fact that the ALMR's as-designed RPS automatically excludes all unprotected events from the licensing basis strongly suggests that a third system is not necessary. However, this analysis was performed for a 1000 MW metal core SFR which results in strong inherent feedback mechanisms that help protect the core during transients (35) (36). A larger reactor may be more sensitive to ULOFs or UTOPs and may require more of its RPS (32) (21) (34), but considering the large margin built into the ALMR's RPS, it is hard to conceive of a situation where a designer would challenge that margin.

4.6 Summary

First, the efficacy of the two scram system design as proposed in the reference plant, the ABR-1000, was evaluated. One of the TNF's unique features is that sequences with release frequencies below a mean threshold frequency of $10^{-7}/\text{yr}$ can be screened from the design basis, a very significant feature in regard to the RPS system. Events that include failure of the RPS are not included in LBEs since the failure probability of the Reactor Protection System (RPS) is small enough to push unprotected accidents under the $10^{-7}/\text{yr}$ mean frequency FCC cutoff. For example, the conditional failure probability for the ALMR RPS during a TOP is $3 \times 10^{-5}/\text{demand}$ and is $1 \times 10^{-7}/\text{demand}$ for all other transients, while the initiating frequency of a TOP or a LOF is less than 0.007 (5). The high reliability of the RPS means that only protected accidents need to be analyzed as LBEs. While accidents involving failure of the RPS may still be required by the regulator, they will qualify as beyond design basis events and will not drive the design of the RPS. These results indicate that two scram systems perform well enough to push the frequency of unprotected transients below the 10^{-7} frequency cutoff proposed in the TNF, thus nullifying the need for a third, independent scram system. However, the RPS as described in this chapter may not satisfy diversity requirements, so the remainder of this thesis analyzes approaches to enhance the diversity of the RPS in SFRs.

5 Self-Actuated Shutdown System Selection

5.1 Introduction

It should be noted that while the TNF incorporates many risk-based concepts, pillars of traditional regulatory structure, such as defense in depth, are still required. Thus, while the RPS is required to be highly reliable to meet the frequency arguments of the FCC; redundancy, diversity, and independence are still required to satisfy defense in depth requirements (2). For example, the ALMR project started negotiations with the NRC Office of Regulatory Research with two independent SCRAM systems comprising their RPS. The NRC recommended the ALMR add to its defense in depth case, and convinced the ALMR designers to augment their redundant shutdown banks with Curie point latches and add GEMs to the core design (37). Thus, while the frequency of scram failure may push unprotected accidents below the FCC cutoff, the extent to which the RPS is further diversified will, in the end, be a negotiation between the NRC and the applicant.

Therefore, the secondary scram system proposed in the reference design may not satisfy the principles of defense-in-depth as recommended by the NRC due to the similarities between the primary and secondary systems' structural design, trip signals, and reliance on active operation. One approach to address this issue is to incorporate Self-Actuated Shutdown Systems (SASS) into the design.

SASS are simple, inexpensive design modifications that induce scram when core temperatures and/or coolant flow rates reach certain design limits (38) (39). These devices have the potential to diversify the RPS, add to defense-in-depth, and increase scram reliability. The primary design characteristics of SASS are shown in Table 5-1. Over a dozen designs for these systems have been proposed, and several designers have considered

incorporating these devices. This chapter will discuss the ranking process used in the present work to select the most promising designs for incorporation into an SFR.

TABLE 5-1: PRIMARY DESIGN CHARACTERISTICS OF SASS (32).

Characteristics	Design Options
Concept Type	<ol style="list-style-type: none"> 1. Combine sensing, triggering, and lock-release functions 2. Combine sensing and triggering functions; separate lock-release function
Sensor-Trigger Type	<ol style="list-style-type: none"> 1. Melting point operated device 2. Ferromagnetic Curie point operated device 3. Thermal expansion operated device 4. Differential density operated device 5. Hydraulic suspension operated device
Insertion Force	<ol style="list-style-type: none"> 1. Gravity 2. Spring 3. Pneumatic 4. Hydraulic 5. Explosive (e.g. a burst disk)
Reactivity Control	<ol style="list-style-type: none"> 1. Absorber insertion 2. Fuel removal 3. Leakage enhancement
Form of Reactivity Control Material	<ol style="list-style-type: none"> 1. Solid block with perforations 2. Rod bundle 3. Spheres 4. Liquid 5. Sealed assembly
Type of Reactivity Control Material	<ol style="list-style-type: none"> 1. Fuel 2. Boron carbide 3. Tantalum 4. Europium

5.2 Self-Actuated Shutdown Systems Considered

Twelve designs were selected from the open literature, focusing on those potentially applicable to SFRs. The twelve systems identified for review are described below (32) (39) (40) (41) (42) (30) (43) (44) (38) (45) (45):

- Lithium Expansion Module

Liquid lithium thermally expands into dedicated assemblies introducing absorbing material as the core outlet temperature increases.

- Lithium Injection Module

Liquid lithium is pressure-injected via a burst disk or comparable feature into dedicated assemblies in response to a coolant temperature increase, introducing absorbing material.

- Curie Point Latches

Magnetic latches are added to the control rod driveline, holding the rods in place. If the coolant temperature exceeds the curie point of the magnetic latch, the material loses its magnetic properties and the control rods drop into the core by gravity.

- Thermostatic Switches

A variation on Curie point latches, electromagnetic latches on the control rod driveline hold up control rods and are tied directly into the plant electrical supply. Power supply is controlled by temperature switches on the driveline that open the circuit above designed temperature limits. When the circuit is opened, the electromagnetic latches lose their holding strength, dropping the rods into the core by gravity.

- Fusible Link Latches

A third variation on Curie point latches, a low-melting point alloy is added as a fusible link to the CRDL. When the coolant temperature increases above the alloy's melting point, the link melts, dropping the rods into the core by gravity.

- Thermal Volumetric Expansion Drives

Thermal expansion of a working fluid in a piston on the CRDL drives absorbing material into the core in response to a coolant temperature increase.

- Flow Levitated Absorbers

Coolant flow suspends absorbing rods above the active core. If coolant flow is lost, the rods drop into the core by gravity.

- Cartesian Diver

Functions according to the same principle as a Galilean thermometer. Absorbing material with a lower density than the coolant at normal operating temperatures floats, due to its buoyancy, above the active core region. When the temperature of the coolant increases above a design limit, the absorber material becomes denser than the coolant, and sinks into the core.

- Sodium Injection

When the coolant reaches a design limit, a fusible burst disk injects sodium into a pre-voided region in the center of the core, introducing negative reactivity.

- Enhanced Thermal Elongation of Control Rod Drive Line

The CRDL is constructed of a highly expansive alloy that drives the absorber material into the core as the coolant temperature increases.

- Gas Expansion Module

Gas Expansion Modules (GEMs) introduce negative reactivity by increasing neutron leakage out of the core. Dedicated modules on the core periphery are filled with a gas which is compressed above the active core region by sodium flow. If the flow stops, the gas expands, providing enhanced streaming paths for neutrons.

- Leading Channels for Na Voiding

Similar to GEMs in function, peripheral fuel assemblies are modified to have high power to flow ratios, inducing sodium boiling earlier in transients and increasing neutron leakage.

Several designers are considering use of some of the above designs (3) (40):

- **US**: Curie point latches, thermostatic switches, and GEMs.
- **France**: Curie point latches, thermostatic switches, and GEMs.
- **Japan**: Curie point latches, thermostatic switches, volume expansion drives, and GEMs. (Lithium expansion is used in the Toshiba 4S design).
- **India**: Flow-levitated absorbers and Curie point latches.
- **Russia**: Flow-levitated absorbers for the BN-800 and BN-1800.

It should be noted that design options which enhance core flowering are not included in the above list since all existing SFR designs incorporate that feature, and inclusion of this feature is unanimously regarded as good practice (21).

5.3 Ranking Methodology

A two-round ranking methodology was exercised to rank SASS according to their performance in a variety of categories in order to refine the list to select the best performers. This ranking methodology involved assembling a list of performance categories. These categories were assigned an importance weighting, W_{cat} , according to the relative importance of each category in satisfying the designer's goals. Next, the proposed designs were assigned a performance score, P_{cat} , for each category. The results were then used to calculate the weighted performance score, S_{cat} , for each category according to Equation (8).

$$S_{cat} = W_{cat} \times P_{cat} \quad (8)$$

This procedure was completed for each category, and the results were summed to produce a total score, S_{tot} , for each design according to Equation (9).

$$S_{tot} = \sum_i^N S_{cat,i} \quad (9)$$

Nine categories were considered and S_{tot} was calculated for the twelve SASS designs reviewed. The categories reviewed were:

- Passivity
- Resetability
- Response time
- Potential for inadvertent actuation
- Effect on steady state operation
- State of development
- Reliability
- Capital cost of inclusion
- Inspectability/Testability (i.e. capability to perform in-situ testing)

The results are shown in Table 5-2. Note that the weightings used are subjective selections by a subset of project participants. Others may assign different weights, but the methodology will be similar.

TABLE 5-2: FIRST ROUND RANKING OF SASS.

Feature (P_{cat})	Performance Categories (W_{cat})									Overall Rating
	Passivity (5)	Resetability (4)	Response Time (5)	Inadvertent Actuation (4)	Effect on Steady State (5)	State of Development (3)	Reliability (5)	Low Capital Cost (5)	Inspectability (3)	
Lithium Expansion Module	5	5	4	4	3	3	5	2	1	143
Lithium Injection Module	4	1	3	4	4	2	4	1	1	109
Curie Point Latches on CRs	5	5	4	4	4	4	5	5	4	175
Thermostatic Switches on CRs	3	5	4	4	4	4	5	4	4	160
Volume Expansion Drive CRs	5	5	3	4	4	3	5	3	4	157
Fusible Link Latches on CRs	5	1	2	4	4	4	5	5	2	143
Flow-Levitated Absorber	5	5	5	4	2	4	5	4	5	168
Cartesian Diver	5	4	1	4	2	2	4	2	2	114
Sodium Injection	4	1	3	4	2	2	3	1	2	97
Enhanced CRDLE	5	4	3	3	4	3	3	4	3	141
GEM	5	5	5	3	1	5	4	5	2	153
Leading Channels for Voiding	5	4	5	3	2	3	5	5	4	159

The five designs with the largest S_{tot} were further analyzed through a second ranking using the same methodology, but with different categories:

- Long term shutdown capability
- Magnitude of negative reactivity
- Compatibility with heat removal
- Possibility for positive reactivity insertion
- Durability
- Proof of operation
- Accident applicability (ULOF, UTOP, ULHS)

The designs were then ranked in the same manner as was done in the first round. The Curie point latch, thermostatic switch, and flow levitated absorber scored highest, as shown in Table 5-3.

TABLE 5-3: SECOND ROUND RANKING OF SASS.

Feature (P_{cat})	Performance Categories (W_{cat})							Overall Rating
	Long Term Shutdown Capability (5)	Magnitude of Negative Reactivity (5)	Compatibility with Decay Heat Removal (4)	Possibility for Positive Insertion (4)	Durability (4)	Proof of Operation (4)	Accident Applicability (5)	
Curie Point Latches on CRs	5	5	4	5	4	5	3	137
Thermostatic Switches on CRs	5	5	4	5	3	5	3	133
Volume Expansion Drive CRs	4	3	4	3	4	4	3	110
Flow-Levitated Absorber	4	5	3	3	5	5	3	124
Leading Channels for Na Voiding	1	1	5	1	3	2	3	69

5.4 Summary

The Curie point latch, thermostatic switch, and flow levitated absorber scored the highest as a result of the ranking process. Due to their similarity in operation, the Curie point device was judged as representative of the thermostatic switch for more detailed performance analysis (44). The next two chapters will discuss the performance of the Curie point latch and the flow levitated absorber during ULOF and UTOP events.

Before reviewing these analyses, it is important to mention that because of the inherent capability of the reference design to avoid severe fuel damage in unprotected events, the addition of an enhanced or tertiary reactor protection system is not justified based on meeting a severe fuel damage frequency limit such as $10^{-7}/\text{yr}$. The justification is to provide defense-in-depth or to address some specific issue, such as low frequency seismic events, incapacitated plant operating crew, or regulator requirements. For this reason, rather than assessing the overall frequency of core damage for a candidate system modification, the conditional failure probability of the analyzed system to prevent cladding damage is considered given an unprotected event.

6 Curie Point Latch Performance Analysis

6.1 Introduction

Curie point latches (CPL) operate based on a material's Curie point. A Curie point, or Curie temperature, is the point at which a material loses its magnetic properties. The Curie temperature of a ferromagnetic or a ferromagnetic material is the temperature above which it becomes paramagnetic (it is for instance 768 °C for pure iron) (46). Below the Curie temperature the magnetic moments are aligned parallel within magnetic domains in ferromagnetic materials and anti-parallel in ferrimagnetic materials. As the temperature is increased towards the Curie point, the alignment (magnetization) within each domain decreases. Above the Curie temperature, the material is paramagnetic so that magnetic moments are in a completely disordered state. While the temperature increases, thermal motion, or entropy, competes with the ferromagnetic tendency for dipoles to align. When the temperature rises beyond a certain point, called the Curie temperature, there is a second-order phase transition and the system can no longer maintain a spontaneous magnetization, although it still responds paramagnetically to an external field. Below that temperature, there is a spontaneous symmetry breaking and random domains form (in the absence of an external field) (46). This is illustrated in Figure 6-1.

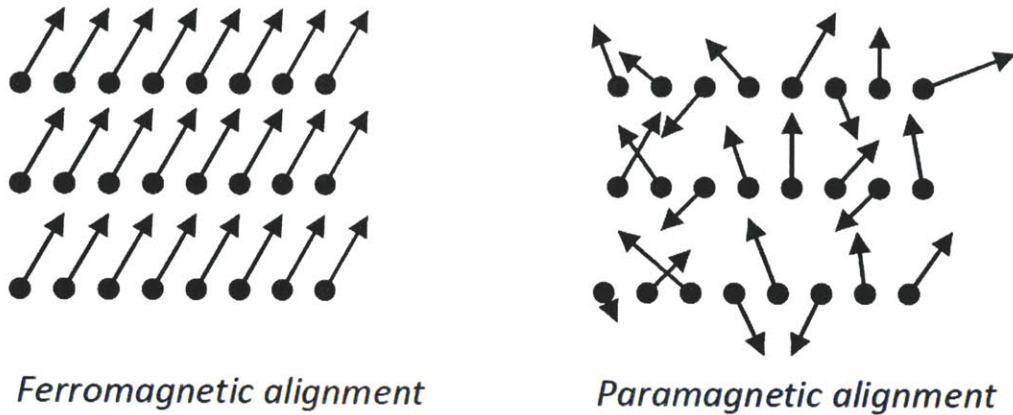


FIGURE 6-1: ILLUSTRATION OF MAGNETIC MOMENTS OF FERROMAGNETIC AND PARAMAGNETIC MATERIALS.

Therefore a curie point will activate with a delay following the initiation of a transient that depends on the time it takes for heat generated in the fuel to transfer to the coolant and then to the Curie point material in the CRDL. This time delay, dictates how quickly the CPL can respond to a transient.

6.2 System Design Description

A CPL would be a simple addition to the reference control assembly design. A CPL would be added to the secondary rod bank to the CRDLs above the absorber bundles. The exact axial placement would have to be optimized but would likely be towards the bottom of the CRDLs, near the connection between the CRDLs and the bundles. This location would allow the CPL to heat up more quickly. A schematic of a possible CPL design is shown in Figure 6-2, and an illustration of such a CPL design in both a latched state and an unlatched state is shown in Figure 6-3.

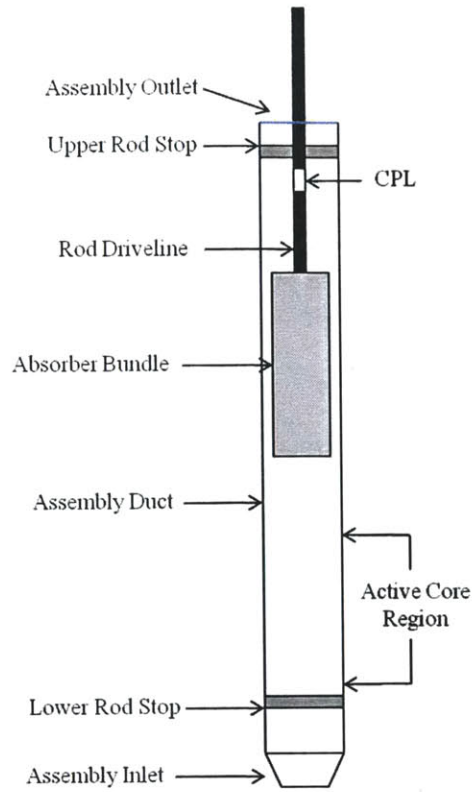


FIGURE 6-2: POSSIBLE CPL DESIGN.

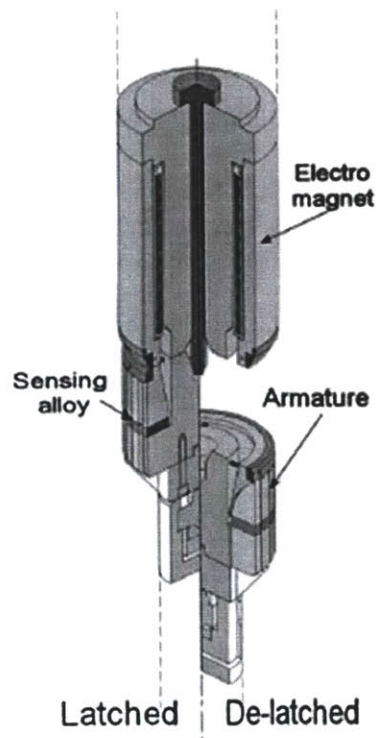


FIGURE 6-3: SCHEMATIC OF A CPL IN A LATCHED AND A DE-LATCHED STATE (43).

6.3 Curie Temperature Selection

A review of the open literature suggests that alloys can be custom-tailored to meet a desired Curie temperature. Japanese researchers have demonstrated that slight changes to an alloy with a Curie temperature of 670 °C can lower the Curie temperature to 630 °C (43) (44). Therefore a designer could select an optimal Curie temperature by analyzing the control assembly axial temperature profile via a systems code like RELAP5-3D during a base case ULOF and UTOP. Representative results are shown in Figure 6-4 and Figure 6-5.

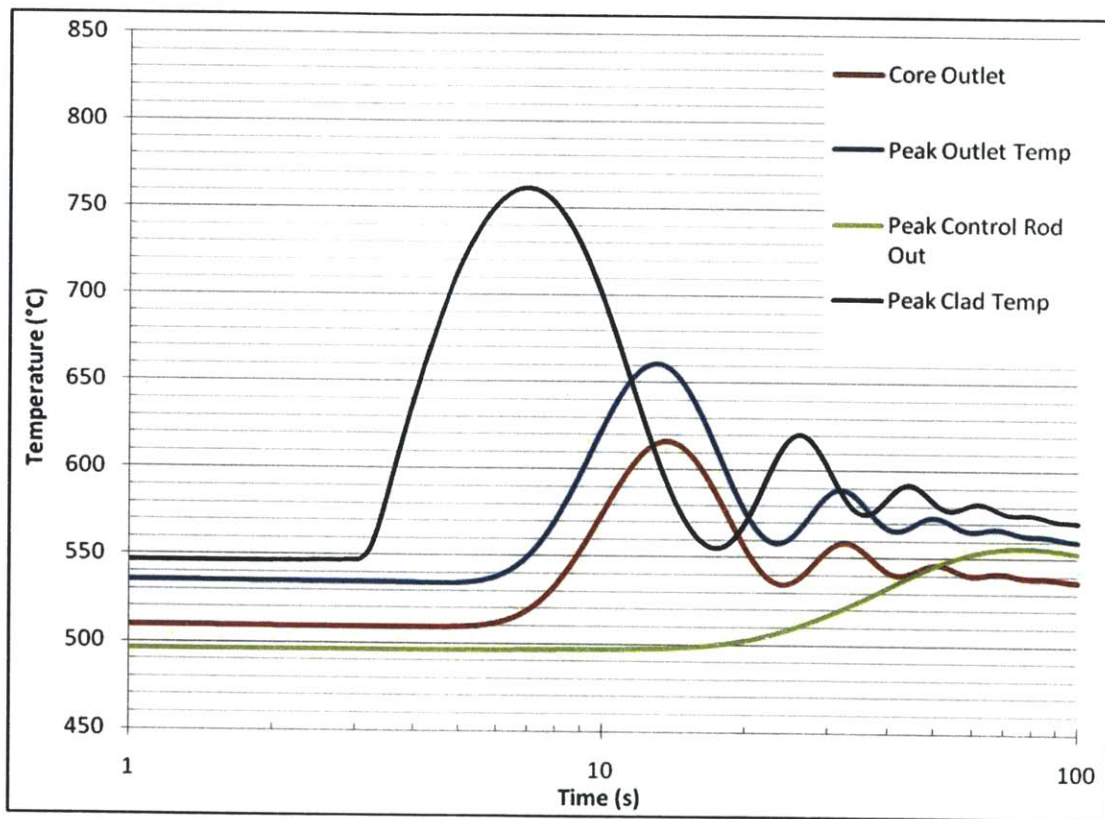


FIGURE 6-4: METAL FUEL ULOF ASSEMBLY OUTLET TEMPERATURES.

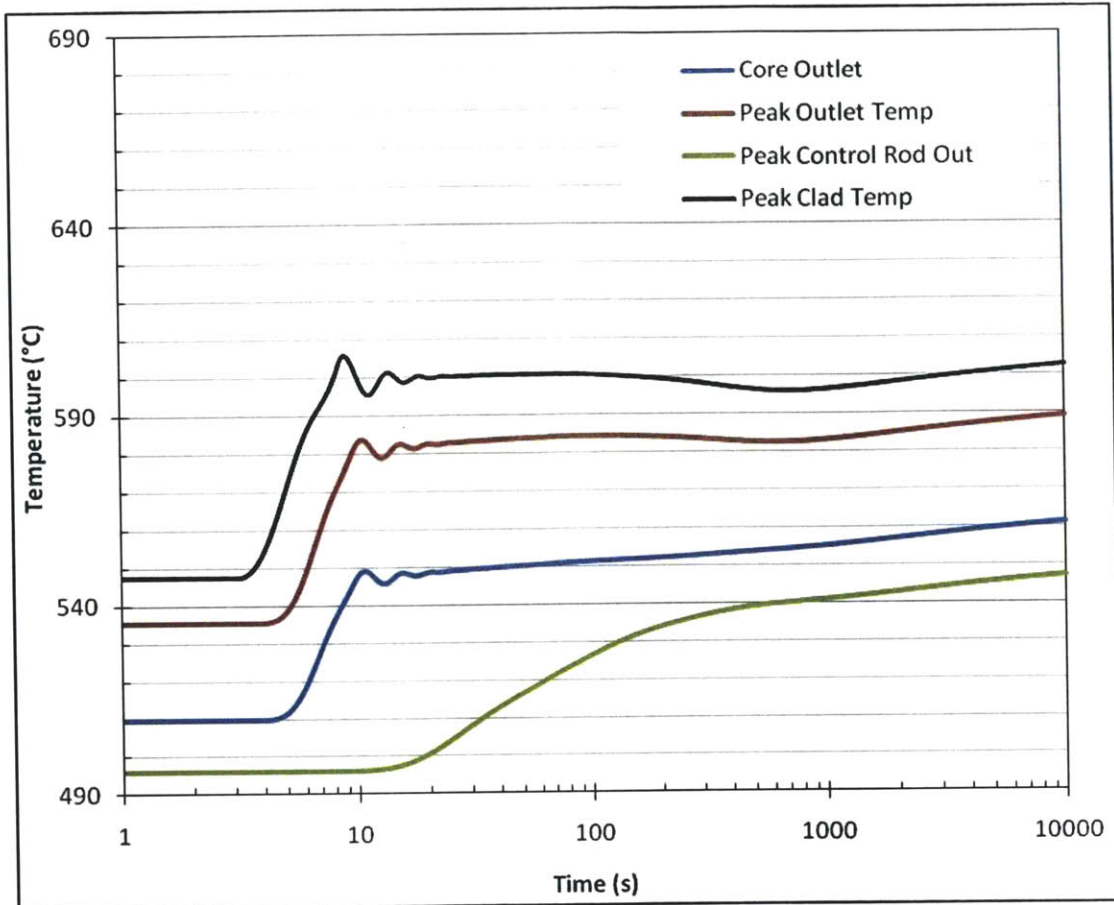


FIGURE 6-5: METAL FUEL UTOP ASSEMBLY OUTLET TEMPERATURES.

The results for this analysis suggest a Curie temperature of 530 °C be selected for the 510 °C core outlet case.

6.4 Unprotected Loss of Flow Performance for a Metal Core

To model SASS performance and calculate the reliability of Curie point latches, the uncertainty analysis methodology described in Chapter 2 was used with RELAP5-3D to model plant performance. This methodology determines transient performance by simulating a large number of cases ($N > 100$) with varying reactor feedback parameters which are randomly and independently sampled from defined probability distribution functions to generate each input for a given transient. Therefore, the sample set spans the uncertainty ranges associated with the feedback parameters. Recall that the parameters sampled were (numerical values are listed in Chapter 2):

- Doppler coefficient
- Axial expansion coefficient
- Sodium density coefficient
- Core radial expansion coefficient
- Control rod driveline expansion coefficient

Next, the CPL was placed on the secondary control rod bank and set to actuate at a mean value of 530 °C, meaning that the latch material would reach its Curie point when the CPL reached 530 °C in the control assembly duct. At 530 °C, the latch would lose its holding strength, dropping the rods into the core at an acceleration of 21.6 cm/s². A 1.5 s delay between the time the sodium surrounding the CPL reaches 530 °C and CPL actuation was implemented as a margin to account for uncertainty in CPL heat up (41) (44). This results in the reactivity insertion shown in Table 6-1, assuming the most reactive rod does not insert.

TABLE 6-1: TIME-DEPENDENT REACTIVITY INSERTION FOLLOWING CURIE POINT ACTIVATION FOR A METAL CORE.

Time (s)	Rho (\$)
0.0	0.0
1.5	0.0
2.0	-0.15
2.5	-1.0215
3.0	-3.9
3.5	-6.7

To account for uncertainty in the Curie temperature, a normal distribution with a mean of 530 °C and standard deviation of 5 °C was defined as the probability density function of the Curie temperature to account for the epistemic uncertainty of the Curie temperature of the latch material (46) (47). This distribution was subsequently sampled randomly to generate the Curie temperature for each simulation.

SFR designers often incorporate a pump coastdown system to maintain reduced coolant flow during a loss of flow transient, thus avoiding a sudden and almost instantaneous flow seizure (34) (21) (33). This reduces the thermal stresses imparted on the core structures and other vessel components. The magnitude of the pump coastdown is often described with the time it takes the flow to decrease to 50% full flow, referred to as the “flow-halving time.” This value is design-dependent and varies for different fuel types (it is typically larger for oxide cores), and designers may select from a range of flow-halving times. To analyze the effects of different flow-halving times, four values that span a range commonly found in literature were selected and simulations were performed for each case. These values are shown in Table 6-2.

TABLE 6-2: FLOW-HALVING TIMES FOR A METAL CORE.

Case	Pump Coastdown – Flow-halving time (s)
1	0
2	3
3	5
4	8

The results of the simulations are shown in Figure 6-6 through Figure 6-9:

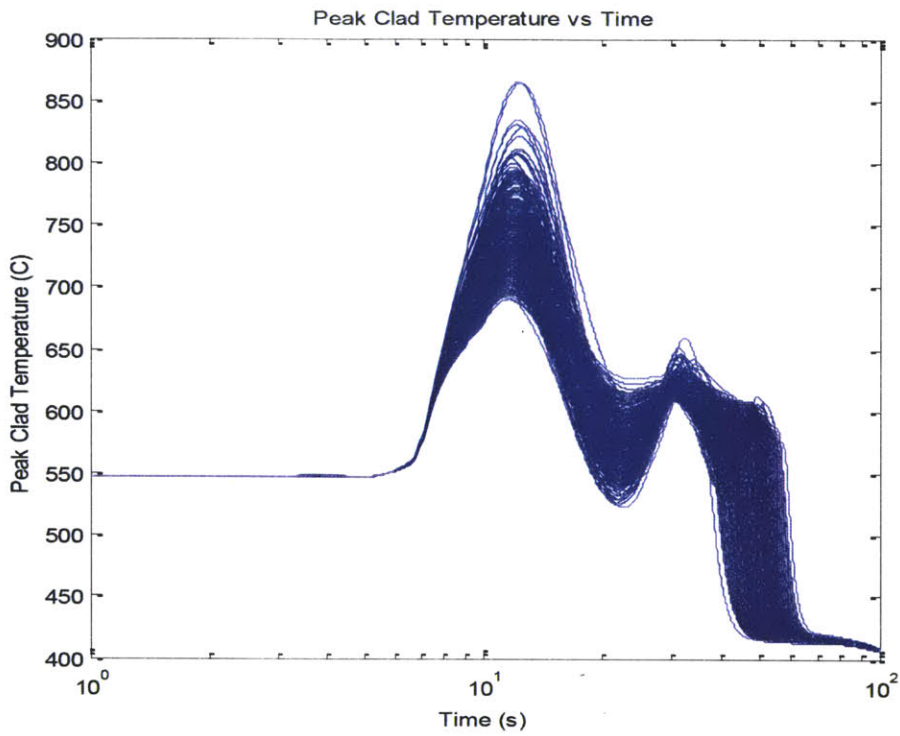


FIGURE 6-6: CPL PERFORMANCE FOR A ULOF WITH INSTANTANEOUS FLOW SEIZURE (METAL CORE).

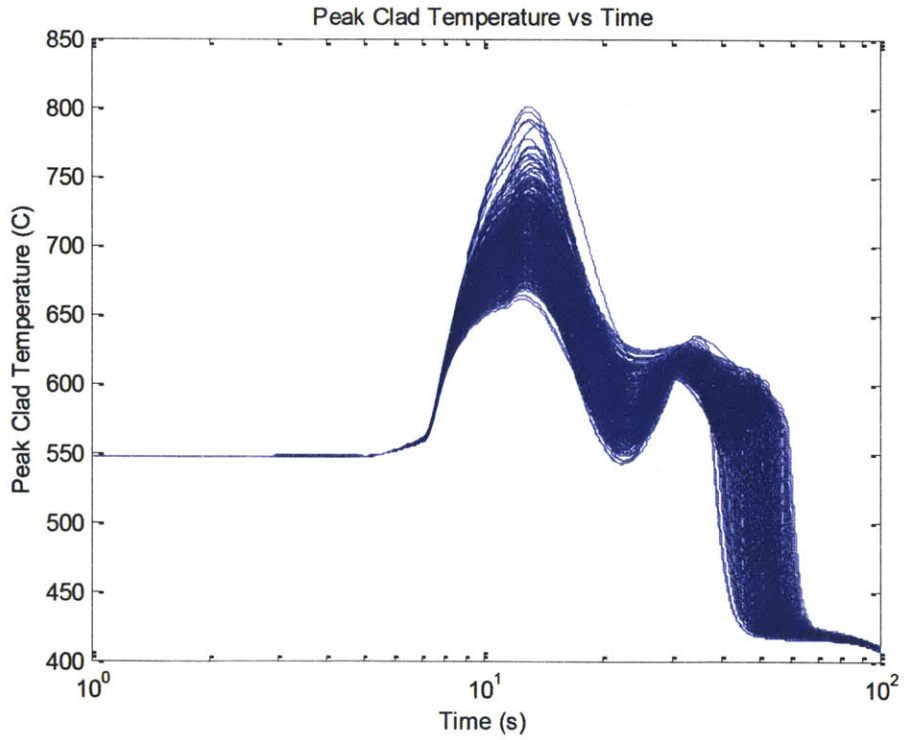


FIGURE 6-7: CPL PERFORMANCE FOR A ULOF WITH A 3 SECOND FLOW-HALVING TIME (METAL CORE).

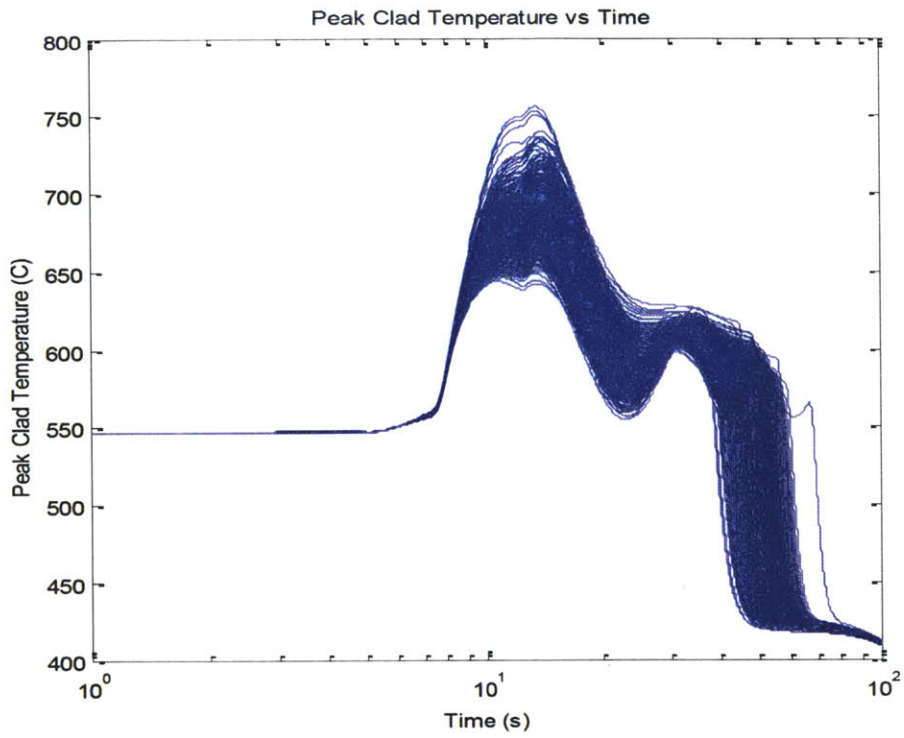


FIGURE 6-8: CPL PERFORMANCE FOR A ULOF WITH A 5 SECOND FLOW-HALVING TIME (METAL CORE).

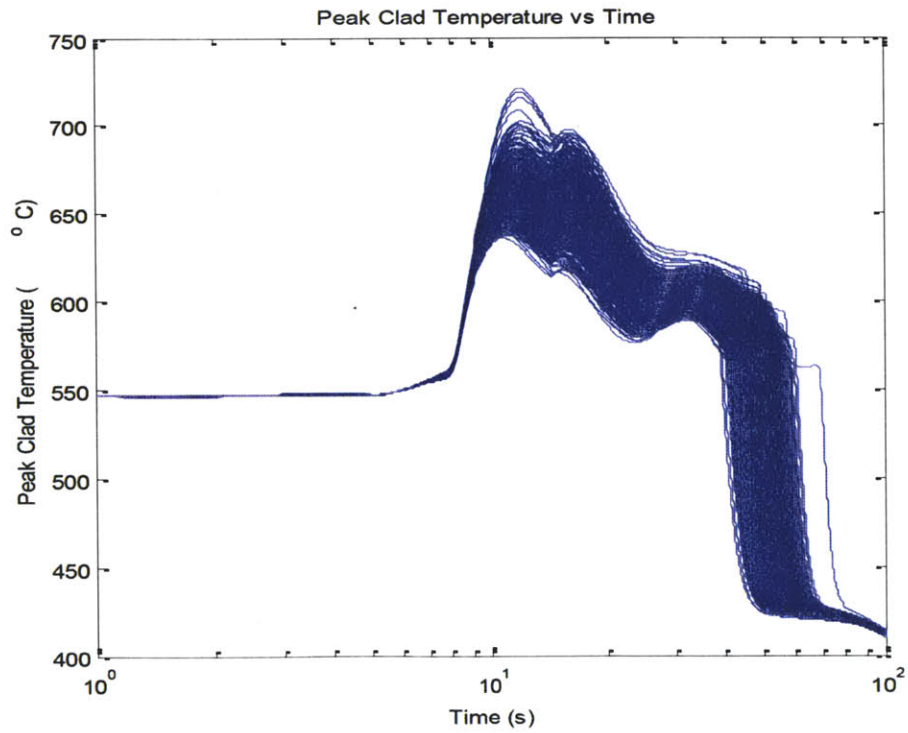


FIGURE 6-9: CPL PERFORMANCE FOR A ULOF WITH AN 8 SECOND FLOW-HALVING TIME (METAL CORE).

The reliability of the CPL given a particular demand is the ratio of successful simulations to total simulations, shown in Equation (10):

$$P(\text{success}|\text{demand}) = \frac{\sum_i^N w_i N_{\text{success},i}}{\sum_i^N (w_i N_{\text{success},i} + w_i N_{\text{fail},i})} \quad (10)$$

The Curie point mechanism is deemed successful if the peak cladding temperature does not exceed 750° C, which can be considered a conservative approximation to cladding failure temperature (48) (49) (50) (51) (52).

The results of this analysis are provided in Table 6-3. Initial reviews of the results suggest the CPL performs well at limiting cladding damage during a LOF, however closer inspection reveals the Curie point latch fails to engage quick enough to mitigate the consequences of the ULOF for almost all cases. Instead the inherent feedbacks shut the reactor down. Comparing the reliability of the inherent mechanisms to the improvements offered by the Curie point latch, it is clear that the performance improvement offered by the CPL is minor, especially when the high reliability of the active scram system is considered. Furthermore, adding a coastdown system also has a substantial affect on mitigating cladding damage.

TABLE 6-3: CPL ULOF RESULTS FOR A METAL CORE.

Case	Pump Coastdown – Flow-halving time (s)	Conditional Cladding Failure Probability
1	0	0.4850
2	3	0.0522
3	5	0.0036
4	8	$\ll 1.0 \times 10^{-5}$

6.5 Unprotected Loss of Flow Performance for an Oxide Core

To model CPL performance and calculate CPL reliability during a LOF in an oxide core, the previously described methodology was employed. The same reactor feedback

parameters were randomly and independently sampled from defined probability distribution functions, this time set to oxide core values.

Again, the Curie point latch was placed on the secondary control rod bank and set to actuate at a mean value of 530 °C (the same value was employed for the oxide core as the metal core because the axial temperature profiles of the coolant are nearly identical) after 1.5 s delay. The resulting reactivity insertion is modeled with the values provided in Table 6-4.

TABLE 6-4: TIME-DEPENDENT REACTIVITY INSERTION FOLLOWING CURIE POINT ACTIVATION FOR AN OXIDE CORE.

Time (s)	Rho (\$)
0.0	0.0
1.5	0.0
2.0	-0.130
2.5	-0.884
3.0	-3.4
3.5	-5.8

As done in the metal core analysis, the uncertainty in the Curie temperature was accounted for by a normal distribution with a mean of 530 °C and standard deviation of 5 °C. This distribution was subsequently sampled randomly to generate Curie temperature for each simulation.

The pump coastdown values used for each case are shown in Table 6-5. These values are greater than those used for the metal core to accommodate the oxide fuel's larger heat capacity and smaller thermal conductivity, meaning that the oxide stores significantly more energy than the metal fuel and releases it more slowly. This necessitates a longer coastdown to ensure proper heat removal (33) (34) (14).

TABLE 6-5: FLOW-HALVING TIMES FOR AN OXIDE CORE (33) (34) (14).

Case	Pump Coastdown – Flow-halving time (s)
1	0
2	5
3	10
4	20

The simulation results are shown in Figure 6-10 through Figure 6-13:

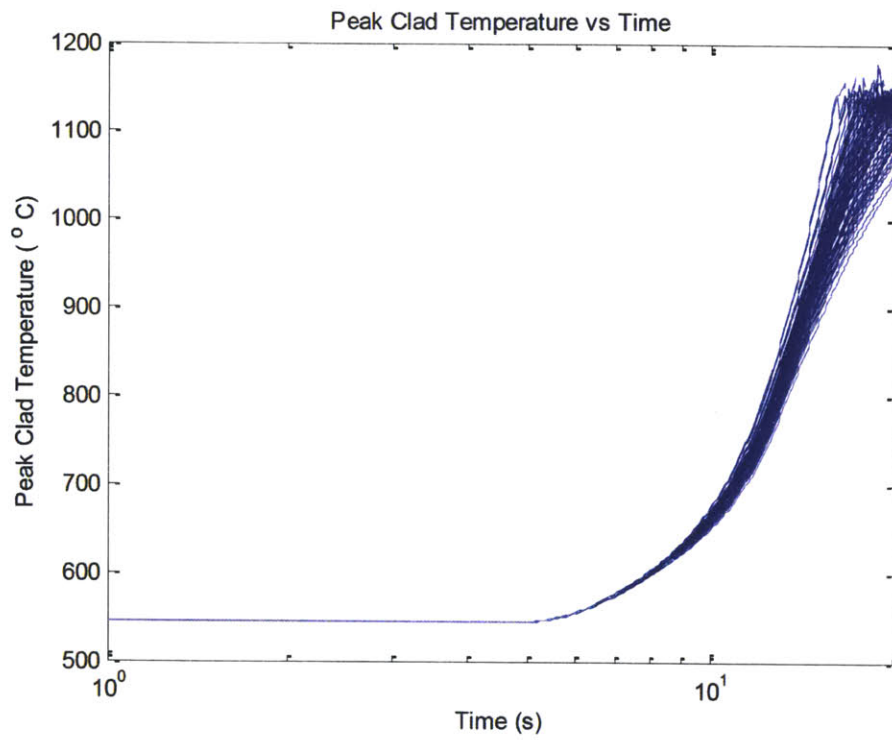


FIGURE 6-10: CPL PERFORMANCE FOR A ULOF WITH INSTANTANEOUS FLOW SEIZURE (OXIDE CORE).

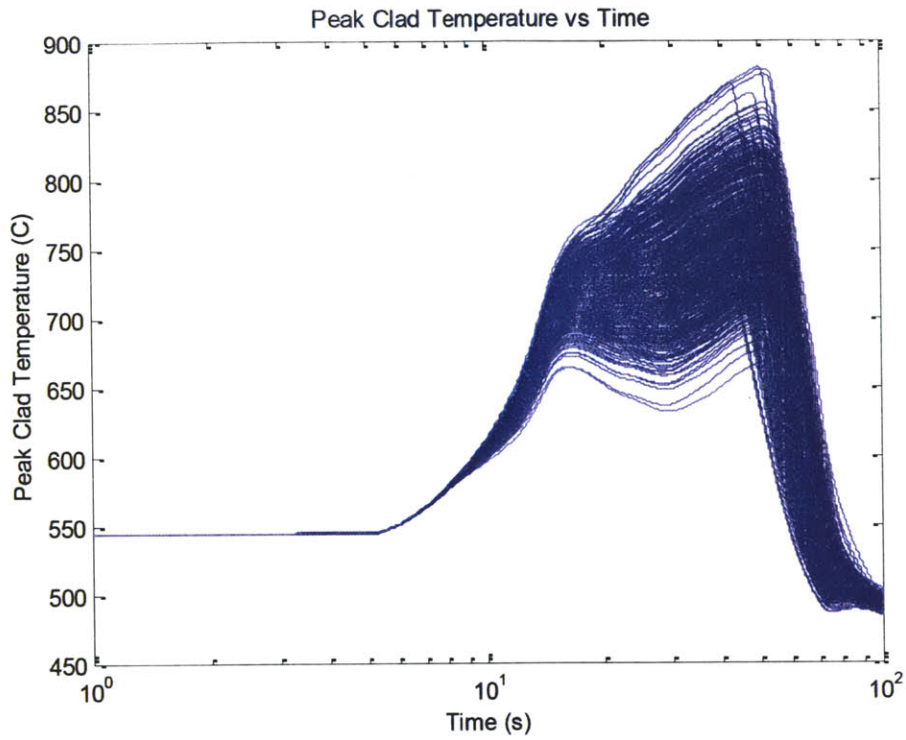


FIGURE 6-11: CPL PERFORMANCE FOR A ULOF WITH A 5 SECOND FLOW-HALVING TIME (OXIDE CORE).

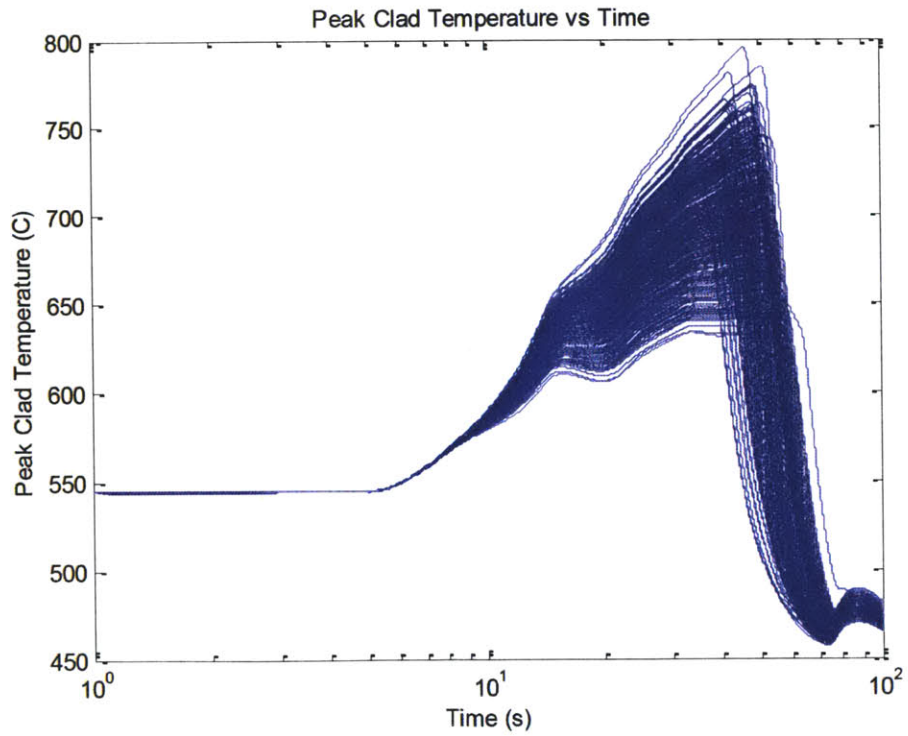


FIGURE 6-12: CPL PERFORMANCE FOR A ULOF WITH A 10 SECOND FLOW-HALVING TIME (OXIDE CORE).

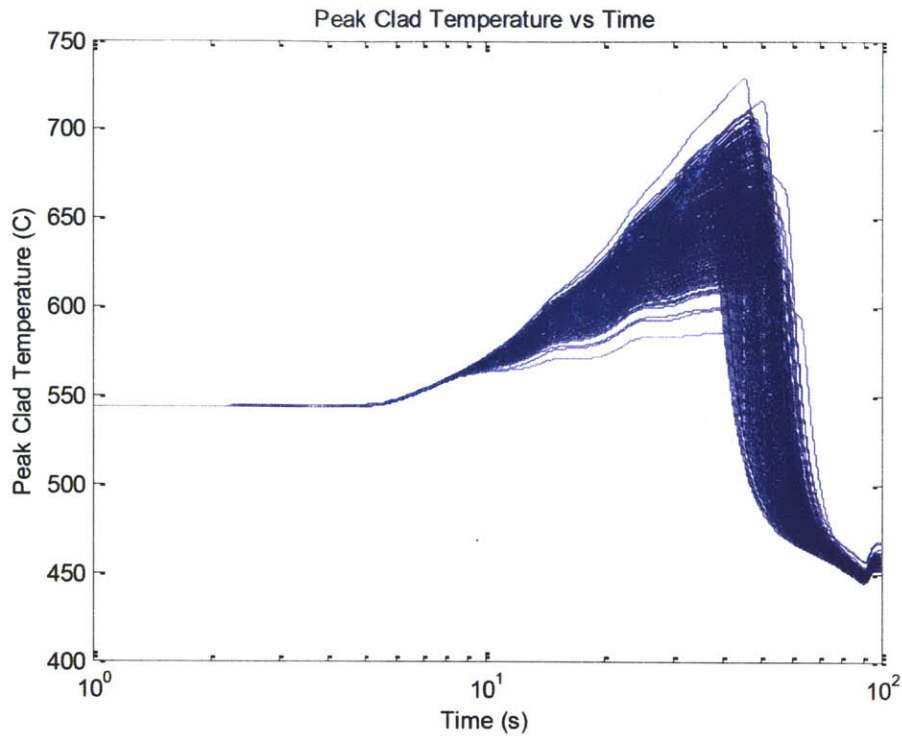


FIGURE 6-13: CPL PERFORMANCE FOR A ULOF WITH A 20 SECOND FLOW-HALVING TIME (OXIDE CORE).

The reliability of the CPL given a particular demand is again calculated using Equation 10, and the CPL is deemed successful if the peak cladding temperature does not exceed 800 °C.

The results of this analysis are provided in Table 6-6. The results indicate a CPL is severely challenged by an oxide core without coastdown; however a CPL offers substantial mitigation potential to more ULOF cases having longer coastdown rates. Comparing the performance between metal cores and oxide cores, the CPL is much more effective in oxide cores, since the inherent feedback mechanisms in the metal core are strong enough to preempt the CPL.

TABLE 6-6: CPL ULOF RESULTS FOR AN OXIDE CORE.

Case	Pump Coastdown – Flow-halving time (s)	Conditional Cladding Failure Probability
1*	0*	~1.000*
2	5	0.4942
3	10	$\ll 1.0 \times 10^{-5}$
4	20	$\ll 1.0 \times 10^{-5}$

* Sodium boiling occurs in this case, causing RELAP to fail so the cladding is assumed to fail whenever sodium boiling occurs.

6.6 Unprotected Transient Overpower Performance for a Metal Core

As described in Chapter 4, UTOPs initially result in an elevated core power (>100%), creating a power to flow mismatch that causes the primary sodium pool to heat up. If the CPL does not actuate before the primary sodium pool heats up to 535 °C, the primary coolant pumps will trip to prevent burnout. At this point, coolant flow will coastdown, initiating a ULOF.

It should be mentioned that the pump trip temperature varies with pump design – EM pumps may have a lower trip point than centrifugal pumps – and therefore the trip temperature varies with reactor design so a designer will select the technology depending on their specific goals and requirements. For this study, the trip point of 535 °C is used (5).

The same methodology used to analyze CPL performance in a ULOF was also used to analyze CPL performance in a UTOP. The results are shown in Figure 6-14. Analyzing these results indicate the CPL does not actuate until the pumps trip, and again the inherent feedback mechanisms shut the reactor down before the CPL actuates, reducing the impact of the CPL on mitigating cladding damage. Quantitatively, the CPL yields a conditional cladding damage probability of 0.2312 given a UTOP.

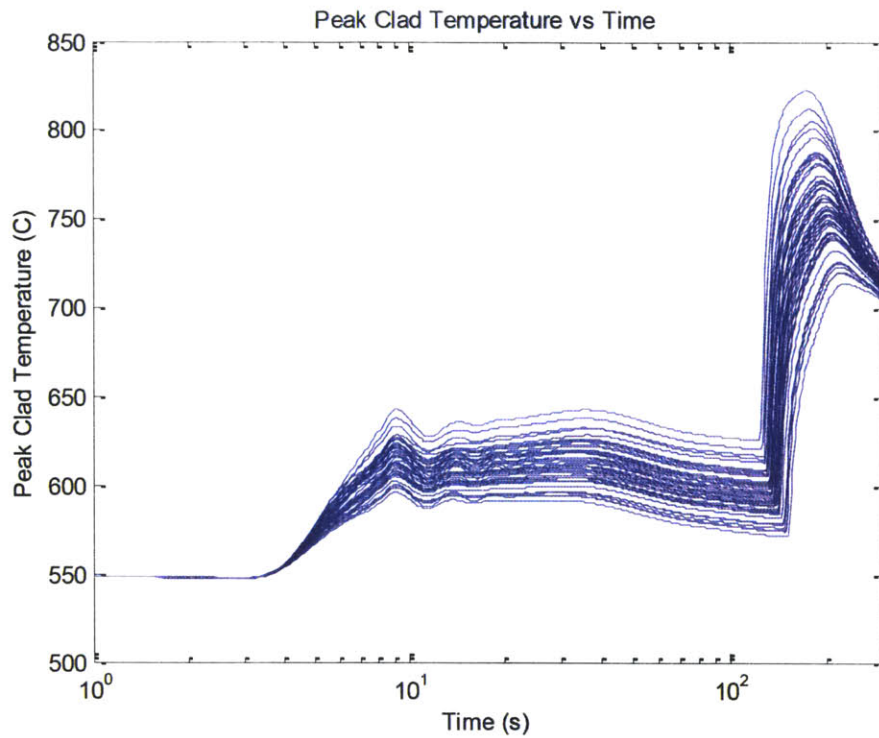


FIGURE 6-14: CPL PERFORMANCE FOR A UTOP (METAL FUEL).

6.7 Unprotected Transient Overpower Performance for an Oxide Core

The same methodology employed to analyze CPL performance during a UTOP in a metal core was employed to analyze CPL performance during a UTOP in an oxide core. The same plant parameters were used, and the results are shown in Figure 6-15. The CPL yields a conditional cladding damage probability of approximately unity given a UTOP, and is generally ineffective at mitigating cladding damage during a UTOP in an oxide core due in large part to the overall severity of a UTOP in an oxide core.

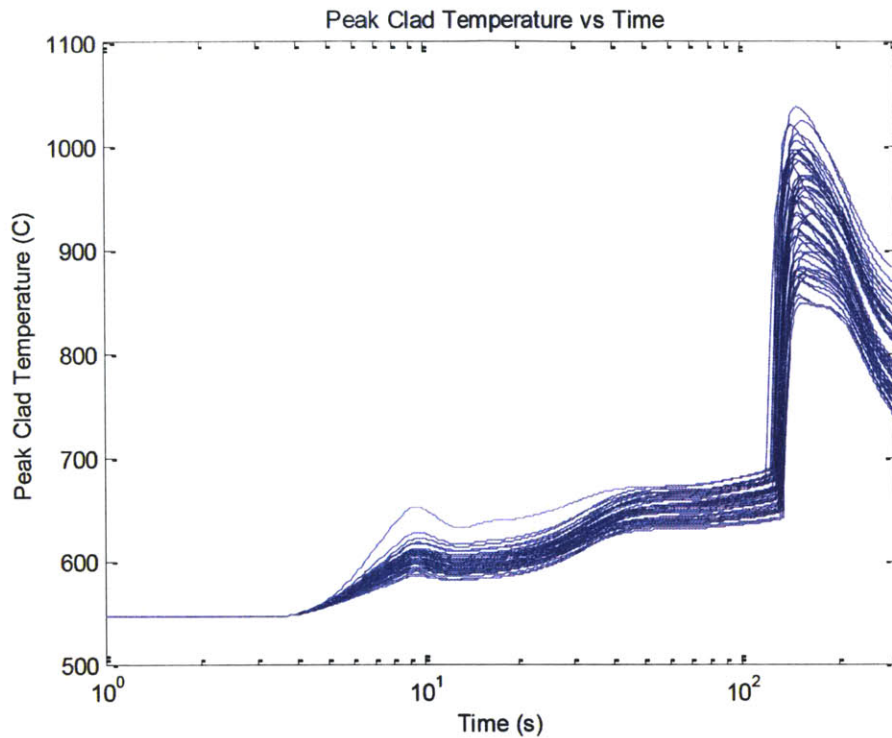


FIGURE 6-15: CPL PERFORMANCE FOR A UTOP (OXIDE CORE).

6.8 Potential Design Improvements

The results of the CPL performance analysis suggest that the CPL design analyzed responds too slowly to effectively mitigate ULOFs and UTOPs in metal cores. This can be partially explained by examining the different temperature profiles in Figure 6-4 and Figure 6-5. The control rod duct temperature response lags behind the hot assembly and core outlet temperature responses by over 50 seconds during a ULOF and over 100 seconds during a UTOP. Placing the CPL higher on the latch so it is exposed to the bulk core outlet temperature may enable the CPL to respond more quickly during a transient. This proposed design is illustrated in Figure 6-16.

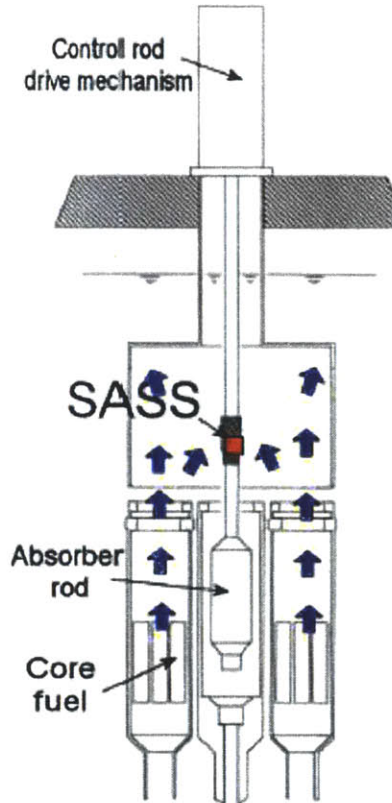


FIGURE 6-16: PROPOSED CPL PLACEMENT IN CORE OUTLET PATH.

Since the core outlet temperature is 12 °C hotter than the control rod assembly temperature during steady state, the CPL activation temperature was increased to 542 °C. The same analysis procedure was performed for a ULOF and a UTOP for both a metal core and an oxide core. Characteristic flow-halving times of 3 and 10 seconds were selected for the metal core and oxide core respectively (14) (33). The simulation results are shown in Figure 6-17 through Figure 6-20.

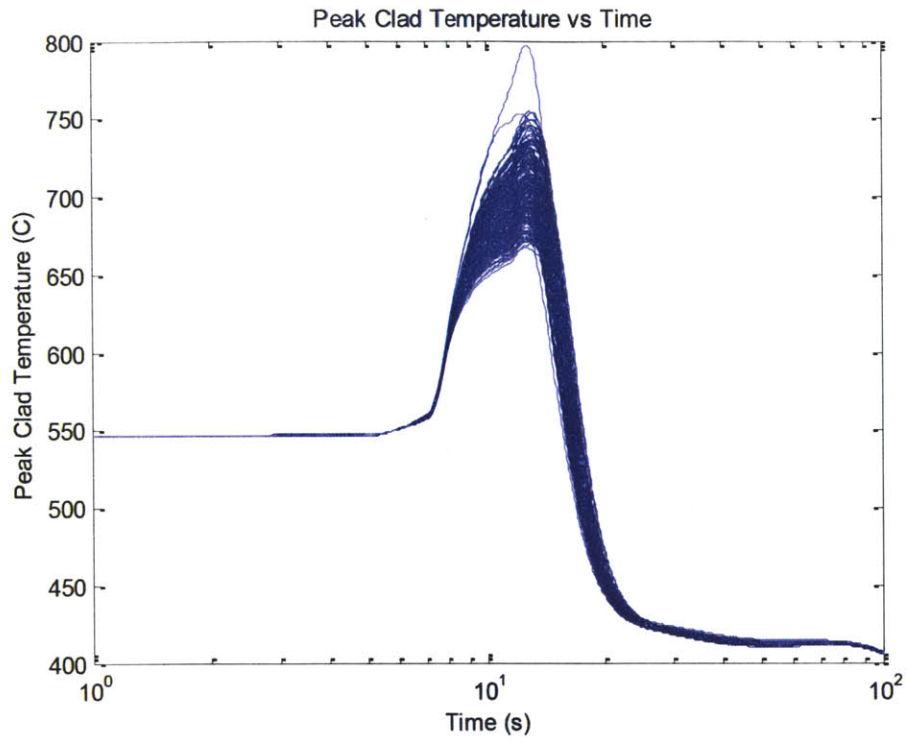


FIGURE 6-17: MODIFIED CPL PERFORMANCE DURING A ULOF (METAL CORE).

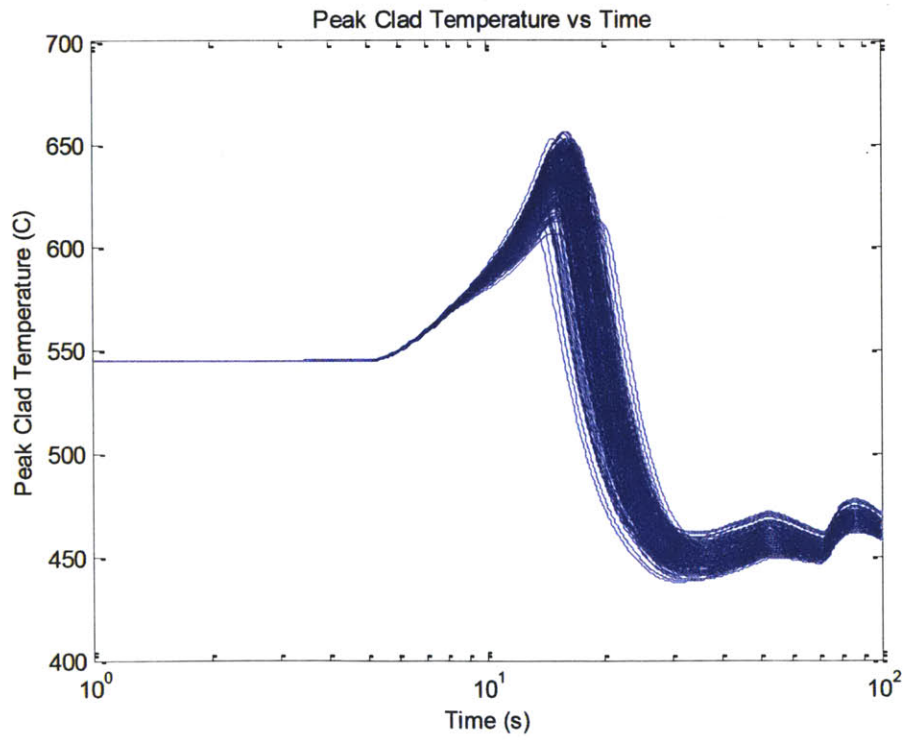


FIGURE 6-18: MODIFIED CPL PERFORMANCE DURING A ULOF (OXIDE CORE).

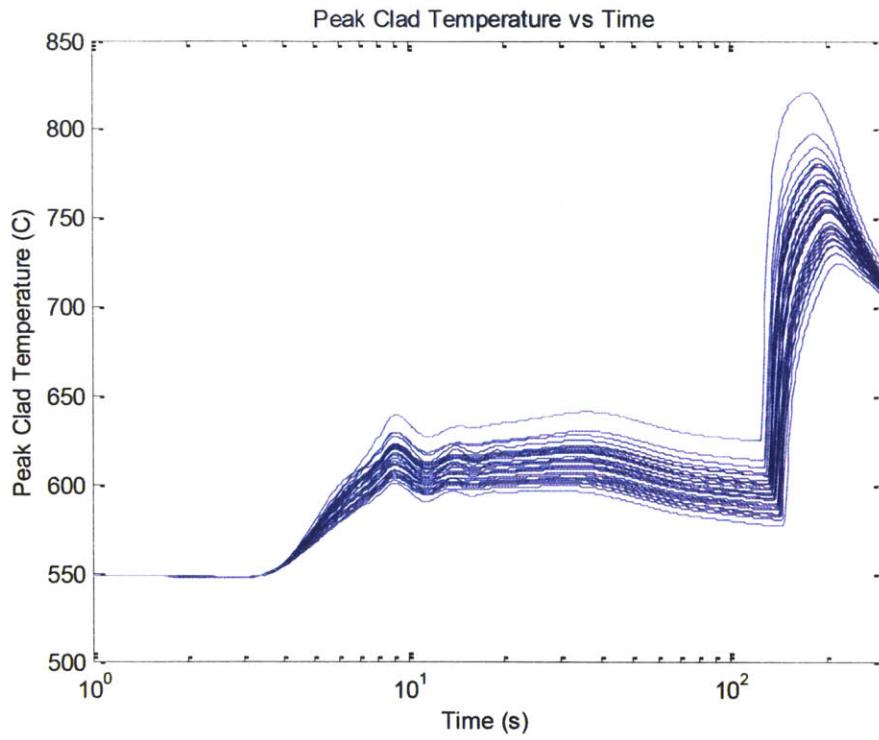


FIGURE 6-19: MODIFIED CPL PERFORMANCE DURING A UTOP (METAL CORE).

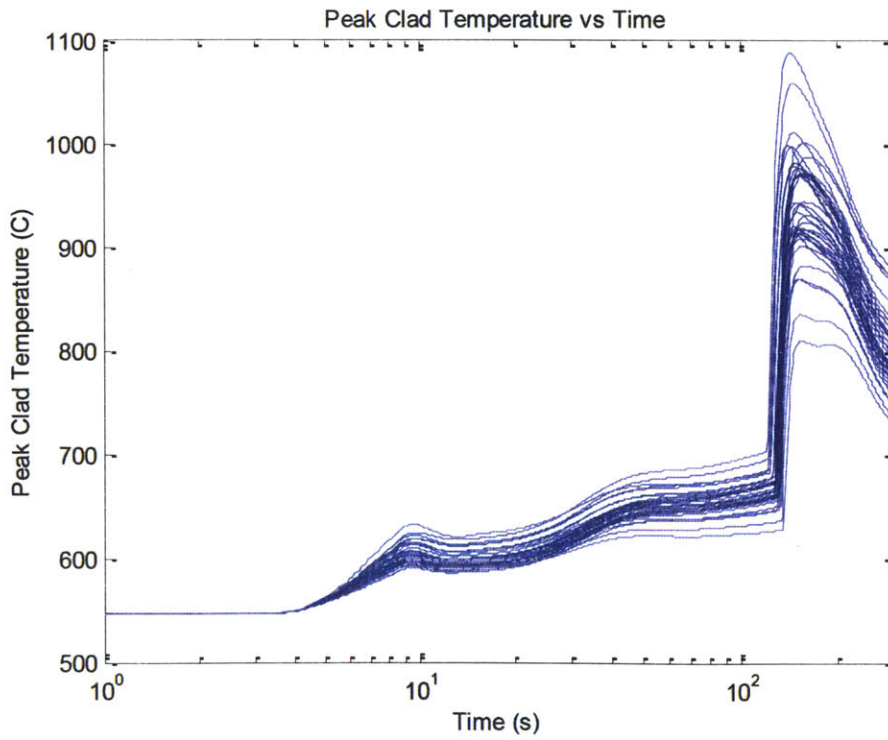


FIGURE 6-20: MODIFIED CPL PERFORMANCE DURING A UTOP (OXIDE CORE).

Applying the same failure models as used previously in this chapter yield the results provided in Table 6-7.

TABLE 6-7: CPL DESIGN MODIFICATION PERFORMANCE RESULTS.

Transient and Fuel Type	Conditional Probability of Cladding Failure Given Unprotected Transient
ULOF – Metal Fuel	6.7074×10^{-5}
ULOF – Oxide Fuel	$\ll 1.0 \times 10^{-5}$
UTOP – Metal Fuel	0.2684
UTOP – Oxide Fuel	~ 1.000

6.9 Impact on Reactor Operations

CPLs are being studied in Japan (where oxide fuel is the norm), and the preliminary results from that research confirms the general feasibility of CPLs for use in SFRs (44). Alloys with Curie points in the temperatures of interest in SFRs have been identified. Thermal and irradiation testing is in progress to determine if any hysteresis occurs over time (44). The technical constraints that may limit Curie point latches are: their useful lifetime; and how exactly the material’s Curie temperature changes with time due to radiation and thermal exposure. Experimental results from the JAEA suggest no significant changes occur, but full-scale in-pile testing remains to be conducted. Nonetheless, the JAEA designers pose a lifetime fluence limit at $6.0 \times 10^{18} \text{ n/cm}^2 > 0.1 \text{ MeV}$ (44) (47).

With regard to safety, CPLs do not introduce any safety concerns beyond the issue of spurious actuation. CPLs may accidentally release the rods into the core due to abnormal behavior, scrambling the reactor. An unanticipated scram would stress the plant in a negative way that may cause thermal shocks to the reactor systems, and reduce the plant’s capacity factor substantially (32) (53). Ideally, CPLs will not affect steady state operation, and will have a low probability of accidental operation. These requirements may be met if Curie point materials successfully satisfy rigorous testing regimes (44). Furthermore, while the CPL does not perform as well if placed on the driveline in the control assembly flow path, it will be

exposed to fewer thermal transients at that location as opposed to if it were placed on the driveline in the bulk core outlet (45). This is one drawback to placing the CPL in the bulk core outlet flow, and may force the designer to apply a higher actuation temperature to the CPL to enhance margin. One other issue is the feasibility of periodic in-situ testing since this would require a short period of excessively high core outlet temperatures.

6.10 Economic Analysis and Results

CPLs are rather inexpensive with only the material and manufacturing costs driving the price. When compared to the estimated cost of the control rod drives, \$10 million (1994 \$), or 1.3% of the total plant cost (54) (55), it is unlikely CPLs will reduce total plant cost by a significant amount since the control rod drives would still be required for the primary rods, and would likely be required for the smaller number of secondary rods with the CPLs as well.

It should also be mentioned that a detailed in-situ testing program would need to be developed to verify and validate consistent Curie point operability over the life of the plant (6). Such a program would likely require that the CPLs be taken out of the vessel periodically and have operability tested to ensure proper function so the plant operator could take credit for them as safety systems.

6.11 Summary

CPLs offer a way to enhance RPS diversity by introducing a passive scram actuation signal. While their performance improvement in metal cores is minor compared to the performance of the inherent feedback mechanisms in shutting the reactor down during unprotected transients, CPLs are more effective at mitigating cladding damage in oxide cores where the inherent feedbacks are not as strong. CPL performance can also be enhanced by altering the placement on the driveline so the CPLs are exposed to different temperature profiles, e.g. placing the CPLs on the driveline so they are exposed to the bulk core outlet

flow. Any changes in placement, however, must not compromise CPL margin to spurious actuation. Success is also dependent on having a sufficiently long pump coastdown time. More testing and analysis is needed to verify CPL durability and robustness, but considering the high reliability of the active RPS, CPLs do not offer a convincing cost-benefit justification without a strong external driver such as regulator requirements to satisfy further defense-in-depth.

7 Flow Levitated Absorber Performance

7.1 Introduction

Flow levitated absorbers (FLA) are control materials designed into a shape having a large drag coefficient so that the material is suspended by the coolant flow (56). A simplified schematic of a potential design is shown in Figure 7-1. As mentioned in Chapter 6, a scram in an SFR is a dramatic event that can decrease the lifetime of in-core components due to thermal shock, so preventing inadvertent actuation of the FLAs is desirable. Therefore, FLAs should be designed with a margin between full coolant flow and the flow rate at which the coolant can no longer suspend the absorber. Literature recommends an actuation flow rate of 40% of full flow to account for this margin (56).

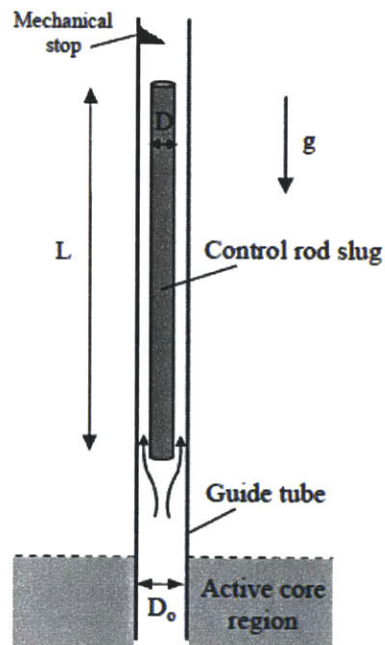


FIGURE 7-1: SIMPLIFIED SCHEMATIC OF AN FLA.

In order to maximize the amount of absorber material contained in the FLAs while engineering enough drag into the absorber bundles, a tradeoff must be achieved between the two competing effects. There are several ways to balance these factors: incorporating a drag

plate at the top or bottom of the control rod; fabricating the absorber material as many small spheres; or manufacturing the absorber material as annular plates among other options (56) (39). Each of these designs can achieve the desired results, so it is up to the designer's discretion as to which option is selected.

7.2 System Design Description

For this analysis, the flow rate through the control assemblies is not altered, and the mass of the absorber material contained in the reference control rod design is conserved. It should be noted that a designer may wish to increase the flow rate to accommodate a larger absorber mass, but the consequences on thermal hydraulic, neutronic, and material performance of this decision must be considered. No specific drag-enhancing design was selected since those specifics do not affect shutdown performance, and proof of concept was demonstrated in previous literature (56). A set point of 40% full flow was selected as the point when the absorber begins to descend into the core. The performance of the FLAs was analyzed with RELAP5-3D for both a metal core and an oxide core. The following sections discuss the results.

7.3 Unprotected Loss of Flow Performance for a Metal Core

To model the performance of and calculate the reliability of FLAs during a loss of flow event, the uncertainty analysis methodology described in Chapter 2 was used with RELAP5-3D to model plant performance for a metal core. This methodology determines transient performance by simulating a large number of cases ($N > 100$) with varying reactor feedback parameters which are randomly and independently sampled from defined probability distribution functions to generate each input for a given transient. Therefore, the sample set spans the uncertainty ranges associated with the feedback parameters (as noted in Chapter 2). The parameters sampled were:

- Doppler coefficient
- Axial expansion coefficient
- Sodium density coefficient
- Core radial expansion coefficient
- Control rod driveline expansion coefficient

The FLAs were placed on the secondary control rod bank and set to actuate at 40% full flow, meaning that the absorber material would drop into the core. This results in the reactivity insertion shown in Table 7-1.

TABLE 7-1: FLA REACTIVITY INSERTION TABLE FOR A METAL CORE.

Time (s)	Rho (\$)
0.0	0.0
1.5	-0.15
2.0	-1.0215
2.5	-3.9
3.0	-6.7

Finally, as with the CPL analysis, separate simulations were performed for the case of different pump coastdown rates as shown in Table 7-2.

TABLE 7-2: FLOW-HALVING TIMES FOR A METAL CORE.

Case	Pump Coastdown – Flow-halving time (s)
1	0
2	3
3	5
4	8

The results are shown in Figure 7-2 through Figure 7-5. Note the results are bunched more tightly together than what was seen in the CPL analysis. This is because the FLA shuts the reactor down much more quickly than the CPL (almost immediately) so the temperature

profiles with the FLA are more dependent on the thermophysical and transport properties of the fuel, clad, coolant, and structural materials rather than the reactivity feedbacks; and since the uncertainties in the thermophysical and transport properties are not accounted for, a more narrow spread in temperature profiles is expected.

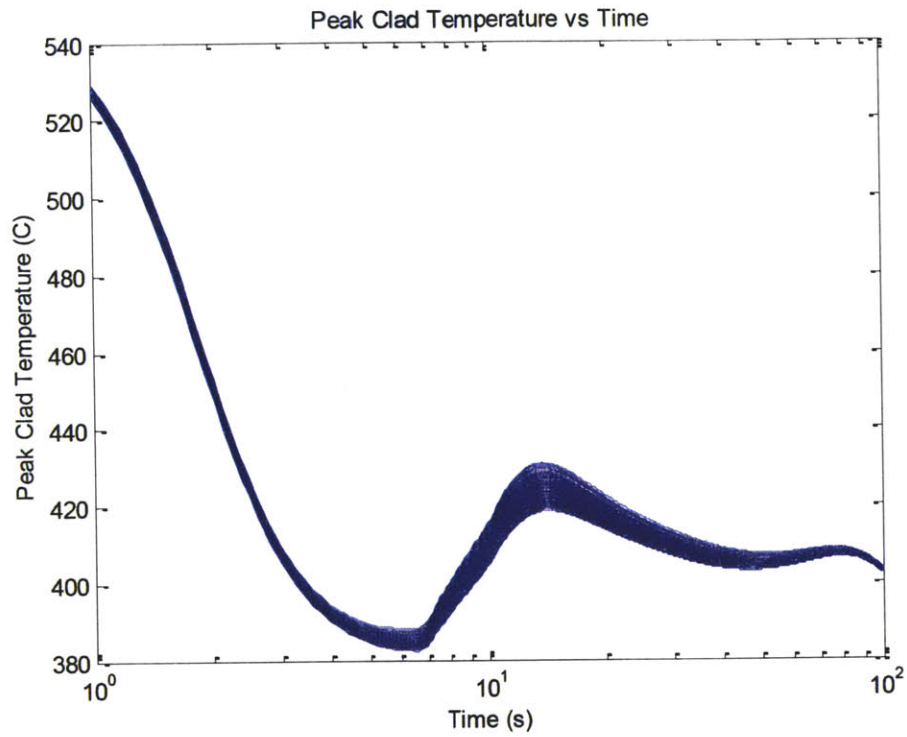


FIGURE 7-2: FLA PERFORMANCE FOR A ULOF WITH INSTANTANEOUS FLOW SEIZURE (METAL CORE).

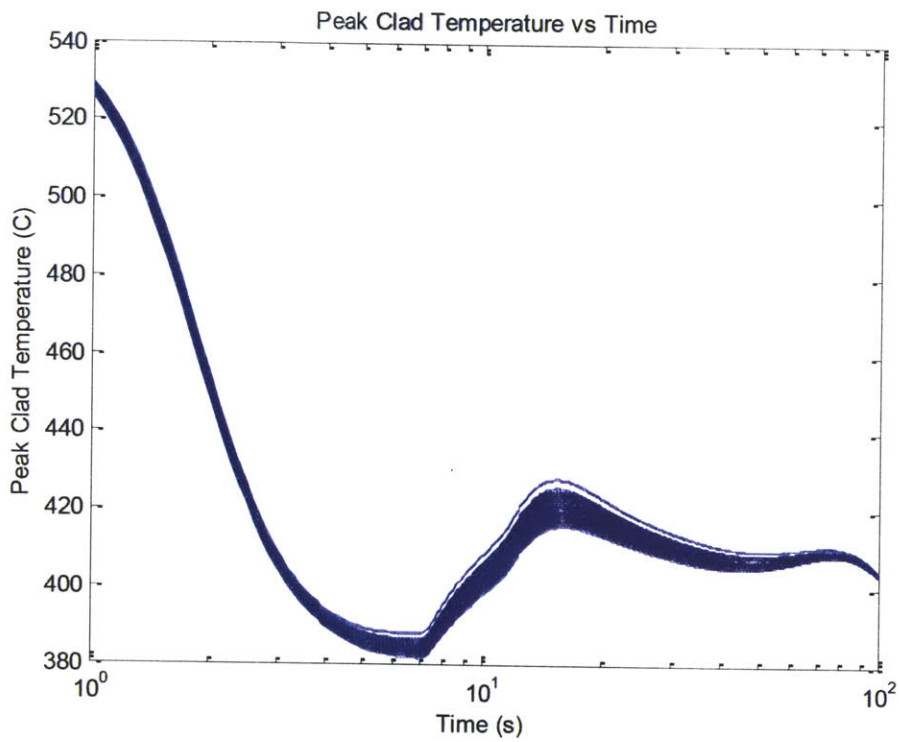


FIGURE 7-3: FLA PERFORMANCE FOR A ULOF WITH A 3 SECOND FLOW-HALVING TIME (METAL CORE).

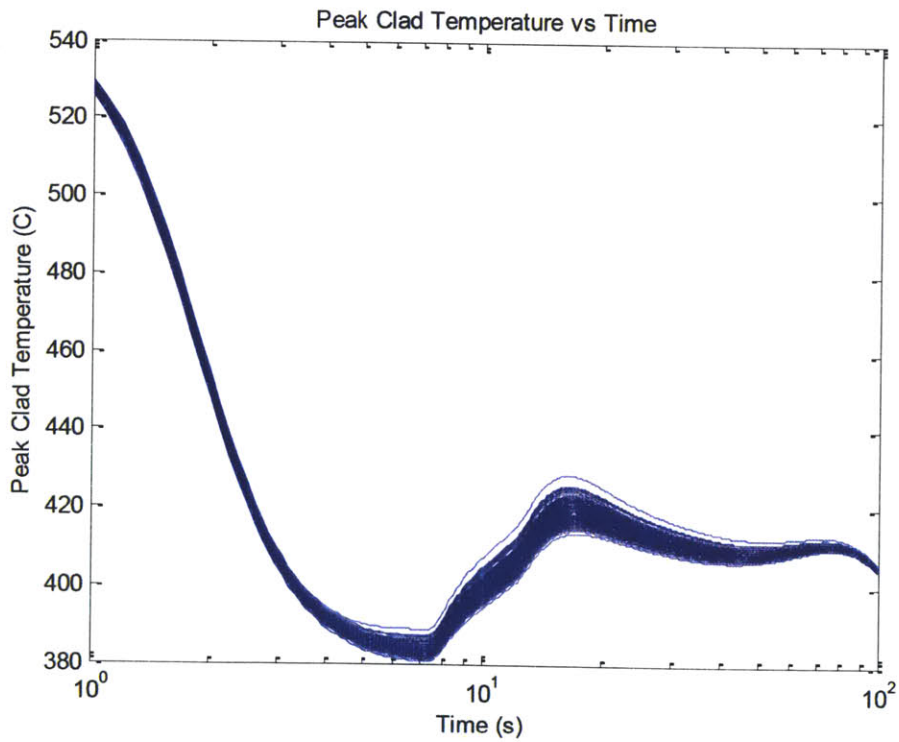


FIGURE 7-4: FLA PERFORMANCE FOR A ULOF WITH A 5 SECOND FLOW-HALVING TIME (METAL CORE).

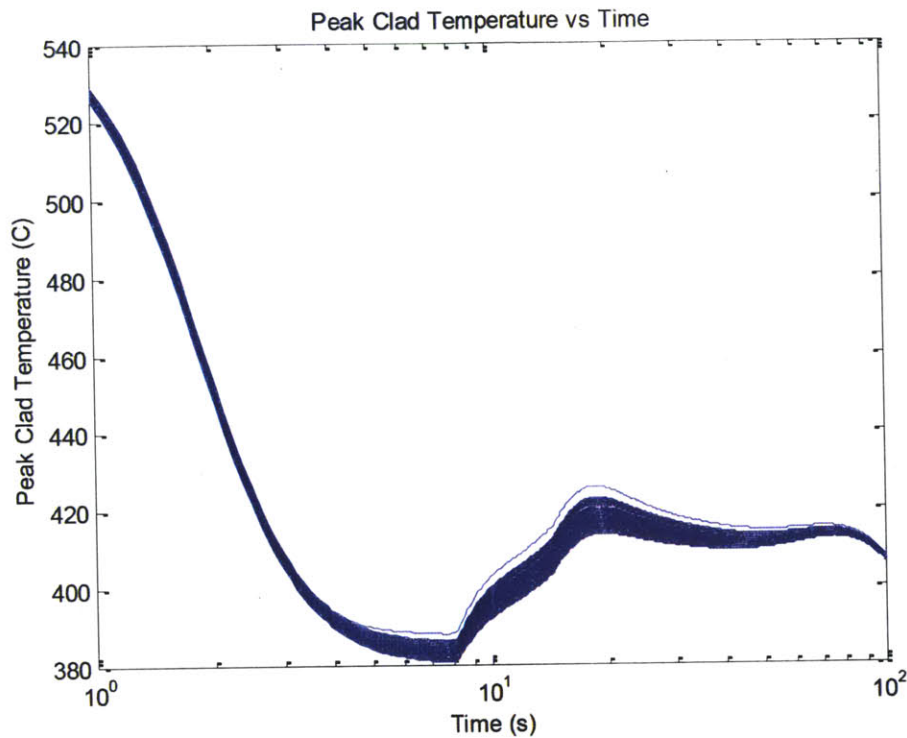


FIGURE 7-5: FLA PERFORMANCE FOR A ULOF WITH AN 8 SECOND FLOW-HALVING TIME (METAL CORE).

Equation 10 was used to calculate the reliability of the FLA given failure occurs when cladding temperatures exceed 750 °C, which can be considered a conservative approximation to failure.

As seen in Figure 7-2 through Figure 7-5, the peak cladding temperature does not exceed 750 °C so no cladding failures are observed. Therefore the results of this analysis show that the FLAs respond almost immediately to a loss of flow, and pump coastdown has no effect on FLA performance, although a longer pump coastdown reduces peak cladding temperature during the transient. In light of these results, the reliability of FLAs is practically unity for internally initiated ULOFs. The rules of probability suggest a passive system like FLAs can never achieve a reliability of unity, since uncertainties in the thermal properties of the coolant, clad, fuel, and structures, combined with the uncertainties in flow patterns, power peaking, clad/fuel eutectic formation, core deformation – to name a few – may lead to an

extremely rare event where the cladding fails. These uncertainties were not accounted for in this analysis since this event would be rare enough to be considered negligible in terms of overall plant performance. Consequently the reliability of FLAs is taken as unity for internally initiated ULOFs.

The dominant failure mode for FLAs is then the physical disruption of absorber insertion, most likely induced by seismic events. This is of particular interest since seismic events are a leading initiator of ULOFs. Therefore the conditional failure probability of FLAs given a ULOF is best calculated as the conditional failure probability of control rods during insertion into reactor core given core deformation during an earthquake. This value is design dependent, and is 1.0×10^{-4} for the ALMR (5). Note this value also applies to active scram systems and CPLs, but was not incorporated in the previous reliability results for those systems. Methods that can reduce rod insertion failure are described in Chapter 8.

7.4 Unprotected Loss of Flow Performance for an Oxide Core

To model FLA performance and reliability during a ULOF in an oxide core, the same analysis methodology was employed. The same sampling parameters were used, just adjusted to oxide fuel values.

Again, the FLAs were placed on the secondary control rod bank and set to actuate at 40% full flow, meaning that the absorber material would drop into the core. The resulting reactivity insertion is modeled with the same values as shown in Table 7-3. It should be mentioned that since the oxide core has a softer neutron spectrum than that encountered in the metal core, the absorber worth would likely be greater in the oxide core. However, the overall impact of such a large (in magnitude) negative reactivity insertion is insensitive to the resulting difference since both cases reduce the multiplication eigenvalue of the core below 0.99, shutting the reactor down.

TABLE 7-3: FLA REACTIVITY INSERTION FOR AN OXIDE CORE.

Time (s)	Rho (\$)
0.0	0.0
1.5	-0.130
2.0	-0.884
2.5	-3.4
3.0	-5.8

Finally, as with the CPL analysis, separate simulations were performed for the case of different pump coastdown rates as shown in Table 7-4.

TABLE 7-4: FLOW-HALVING TIMES FOR AN OXIDE CORE.

Case	Pump Coastdown – Flow-halving time (s)
1	0
2	5
3	10
4	20

The results are shown in Figure 7-6 through Figure 7-9. Again, note the results are bunched more tightly together than what was seen in the CPL analysis. This is because the FLA shuts the reactor down much quicker than the CPL (almost immediately) so the temperature profiles with the FLA are more dependent on the thermophysical and transport properties of the fuel, clad, coolant, and structural materials rather than the reactivity feedbacks; and since the uncertainties in the thermophysical and transport properties are not accounted for, a more narrow spread in temperature profiles is expected.

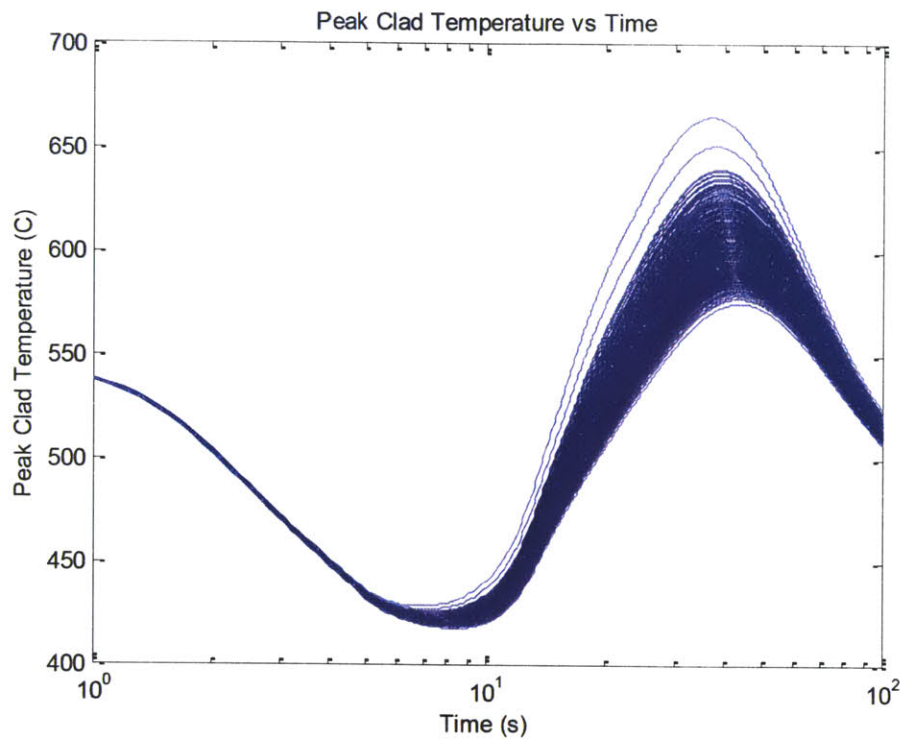


FIGURE 7-6: FLA PERFORMANCE FOR A ULOF WITH INSTANTANEOUS FLOW SEIZURE (OXIDE CORE).

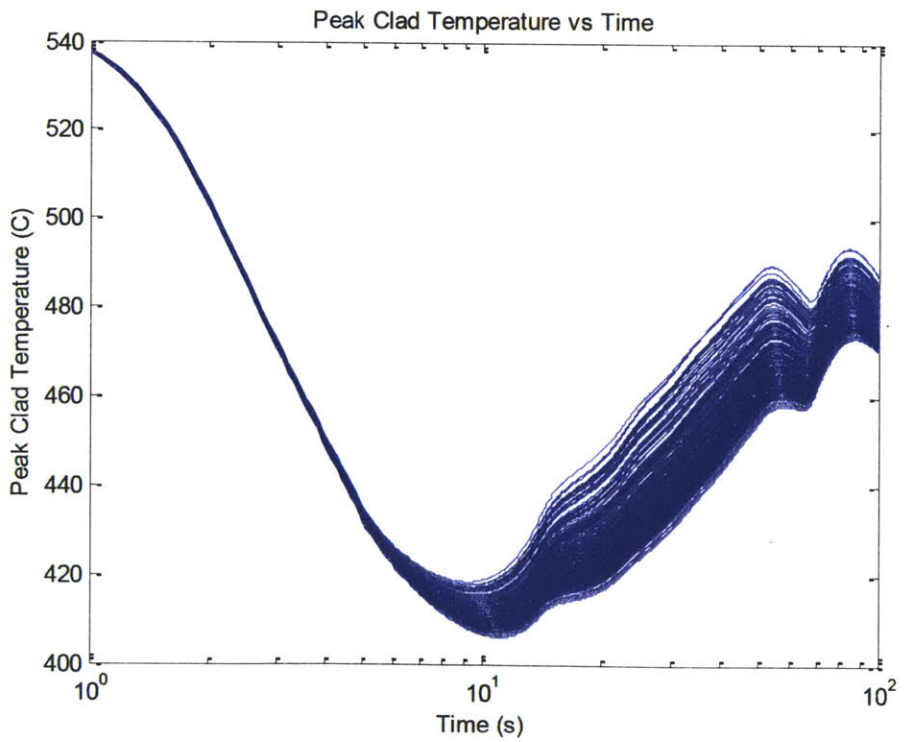


FIGURE 7-7: FLA PERFORMANCE FOR A ULOF WITH A 5 SECOND FLOW-HALVING TIME (OXIDE CORE).

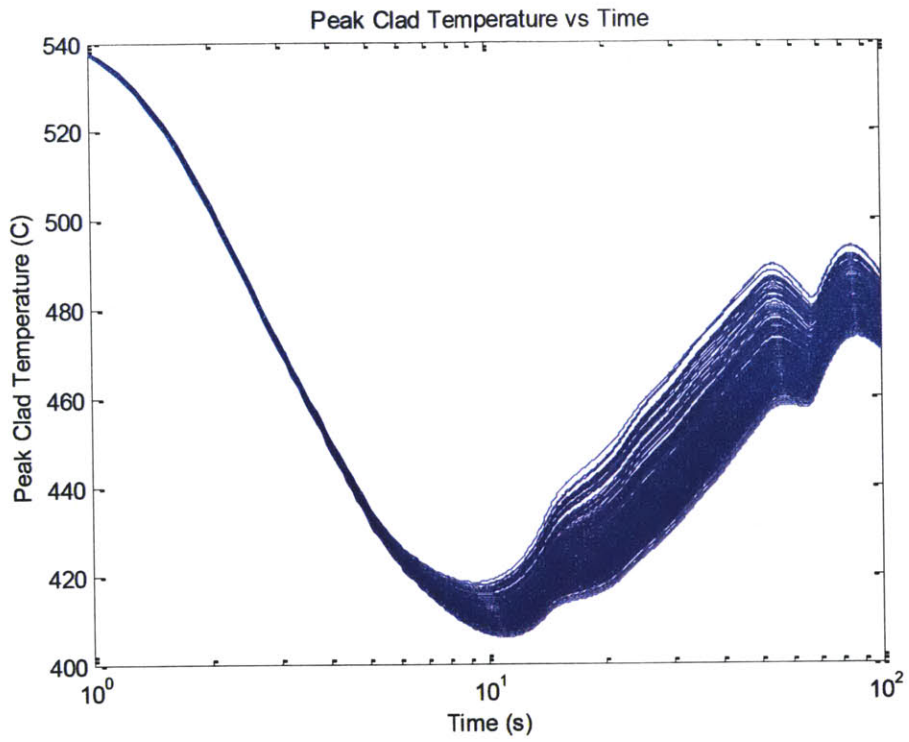


FIGURE 7-8: FLA PERFORMANCE FOR A ULOF WITH A 10 SECOND FLOW-HALVING TIME (OXIDE CORE).

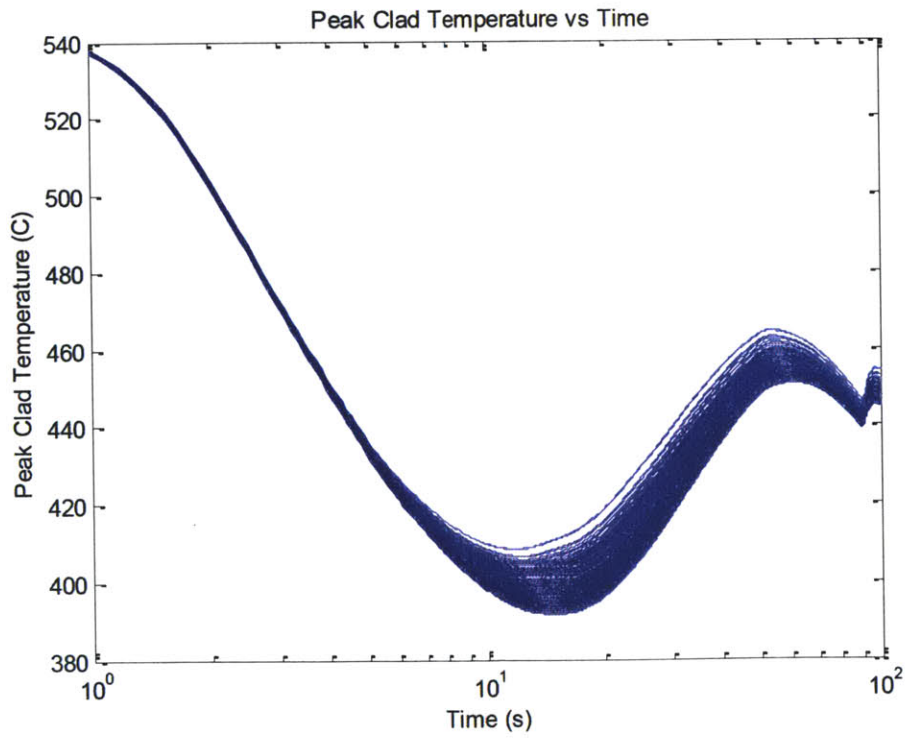


FIGURE 7-9: FLA PERFORMANCE FOR A ULOF WITH A 20 SECOND FLOW-HALVING TIME (OXIDE CORE).

Equation 10 was used to calculate the reliability of the FLA given a particular demand, with failure occurring when the peak cladding temperature exceeds 800 °C, which can be considered a conservative approximation to cladding failure.

As seen in the metal core analysis, and as seen in Figure 7-6 through Figure 7-9, the peak cladding temperature never exceeds 800 °C. Therefore, the results of this analysis show the FLAs respond almost immediately to a loss of flow, and pump coastdown is the dominant factor affecting peak cladding temperature during the transient. As with the metal core analysis, the reliability of FLAs is practically unity for internally initiated LOFs. But since the dominant failure mode for FLAs is the physical disruption of absorber insertion, the conditional failure probability of FLAs given a ULOF is best calculated as the conditional failure probability of control rods during insertion into reactor core given core deformation. This value is design dependent, and for PRISM is given as 1.0×10^{-4} .

7.5 Unprotected Transient Overpower Performance

As mentioned in Chapters 4 and 6, UTOPs initially produce an elevated core power (>100%), creating a power to flow mismatch that causes the primary sodium pool to heat up. This sequence of events would have little to no effect on a FLA since a UTOP would only slightly decrease the mass flow rate of the sodium due to its decreased density, and thus not significantly alter the coolant flow. However, the primary sodium pool will eventually heat up to a temperature that trips the primary pumps to prevent burnout. At this point, coolant flow will coastdown, and the FLAs will drop into the core, shutting the reactor down. Therefore, a UTOP would have to progress unencumbered until the pump inlet temperature reaches this trip point. At this point, the FLA will shut the reactor down with the same effect encountered during a ULOF.

7.6 Impact on Reactor Operations

During steady state full power operations, flow levitated absorbers would not impact reactor performance negatively since any plausible flow perturbation would not reduce coolant flow to less than 40%. However, FLAs would impact startup and low power operations. During startup operations, the reactor core is gradually raised from cold zero power to hot zero power to hot full power. This is a dynamic process that balances many factors including core power, primary coolant flow rates, intermediate coolant flow rates, and steam flow rates to avoid introducing large thermal stresses in plant components. Typically primary coolant flow and core power are carefully matched so the coolant does not flow at 100% during low power operations. This poses a problem for FLAs during startup operations since primary coolant flow will be below 40% full flow, meaning the FLAs will not be suspended.

In order to overcome this challenge, the designer must compensate by changing the startup procedures to maintain high flow rates during low power operations. Unfortunately this would lead to power-flow mismatches that could stress components in the primary, intermediate, and steam loops, reducing their operational lifetime. The same issue exists for another SASS design mentioned in Chapter 3 – GEMs.

Another solution to this problem is to lift the FLAs by a traditional control rod latch and driveline that would electromagnetically hold the FLAs up when desired. When primary coolant flow rates exceed 40% full flow the latches would be disengaged, allowing the coolant flow to suspend the FLAs. To prevent the traditional latches and drives from interfering with FLA operation during a transient, the latches and drivelines could be withdrawn above a stop that would limit the rise of the FLA. This is demonstrated in Figure 7-10. Such a design would alleviate the challenges to reactor startup posed by flow dependent SASS in a way unique to FLAs, and non-applicable to GEMs. It should be noted

that this system would only function for a rod assembly design, so it would not work if spheres are employed to hold the absorbing material.

Furthermore, this design could also address the issue of inadvertent withdrawal due to accidental pump startup, or higher than anticipated natural convection flow. This scenario must be accounted for in plant performance analysis, and the FLA's susceptibility (as for any flow-dependent SASS device) to this phenomenon is a major drawback. Also, natural convection flow rates must be accurately characterized since they could challenge the long term shutdown performance of a FLA. The traditional rod stop and driveline design discussed previously in this section would help alleviate concerns for accidental withdrawal because the drivelines could be programmed to drive into the core, latch to the FLA, and lock position, preventing the FLA from rising out of the core. This is also illustrated in Figure 7-10.

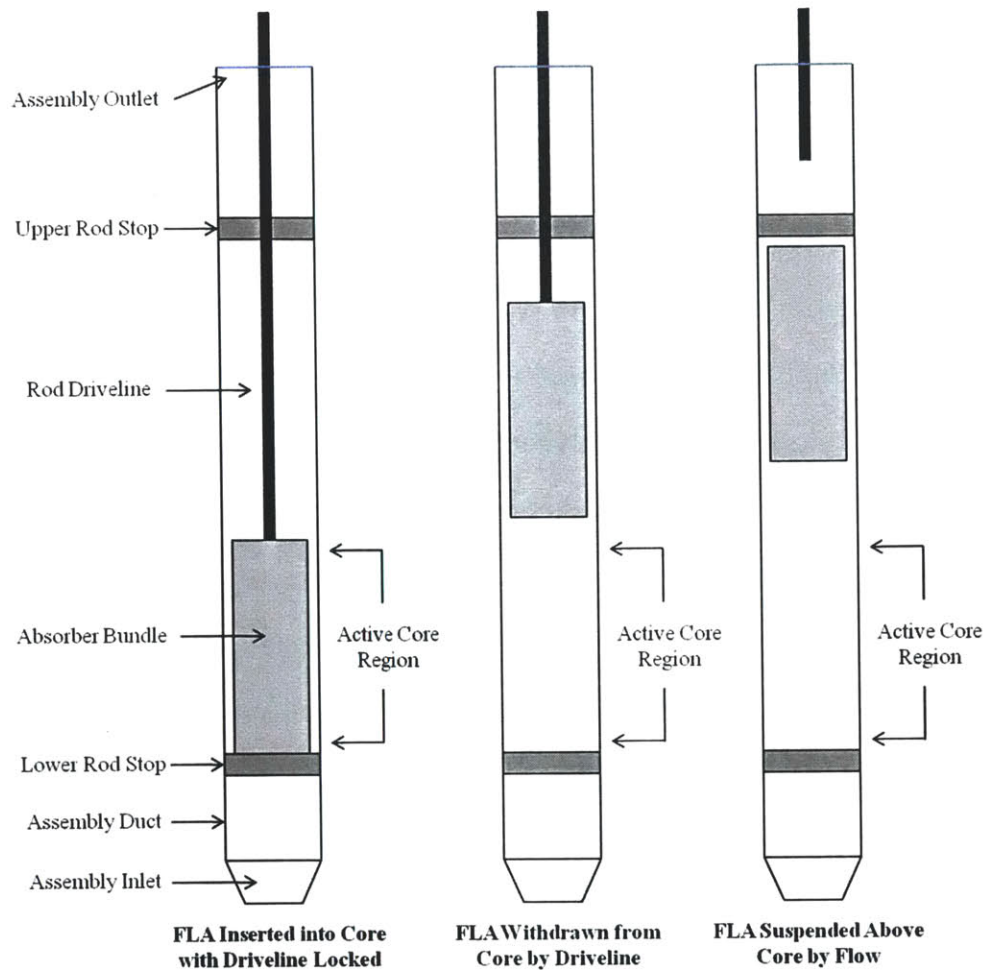


FIGURE 7-10: PROPOSED FLA-TRADITIONAL CR DRIVELINE DESIGN.

One major uncertainty associated with this design is demonstrating to the operators that the FLA is decoupled from the latch and driveline, thereby enabling them to rely on FLA operation during an accident. A level indicator on the driveline and a sonic sensor in the core could address this problem, but whichever option is selected, the designer would have to demonstrate the function of this system during design, pre-operation, and throughout the plant's lifetime.

7.7 Economic Analysis and Results

Like CPLs FLAs are rather inexpensive, but when compared to the estimated cost of the control rod drives, \$10 million (1994 \$), or 1.3% of the total plant cost (54) (55), it is

unlikely FLAs will reduce total plant cost by a significant amount, especially if control drivelines are employed to address the operability concerns mentioned previously. It should also be mentioned that, as with CPLs, a detailed in-situ testing program would need to be developed to verify and validate consistent FLA operation over the life of the plant (6). This may impact the net FLA economic impact on SFRs.

7.8 Summary

FLAs enhance RPS diversity, and, unlike CPLs, significantly enhance ULOF performance for both metal and oxide cores. However, considering the high reliability of the active RPS, FLAs do not offer a convincing cost-benefit argument for their inclusion without a strong external driver such as regulator requirements to satisfy further redundancy and defense-in-depth. This is compounded by the negative impact hydraulically driven SASS have on reactor operations.

8 Seismic Considerations for Reactor Protection Systems

8.1 Introduction

Licensing an SFR via the TNF illuminated challenges to TNF safety goals with regard to seismic hazards. This is because SFRs are susceptible to reactivity insertions, sloshing, and other seismically induced potential failure modes not encountered in LWRs. Most modern designers attempt to reduce this risk by including seismic isolators. Although isolators should be useful in most scenarios, in very rare large earthquakes, the isolators could fail, leading to plant damage states that are difficult to analyze and would likely lead to a large release. One step often found in the event sequences of these severe earthquakes is the failure of the RPS (5). This chapter will investigate ways to improve the shutdown performance of the RPS during seismic events.

8.2 Seismic Impacts on Sodium Fast Reactors

Seismic events are a particularly important issue in the safety analysis of SFRs. Two important characteristics of SFRs in this context are high operating temperatures and low pressures. The high temperature condition requires the component walls to be of limited thickness to bound thermal stresses. Furthermore, relatively thin walls are possible because of the low operating pressure. Conversely, with regard to seismic stresses, component walls need to be thick. The optimum design choice must achieve a balance that satisfies both these requirements, which leads to a tradeoff that introduces vulnerabilities from a seismic perspective (57). To compound these issues, SFRs are susceptible to seismically induced potential failures that LWRs are not, e.g. reactivity insertion and sloshing (9). The application of the TNF for SFR licensing requires the evaluation of seismic events with a very low frequency of occurrence, such that it is difficult to quantify the maximum peak ground acceleration, especially vertical.

Therefore, when applying the TNF to SFRs, it was observed that seismically induced failures presented the greatest challenge to the reference design. The main failure mode is failure of the decay heat removal system due to a seismic initiator that also causes a reactivity insertion (5). Most SFRs attempt to mitigate seismic consequences with seismic isolators. Although isolators should be useful in most scenarios, in very rare large earthquakes, the isolators could fail leading to plant damage states that are difficult to analyze and would likely lead to a large release (58).

8.3 Reactor Protection System Design Alternatives

The unique challenges posed to current SFR RPS designs under the TNF by seismic events motivates the investigation of RPS alternatives that may improve RPS performance during such events. According to the ALMR PRA, seismic events provide a substantial challenge to the design of the RPS. The potential for common cause failure of the RPS in these events makes it difficult to provide assurance that the TNF limit curve can be satisfied. Two design modifications were analyzed: articulated control rods, and anticipatory scram systems.

8.4 Articulated Control Rods

The lateral and vertical movement of core structures during a seismic event may impede control rod insertion by obstructing the rod's entry path. To overcome this difficulty, articulated control rods are offered as a potential design addition, especially for the backup scram system. Control rods designed with multiple degrees of motion, and a more forgiving clearance, may decrease the insertion time in the event of an earthquake by up to 17% compared to the insertion time of traditional rods, resulting in a full stroke insertion time of about 2.5 s compared to 3.0 s (59) (60).

Articulated rods may enhance scram performance in the case of core deformation at negligible additional cost, but would not affect normal operations. Detailed mechanical analysis and testing would need to be performed to determine the exact improvements, but mechanical analysis of the EBR-II's scram system suggest contact with the guide tubes during a seismic event increased the insertion time by up to 100% (59).

8.5 Seismic Anticipatory Scram System

Earthquakes produce two waves: primary waves (p-waves) and secondary waves (s-waves). P-waves travel nearly twice as fast as s-waves and therefore arrive at a location before the much more damaging s-waves. This time delay, or residual time, ranges from 0.2 s to 3.0 s, and times longer than 0.5 s would easily enable a pre-emptive scram. Both waves are easily detectable, so an anticipatory scram system with seismic sensors located on the plant site may be able to signal a scram prior to the arrival of s-waves. A simplified anticipatory scram system was deployed at EBR-II, and may enhance an SFR's safety performance during a seismic event, at little additional cost (59).

An anticipatory scram system would not introduce a significant cost increase to the SFR. The major economic concern arises from false alarm scram signals. These would result in unplanned outages, decreasing an SFR's capacity factor. A multi-positive sensor logic structure (2-out-of-3, etc.) would help prevent spurious scrams. Also, periodic in-situ testing is also an issue, since full simulation of an earthquake is unfeasible, however testing the accelerometers may serve as a surrogate path.

8.6 Summary

Articulated rods may enhance RPS performance during seismic events, but detailed testing needs to be conducted to confirm the efficacy of such rods. Furthermore, the magnitude of seismic events for which articulated rods may have a noticeable impact on

performance may also result in damage to other plant components that would override the improvement to the RPS.

Anticipated scram systems may enhance RPS performance during seismic events, but the detailed efficacy of such a system is highly dependent on the geologic conditions at the plant, and the seismic characteristics of each earthquake since those factors affect the residual time between p-wave and s-wave arrival. As with the articulated rods, the magnitude of seismic events for which an anticipatory scram system may have a noticeable impact on performance may also result in damage to other plant components that would override the improvement to the RPS.

9 Summary, Conclusions, and Recommendations for Future Work

9.1 Summary

SFRs are gaining renewed interest from the global community thanks to their unique capabilities. However cost concerns temper SFR deployment. Design features aimed at addressing concerns over the severity and likelihood of ECDAs are considered to be a contributing factor to the cost premium of SFRs. However, when considered from a risk perspective, such as that provided by the TNF, ECDAs occur with a low enough frequency that they may be excluded from the design basis, allowing designers to remove unnecessary margin. This thesis investigated how RPS design alternatives can affect SFR economics under the context provided by the TNF through three major evaluations: 1) the efficacy of a two-scrum system RPS was investigated as a means to preclude unprotected transients from the design basis; 2) SASS performance was analyzed as a way to enhance RPS diversity and performance; and 3) articulated control rods and anticipatory scram systems were studied as a way to address the challenges seismic events pose to SFRs.

9.2 Conclusions

One of the TNF's unique features is that sequences with release frequencies below a mean threshold frequency of $10^{-7}/\text{yr}$ can be screened from the design basis, a very significant feature in regard to the RPS system. Events that include failure of the RPS are not included in SFR LBEs since the failure probability of their two independent subsystem RPS is small enough to push unprotected accidents under the $10^{-7}/\text{yr}$ mean FCC. For example, the failure probability for the ALMR RPS during a TOP is $3 \times 10^{-5}/\text{demand}$ and is $1 \times 10^{-7}/\text{demand}$ for all other transients; while the frequency of challenging transients initiating scram start at 0.001/yr for TOPs and 0.007/yr for LOFs (5), hence their product is less than $10^{-7}/\text{yr}$. The high reliability of the RPS means that only protected accidents need to be analyzed as LBEs.

While consideration of accidents involving failure of the RPS may still be required by the regulator, they will qualify as beyond design basis events and therefore should not drive the design of the RPS system. These results indicate that two scram systems perform well enough to push the frequency of unprotected transients below the $10^{-7}/\text{yr}$ frequency cutoff proposed in the TNF, thus nullifying the need for a third, independent scram system.

SASS have the potential to improve RPS performance by adding to the defense-in-depth case, and increasing scram reliability. Plant performance simulations were conducted to analyze SASS performance for Curie point latches and flow levitated absorbers. CPLs were found to marginally reduce the conditional cladding damage probability for metal cores because of their rapid inherent feedback effects, but were more effective for the more sluggish oxide cores given reasonably long pump coastdown times. FLAs are very effective at mitigating ULOFs for both fuel types, but are limited in response during UTOPs. However, inclusion of SASS necessitates evaluating the lifetime impact of such systems. For example, the use of FLAs complicates startup procedures as flow rates are increases.

Ultimately, when considered from a risk-informed perspective, a traditional, diverse RPS appears to be adequate to assure a very low core damage frequency for unprotected events with the possible exception of seismic events. In light of this, a clear rationale and objective is needed to justify the inclusion of a tertiary system or additional feature such as SASS. In particular, there is no a priori assurance that the added system does not have a common mode failure mechanism with the existing RPS, which as a consequence would provide little additional defense-in-depth. Although the reference design includes isolation against horizontal seismic accelerations, low frequency high acceleration seismic events remain an area of high uncertainty and regulatory unpredictability, while the issue of vertical acceleration also needs to be addressed. The need for further refinement of the TNF in this regard is a major finding of the larger study – *“Risk-Informed Balancing of Safety, Non-*

Proliferation, and Economics for the Sodium-Cooled Fast Reactor,” supported by the U.S. Department of Energy under NERI contract DE-FG07-07ID14888 – of which this thesis is but one part. The use of articulated safety rods as one of the diverse means of reactivity insertion and the implementation of an anticipatory seismic scram system may be the most cost-effective alternatives to provide defense in depth in light of the SFRs susceptibility to seismic events.

Furthermore, in assessing the response of the reference design to unprotected events, it was assumed that credit could only be granted for safety-grade components in the safety analysis of LBEs. In the reference design, there are no safety-grade equipment for full power heat removal, so when analyzing UTOP and ULOF accidents, the intermediate heat removal system was also assumed to fail. Thus, in the analyses performed with RELAP5-3D, it is reasonable to assume that cladding failure would not be predicted to occur for either the UTOP or ULOF scenarios if the heat removal system is regarded to be functional.

9.3 Future Work

This thesis provided a survey of RPS design alternatives under the context of the TNF, but there remain many uncertainties when it comes to RPS performance that should be addressed to properly select and optimize the RPS, not to mention work in other areas not addressed in this thesis such as extending control rod lifetimes.

First, a more accurate and flexible systems code that incorporates better multiphysics phenomena than which currently exist with RELAP5-3D should be developed to better model the complex phenomena of unprotected transients.

Regarding SASS, there is room for both detailed design optimization, and development of other innovative mechanisms for shutdown, such as hybrid designs that incorporate the best features of various SASS designs. For metal cores specifically, speed of

actuation is a key area for improvement, and both cores would benefit from a fast acting design during a UTOP. Furthermore, an improved sampling scheme that accounts for uncertainties in the thermophysical and transport properties of the core materials would also reduce uncertainty and provide a more accurate model. The accuracy of the cladding failure model could also be substantially improved by adopting better fuel-clad eutectic models and cladding creep models, as discussed by Denman (19). Detailed in-situ testing plans for the SASS should be developed to address lifetime proof of operation requirements. For example, raising the core outlet temperature to demonstrate CPL action is probably not a desirable procedure. All of these efforts precede experimental testing needed to confirm the analytical computational methods.

Regarding seismic issues, the impacts of advanced isolation systems on RPS performance during seismic events needs to be analyzed. Detailed computational models to analyze the structural mechanics of complex rod geometries during seismic events would also benefit SFR designers. Finally, a detailed economic model of a generic SFR RPS should be developed that would support meaningful cost/benefit analysis, as well as lifetime economics of proposed designs.

References

1. *A Cost-Effective U-235 Once-Through Startup Mode for SFRs*. Fei, T., Shwageraus, E., and Driscoll, M. Hollywood, FL : Transactions of the American Nuclear Society, 2011. 2011 ANS Annual Meeting (forthcoming).
2. NRC . *Feasibility Study for Development of a Risk-Informed, Performance Based Alternative to Plant Licensing*. Office of Nuclear Regulatory Research. Washington D.C. : Nuclear Regulatory Commission, 2007. NUREG-1860.
3. IAEA. *Fast Reactor Database 2006*. IAEA-TECDOC-1531. s.l. : International Atomic Energy Agency, 2006.
4. U.S. Department of Energy. *A Technology Roadmap for Generation IV Nuclear Energy Systems*. 2002.
5. El-Sheikh, K.A. Probabilistic Risk Assessment of the Advanced Liquid Metal Reactor. *GEFR-00873*. San Diego, CA : GE Nuclear Energy, 1994. GEFR-00873.
6. U.S. NRC/U.S. Code of Federal Regulations. *Appendix A to Part 50 - General Design Criteria for Nuclear Power Plants*. s.l. : U.S. Government Printing Office.
7. U.S. NRC. *Pre-application safety evaluation report for the PRISM*. Washington, D.C. : U.S. NRC, 1994. NUREG-1368.
8. *Fast Reactor Fuel Type and Reactor Safety Performance*. Wigeland, R. and Cahalan, J. Paris, France : s.n., 2009. GLOBAL'09. p. 9445.
9. Johnson, Brian C. *Application of the Technology Neutral Framework to Sodium-Cooled Fast Reactors*. Department of Nuclear Science and Engineering, MIT. Cambridge, MA : MIT, 2010. PhD Thesis.
10. *The EBR-II PRA: Lessons Learned Regarding Passive Safety*. Hill, D. J., et. al. 1998, Reliability Engineering and System Safety, Vol. 62, pp. 43-50.
11. LANL. *MCNP Users Guide*. s.l. : LANL, 2005. LA-CP-03-0245.
12. LANL. *NJOY 99.0 Users Manual*. s.l. : Oak Ridge National Labs - RSICC, 2000. PSR-480.
13. *S-PRISM Oxide and Metal Fuel Core Designs*. Dubberley, A., et al. Baltimore, MD : s.n., 2000. Proceedings of ICON8.
14. Morris, E. Uncertainty in Unprotected Loss of Heat Sink, Loss of Flow, and Transient Overpower Accidents. *ANL-AFCI-205*. s.l., Argonne, IL : Argonne National Laboratory, 2007.
15. Memmott, Matthew J. *THERMAL-HYDRAULIC ANALYSIS OF INNOVATIVE FUEL CONFIGURATIONS FOR THE SODIUM FAST REACTOR*. Department of Nuclear Science and Engineering, MIT. Cambridge, MA : MIT, 2009. PhD Thesis.
16. RELAP5-3D Dev. Team. RELAP5-3D© Code Manual Volume I: Code Structure, System Models and Solution Methods. *INEEL-EXT-98-00834*. Idaho Falls, ID : Idaho National Laboratories, April 2005.
17. Langewisch, Dustin R. *Uncertainty and Sensitivity Analysis for Long-Running Computer Codes: A Critical Review*. Department of Nuclear Science and Engineering, MIT. Cambridge, MA : MIT, 2009. S.M. Thesis.
18. *Applying the Technology Neutral Framework to Evaluate Core Outlet Temperature Changes in a Sodium Fast Reactor*. Denman, M. R., Todreas, N. E., Driscoll, M. J. San Diego, CA : International Congress on Advances in Nuclear Power Plants, 2010.
19. Denman, M. R. *Probabilistic Transient Analysis of Fuel Choices for Sodium Fast Reactors*. NSE, MIT. Cambridge, MA : MIT, 2011.
20. Ang, H-S and Tang, W.H. *Probability Concepts in Engineering*. s.l. : Wiley, 2007.

21. *Probabilities of Inherent Shutdown of Unprotected Events in Innovative Liquid Metal Reactors*. Mueller, C. and Wade, D. Seattle, WA : s.n., 1988. ANS Topical Meeting on Safety of Next Generation Power Reactors.
22. McCormick, N. J. *Reliability and Risk Analysis*. New York, NY : Academic Press, 1981. ISBN-0-12-482360-2.
23. ANL. *Advanced Burner Reactor 1000MWh Reference Concept*. s.l. : ANL, 2007. ANL-AFCI-202.
24. *PRISM-Liquid Metal Cooled Reactor Plant Design and Performance*. Kwant, W. and Boardman, C. 1992, Nuclear Engineering and Design, Vol. 136, pp. 111-120.
25. Gluekler, E. L., et. al. *ALMR Summary Plant Design Description*. s.l. : GE, 1995. GEFR-00941.
26. *S-PRISM Metal Core Margins to Severe Core Damage*. Dubberley, A.E., et al. Baltimore, MD : s.n., 2000. ICONE 8. p. # 8001.
27. Dubberley, A. E., et. al. *ALMR Mod B Core Design and Analysis Report*. s.l. : GE, 1993. GEFR-00923.
28. CEA. Generation IV: Development of the first prototype reactor. *CEA News*. 2010. Vol. Autumn 2010.
29. *Studies on French SFR Advanced Core Designs*. Mignot, G., et al. Anaheim, CA : 2008 ICAPP, 2008. 2008 ICAPP.
30. *A Next Generation Sodium Cooled Fast Reactor Concept and its R&D Program*. Ichimiya, M., Mizuno, T. and Kotake, S. 3, Ibaraki, Japan : s.n., 2007, Nuclear Engineering and Technology, Vol. 39, pp. 171-186.
31. *Development of Advanced Loop-Type Fast Reactors in Japan (1): Current Status of JSFR Development*. Kotake, S., et al. Anaheim, CA : s.n., 2008. 2008 ICAPP.
32. Argonne National Laboratory. *Severe Accident Approach - Final Report: Evaluation of Design Measures for Severe Accident Prevention and Consequence Mitigation*. s.l. : ANL, 2010. ANL-GENIV-128.
33. *Influence of Metal and Oxide Fuel Behavior on the ULOF Accident in 3500MWh Heterogeneous LMR Cores and Comparison with other Large Cores*. Royle, P., et al. Snowbird, UT : s.n., 1990. International Topical Meeting on Fast Reactor Safety.
34. *Performance of Metal and Oxide Fuels During Accidents in a Large Liquid Metal Cooled Reactor*. Cahalan, J., et al. Snowbird, UT : s.n., 1990. International Topical Meeting on Fast Reactor Safety.
35. *The Safety of the IFR*. Wade, D. C., et. al. 1997, Progress in Nuclear Energy, Vol. 31, pp. 63-82.
36. *EBR-II DRIVER FUEL QUALIFICATION FOR LOSS-OF-FLOW AND LOSS-OF-HEAT-SINK TESTS WITHOUT SCRAM*. LAHM, C.E., et al. 101, Idaho Falls, ID : North-Holland Publishing, 1987, Nuclear Engineering and Design, pp. 25-34.
37. Ivans, W. *The Current Nuclear Regulatory Environment: A PRISM Perspective*. Department of Nuclear and Radiological Engineering, University of Florida. Gainesville, FL : University of Florida, 2006. M.S. Thesis.
38. Pope, M., Driscoll, M., Hejzlar, P. *Reactor Physics Design of a Supercritical CO₂-Cooled Fast Reactor*. MIT. s.l. : CANES, 2004. MIT-ANP-TR-104.
39. Combustion Engineering, INC. *Self-Actuated Shutdown System for a Commercial Size LMFBR*. s.l. : Combustion Engineering, INC., 1978. NP-846, Research Project 897-1.
40. IAEA. *Absorber Materials, control rods, and designs of shutdown systems for advanced liquid metal fast reactors*. s.l. : IAEA, 1995. IAEA-TECDOC-884.
41. *Assessment of Proposed Passive Prevention and Mitigation Measures for Future Fast Breeder Reactors*. Ieda, et. al. Pittsburgh, PA : s.n., 1994. International Conference on Advanced Reactor Safety.

42. *Improving the Safety of Cores for Commercial FBRs*. Inagaki, et. al. Pittsburgh, PA : International Conference on Advanced Reactor Safety, 1994.
43. *Development of Advanced Loop-Type Fast Reactor in Japan (5): Adoption of Self-Actuated Shutdown System to JSFR*. Nakanishi, S., et. al. Anaheim, CA : 2008 ICAPP, 2008.
44. *Development of Passive Shutdown System for SFR*. Nakanishi, S., et. al. s.l. : ANS, 2009, Nuclear Technology, Vol. 170, pp. 181-188.
45. *A Magnetic Curie Point Inherent Shutdown Assembly (ISA) for LMFBR Plants*. Sowa, E., Josephson, J. s.l. : ANS, 1975. Transactions of the American Nuclear Society.
46. *Criterion for Ferromagnetism from Observations of Magnetic Isotherms*. Arrott, A. 6, s.l. : Physical Review, 1957, Vol. 108.
47. *Demonstration of Control Rod Holding Stability of the Self Actuated Shutdown System in JOYO for Enhancement of Fast Reactor Inherent Safety*. Takamatsu, M., et. al. 3, 2007, Nuclear Science and Technology, Vol. 44, pp. 511-517.
48. *Metallic Fast Reactor Fuel*. Hoffman, G., Walters, C. and Bauer, T. 1, Idaho Falls, ID : s.n., 1997, Progress in Nuclear Energy, Vol. 31, pp. 83-110.
49. *Cladding Failure Margins for Metallic Fuel in the Integral Fast Reactor*. Bauer, T., et al. Lausanne, Switzerland : s.n., 1987. SMiRT'87. Vol. C.
50. *Eutectic Penetration Times in Irradiated EBR-II Driver Fuel Elements*. Betten, P.R., Bottcher, J.H. and Siedel, B.R. San Francisco, CA : s.n., 1983. ANS Winter Meeting. p. # 83104775.
51. *Fuel/cladding compatibility in U- 19Pu-10Zr/ HT9-clad fue at elevated temperatures*. Cohen, A.B., Tsai, H. and Neimark, L.A. 204, Argonne : Elsevier Science Publishers B.V., 1993, Journal of Nuclear Materials, pp. 244-251.
52. *Behavior of Low-burnup Fuels for the Integral Fast Reactor at Elevated Temperatures in Ex-Reactor Tests*. Tsai, H. Kyoto, Japan : s.n., 1991. Conference on Fast Reactors and Related Fuel Cycles.
53. Hagan, J. W., et. al. *Parametric Scram Transient Analyses for the FFTF Fast Test Reactor*. 1967. BNWL-657.
54. Gokcek, O., et. al. *ALMR 1994 Capital and Busbar Cost Estimates*. s.l. : GE, 1994. GEFR-00940.
55. Nitta, Christopher. *Applying Risk Informed Methodologies To Improve the Economics of Sodium-Cooled Fast Reactors*. Department of Nuclear Science and Engineering, MIT. Cambridge, MA : MIT, 2010. S.M. Thesis.
56. Specht, E. R., et. al. *Hydraulically Supported Absorber Balls Shutdown System for Inherently Safe LMFBRs*. Canoga Park, CA : Rockwell International - Atomics International Division. AT(04-3)-824.
57. *Seismic Risk Evaluation within the Technology Neutral Framework*. Johnson, B., Apostolakis, G. San Diego, CA : s.n., 2010. 2010 ICAPP.
58. IAEA. *Seismic Analysis of Liquid Metal Fast Breeder Reactors*. s.l. : IAEA, 1989. IAEA-TECDOC-514.
59. *Scram Reliability under Seismic Conditions at the Experimental Breeder Reactor II*. Roglans, J., et. al. s.l. : ANS, 1995, Nuclear Engineering and Design, Vol. 160, pp. 399-410.
60. *SCRAM and Nonlinear Reactor System Seismic Analysis for a Liquid Metal Fast Reactor*. Morrone, A., et. al. 1976, Nuclear Engineering and Design, Vol. 38, pp. 555-566.

Appendix A – MCNP Model

For more information, and a detailed description of the input, please refer to the MCNP5 manual (11).

message:

datapath=/home/CODES/mcnp/mcnplib \$ Squadron datapath=C:\XSFiles \$
PC

Reactivity Worth -Central Rod Insertion 100.00 %

400

c In order to convert to a text document, click save as and then select the .pm extension (space delimited)

c the following are the input data to create this mcnp input deck

c Assembly Pitch n/cycle k-guess Skip Cycles Active Cycles Total Cycles Total n Average
Enrichment 19.75% 22.1%

c 16.142 4600 1 250 250 500 1150000

c

c Zone 1 Fuel

c Pin Pitch Fuel Radius Gap Thickness Clad Thickness smear density Average Fuel
DensiTRU Enrich

c 0.8909 0.278425 0.0431 0.056 75% 15.7 17.30%
18.28%

c Pitch Offset Pins/Assembly Wrap Thickness # of assemblies 78

c 0.8909 271 0.1307

c

c Zone 2 Fuel

c Blanket Pitch Blanket Radius Gap Thickness Clad Thickness Pins/Assembly Wrap
Thickness TRU Enrich

c 0.8909 0.278425 0.0431 0.056 271 0.13074 21.62%
of assemblies 102

c

c Zone 3 Fuel (NA)

c Blanket Pitch Blanket Radius Gap Thickness Clad Thickness Pins/Assembly Wrap
Thickness TRU Enrich

c 0.8909 0.278425 0.0431 0.056 271 0.13074 0.00%

c

c Control Rod Drive Parameters

c CRD Pitch Clad OD Clad ID Pellet RadiuInsert %CRD 1 Distance Into theCR Ht.
Standard CRD 2 Distance Into the CCR Ht. Standard

c 4.82395 2.344 2.274 2.0965 100.00 -5.02 86.3 -5.02
86.3

c Inner Duct Thickness Inner Duct Gap

c 0.394 0.4 0.755

c

c Reflector Parameters

c Relector Pitch refl radius Pins/Assembly

c 0.77127 0.7705 91

c

c Shield Parameters

c Shield Pitch Shield Radius Shield Gap Shield Clad Pin OD Pins/Assembly

c 3.34034 1.2765 0.142 0.25 3.337 19

c

c Duct Parameters

c Duct Gap Ductg Wall Thickness

c 0.432 0.394

c

c Axial Parameters

```

c Upper Handeling Socket      Duct Standoff      Upper End Plug Thickness      Upper Plenum
Thickness
c 30.48          78.74          2.54          124.46
c Core Height      Lower Shield ThicknesNosepiece      Nozzel Thickness
c 81.28          124.46          35.6          91.44
c Grid Support Height      Lower Na Thickness
c 15.24          100
c
c Materials
c rhocol rhozr HT9 Density      SuperDense HT9      Clad Areawrap area      Coolant
Temperature      Thermal Expansion
c 0.8678 6.5 7.76      =mat= 3 9.4543 =mat=3      0.061487 0.0134248      355oC
alpha delta T
c 0.8500 6.5      =7.76*(1+wrap_area/clad_area)      432.5oC
0.00002 0
c 0.8321 6.5      510oC
c void= no      no duct= no
c the above are the input data to create this mcnp input deck
c
c cell specification
c cell # mat # Density      Surface Definitions UniveImportanVolumes for Tallies
c Begin Zone 1
1 1 -15.70000000 -11 405 -407 u=2 imp:n=1 vol= 19.79475 $ high enr
=-H481
2 3 -7.7600000000 -11 -405 u=2 imp:n=1      $lower plug
3 2 -0.8677843273 11 -12 -407 u=2 imp:n=1      $ gap
4 3 -9.4542733673 12 -13 -409 u=2 imp:n=1      $ clad HT9 ASTM A826-88
5 5 0.0000795149 -12 407 -408 u=2 imp:n=1      $ gas plenum
6 3 -7.7600000000 -12 408 -409 u=2 imp:n=1      $ upper plug
7 4 -0.8677843273 13 -405 u=2 imp:n=1      $ coolant around lower plug
50 40 -0.8500273421 13 -407 405 u=2 imp:n=1      $ coolant around fuel region
51 41 -0.8320688846 13 407 u=2 imp:n=1      $ coolant around gas plenum
region
c End Zone 1 / Begin Zone 2      $
10 10 -15.70000000 -1 405 -407 u=4 imp:n=1 vol= 19.79475 $ low enr
=-H499
11 3 -7.7600000000 -1 -405 u=4 imp:n=1      $lower plug
12 2 -0.8620774989 1 -2 -407 u=4 imp:n=1      $ gap
13 3 -9.4542733673 2 -3 -409 u=4 imp:n=1      $ clad HT9 ASTM A826-88
14 5 0.0000795149 -2 407 -408 u=4 imp:n=1      $ gas plenum
15 3 -7.7600000000 -2 408 -409 u=4 imp:n=1      $ upper plug
16 4 -0.8677843273 3 -405 u=4 imp:n=1      $ coolant around lower plug
52 40 -0.8500273421 3 -407 405 u=4 imp:n=1      $ coolant around fuel region
53 41 -0.8320688846 3 407 u=4 imp:n=1      $ coolant around gas plenum
region
c End Zone 2/ Begin Reflector Pin      $
17 3 -7.7600000000 -4 -410 u=7 imp:n=1      $ reflector
18 4 -0.8677843273 4 -410 u=7 imp:n=1      $ coolant around lower plug
c End reflector pin / Begin shield Pin      $
20 15 0.1359553620 -5 -410 u=9 imp:n=1      $ shield Natural Boron is Mat 15
21 5 0.0000795149 5 -6 -410 u=9 imp:n=1      $ gap
22 3 -7.7600000000 6 -7 -410 u=9 imp:n=1      $ clad
23 4 -0.8677843273 7 -410 u=9 imp:n=1      $ coolant
c End shield pin / Begin Guide Tube Pin      $
44 8 0.1385459110 -8 415 -410 u=5 imp:n=1      $ CRD Enriched Boron is Mat
8
45 5 0.0000795149 -8 -415 u=5 imp:n=1      $ He Below CRD
46 5 0.0000795149 8 -9 -410 u=5 imp:n=1      $ He gap
47 3 -7.7600000000 9 -10 -410 u=5 imp:n=1      $ HT9 Clad
48 4 -0.8677843273 10 -410 u=5 imp:n=1      $ coolant

```

```

c End shield pin / Begin Guide Tube Pin $
944 9 0.1385459110 -8 414 -410 u=55 imp:n=1 $ CRD Natural Boron is Mat
9
945 5 0.0000795149 -8 -414 u=55 imp:n=1 $ CRD
946 5 0.0000795149 8 -9 -410 u=55 imp:n=1 $ gap
947 3 -7.7600000000 9 -10 -410 u=55 imp:n=1 $ HT9 Clad
948 4 -0.8677843273 10 -410 u=55 imp:n=1 $ coolant
c End shield pin / Begin Guide Tube Pin $
9144 9 0.1385459110 -8 413 -410 u=955 imp:n=1 $ CRD Natural Boron is Mat
9
9145 5 0.0000795149 -8 -413 u=955 imp:n=1 $ CRD
9146 5 0.0000795149 8 -9 -410 u=955 imp:n=1 $ gap
9147 3 0.0000000000 9 -10 -410 u=955 imp:n=1 $ HT9 Clad
9148 4 0.0000000000 10 -410 u=955 imp:n=1 $ coolant

```

```

c $
c Zone 1 Assembly Layout $
101 40 -0.8500273421 -210 220 -230 -240 -250 -260 $ Zone 1 271 pin
imp:n=1 u=1 lat=2 fill=-10:10 -10:10 0:0 $ Zone 1 271 pin
0000000000111111111111 $ Zone 1 271 pin
0000000000122222222221 $ Zone 1 271 pin
0000000001222222222221 $ Zone 1 271 pin
0000000012222222222221 $ Zone 1 271 pin
0000000122222222222221 $ Zone 1 271 pin
0000001222222222222221 $ Zone 1 271 pin
0000122222222222222221 $ Zone 1 271 pin
0001222222222222222221 $ Zone 1 271 pin
0012222222222222222221 $ Zone 1 271 pin
0122222222222222222221 $ Zone 1 271 pin
1222222222222222222221 $ Zone 1 271 pin
1222222222222222222210 $ Zone 1 271 pin
12222222222222222222100 $ Zone 1 271 pin
122222222222222222221000 $ Zone 1 271 pin
1222222222222222222210000 $ Zone 1 271 pin
12222222222222222222100000 $ Zone 1 271 pin
122222222222222222221000000 $ Zone 1 271 pin
1222222222222222222210000000 $ Zone 1 271 pin
111111111111100000000000 $ Zone 1 271 pin
201 3 -7.7600000000 -427 -428 -429 430 -431 -432 $
imp:n=1 u=101 lat=2 fill=-1:1 -1:1 0:0 $ Fuel assembly in Duct
101 101 101 $
101 1 101 $
101 101 101 $
301 40 -0.850027342 -327 -328 -329 330 -331 -332 $ Duct in Sodium
imp:n=1 u=100 lat=2 fill=-1:1 -1:1 0:0 $
100 100 100 $
100 101 100 $
100 100 100 $

```

```

c $
c Zone 2 Assembly Layout $
102 40 -0.850027342 -21 22 -23 -24 -25 -26 $ Zone 2 271 pin
imp:n=1 u=3 lat=2 fill=-10:10 -10:10 0:0 $ Zone 2 271 pin
0000000000333333333333 $ Zone 2 271 pin
0000000000344444444443 $ Zone 2 271 pin
0000000003444444444443 $ Zone 2 271 pin
0000000034444444444443 $ Zone 2 271 pin
0000003444444444444443 $ Zone 2 271 pin
0000034444444444444443 $ Zone 2 271 pin
0000344444444444444443 $ Zone 2 271 pin

```

000344444444444444444444444444443	\$ Zone 2 271 pin
003444444444444444444444444444443	\$ Zone 2 271 pin
034444444444444444444444444444443	\$ Zone 2 271 pin
344444444444444444444444444444443	\$ Zone 2 271 pin
344444444444444444444444444444430	\$ Zone 2 271 pin
34444444444444444444444444444300	\$ Zone 2 271 pin
3444444444444444444444444443000	\$ Zone 2 271 pin
344444444444444444444444430000	\$ Zone 2 271 pin
34444444444444444444444300000	\$ Zone 2 271 pin
3444444444444444444443000000	\$ Zone 2 271 pin
34444444444444444430000000	\$ Zone 2 271 pin
344444444444443000000000	\$ Zone 2 271 pin
3444444444430000000000	\$ Zone 2 271 pin
3333333333330000000000	\$ Zone 2 271 pin
202 3 -7.7600000000 -427 -428 -429 430 -431 -432 \$	
imp:n=1 u=103 lat=2 fill=-1:1 -1:1 0:0	\$ Fuel assembly in Duct
103 103 103	\$
103 3 103	\$
103 103 103	\$
302 40 -0.850027342 -327 -328 -329 330 -331 -332 \$	\$ Duct in Sodium
imp:n=1 u=300 lat=2 fill=-1:1 -1:1 0:0	\$
300 300 300	\$
300 103 300	\$
300 300 300	\$
c	\$
c Reflector Assembly Layout	\$
103 4 -0.867784327 -35 36 -37 -38 -39 -40	\$ Reflector Assembly 91 Pin
imp:n=1 u=6 lat=2 fill=-6:6 -6:6 0:0	\$ Reflector Assembly 91 Pin
00000066666666	\$ Reflector Assembly 91 Pin
00000677777776	\$ Reflector Assembly 91 Pin
00006777777776	\$ Reflector Assembly 91 Pin
00067777777776	\$ Reflector Assembly 91 Pin
00677777777776	\$ Reflector Assembly 91 Pin
06777777777776	\$ Reflector Assembly 91 Pin
67777777777776	\$ Reflector Assembly 91 Pin
6777777777760	\$ Reflector Assembly 91 Pin
6777777777600	\$ Reflector Assembly 91 Pin
6777777776000	\$ Reflector Assembly 91 Pin
6777777600000	\$ Reflector Assembly 91 Pin
66666666000000	\$
203 3 -7.7600000000 -427 -428 -429 430 -431 -432 \$	
imp:n=1 u=106 lat=2 fill=-1:1 -1:1 0:0	\$
106 106 106	\$
106 6 106	\$
106 106 106	\$
303 4 -0.867784327 -327 -328 -329 330 -331 -332 \$	
imp:n=1 u=600 lat=2 fill=-1:1 -1:1 0:0	\$
600 600 600	\$
600 106 600	\$
600 600 600	\$
c	\$
c Central CRD Assembly Layout	\$
161 4 -0.867784327 -900 901 -902 -903 -904 -905	\$ Control Rod - 7 Pins
imp:n=1 u=980 lat=2 fill=-2:2 -2:2 0:0	\$ Control Rod - 7 Pins
00980980980	\$ Control Rod - 7 Pins
0980955955980	\$ Control Rod - 7 Pins
980955955955980	\$ Control Rod - 7 Pins
9809559559800	\$ Control Rod - 7 Pins
98098098000	\$ Control Rod - 7 Pins

```

624 3 -7.7600000000 -727 -728 -729 730 -731 -732
imp:n=1 u=981 lat=2 fill=-1:1 -1:1 0:0 $ Creates Inner Duct and Puts CRD
inside
981 981 981
981 980 981
981 981 981
724 4 -0.867784327 -627 -628 -629 630 -631 -632
imp:n=1 u=982 lat=2 fill=-1:1 -1:1 0:0 $ Creates Inter Duct Gap and Puts
Inner Duct Inside
982 982 982
982 981 982
982 982 982
824 4 -0.867784327 415 imp:n=1 u=983 fill=181 $How Far doe CRDs Extend
825 4 -0.867784327 -415 imp:n=1 u=983 $Sodium Beneith CRDs
224 3 -7.7600000000 -427 -428 -429 430 -431 -432
imp:n=1 u=984 lat=2 fill=-1:1 -1:1 0:0 $ Creates Outer Duct and puts both
CRD and
984 984 984
984 983 984
984 984 984 $ Bottom Sodium Inside
324 4 -0.867784327 -327 -328 -329 330 -331 -332
imp:n=1 u=950 lat=2 fill=-1:1 -1:1 0:0 $Creates Intra Assembly Duct Gap
950 950 950
950 984 950
950 950 950

c
c Primary CRD Assembly Layout $
106 4 -0.867784327 -900 901 -902 -903 -904 -905 $ Control Rod - 7 Pins
imp:n=1 u=8 lat=2 fill=-2:2 -2:2 0:0 $ Control Rod - 7 Pins
0 0 8 8 8 $ Control Rod - 7 Pins
0 8 5 5 8 $ Control Rod - 7 Pins
8 5 5 5 8 $ Control Rod - 7 Pins
8 5 5 8 0 $ Control Rod - 7 Pins
8 8 8 0 0 $ Control Rod - 7 Pins
604 3 -7.7600000000 -727 -728 -729 730 -731 -732
imp:n=1 u=180 lat=2 fill=-1:1 -1:1 0:0 $ Creates Inner Duct and Puts CRD
inside
180 180 180
180 8 180
180 180 180
704 4 -0.867784327 -627 -628 -629 630 -631 -632
imp:n=1 u=181 lat=2 fill=-1:1 -1:1 0:0 $ Creates Inter Duct Gap and Puts
Inner Duct Inside
181 181 181
181 180 181
181 181 181
804 0 -0.867784327 413 imp:n=1 u=182 fill=181 $How Far doe CRDs Extend
805 4 -0.867784327 -413 imp:n=1 u=182 $Sodium Beneith CRDs
204 3 -7.7600000000 -427 -428 -429 430 -431 -432
imp:n=1 u=108 lat=2 fill=-1:1 -1:1 0:0 $ Creates Outer Duct and puts both
CRD and
108 108 108
108 182 108
108 108 108 $ Bottom Sodium Inside
304 4 -0.867784327 -327 -328 -329 330 -331 -332
imp:n=1 u=800 lat=2 fill=-1:1 -1:1 0:0 $Creates Intra Assembly Duct Gap
800 800 800
800 108 800
800 800 800

c Secondary CRD Assembly Layout

```

```

c
160 4 -0.867784327 -900 901 -902 -903 -904 -905 $ Control Rod - 7 Pins
    imp:n=1 u=888 lat=2 fill=-2:2 -2:2 0:0 $ Control Rod - 7 Pins
    0 0 888 888 888 $ Control Rod - 7 Pins
    0 888 55 55 888 $ Control Rod - 7 Pins
    888 55 55 55 888 $ Control Rod - 7 Pins
    888 55 55 888 0 $ Control Rod - 7 Pins
    888 888 888 0 0 $ Control Rod - 7 Pins
614 3 -7.7600000000 -727 -728 -729 730 -731 -732
    imp:n=1 u=185 lat=2 fill=-1:1 -1:1 0:0 $ Creates Inner Duct and Puts CRD
inside
    185 185 185
    185 55 185
    185 185 185
714 4 -0.867784327 -627 -628 -629 630 -631 -632
    imp:n=1 u=186 lat=2 fill=-1:1 -1:1 0:0 $ Creates Inter Duct Gap and Puts
Inner Duct Inside
    186 186 186
    186 185 186
    186 186 186
814 4 -0.867784327 414 imp:n=1 u=187 fill=181 $How Far doe CRDs Extend
815 4 -0.867784327 -414 imp:n=1 u=187 $Sodium Beneith CRDs
214 3 -7.7600000000 -427 -428 -429 430 -431 -432
    imp:n=1 u=188 lat=2 fill=-1:1 -1:1 0:0 $ Creates Outer Duct and puts both
CRD and
    188 188 188
    188 187 188
    188 188 188 $ Bottom Sodium Inside
314 4 -0.867784327 -327 -328 -329 330 -331 -332
    imp:n=1 u=850 lat=2 fill=-1:1 -1:1 0:0 $Creates Intra Assembly Duct Gap
    850 850 850
    850 188 850
    850 850 850

c
c Shield Assembly Layout
107 4 -0.867784327 -41 42 -43 -44 -45 -46 $Shield 17 Pins
    imp:n=1 u=10 lat=2 fill=-3:3 -3:3 0:0 $Shield 17 Pins
    0 0 0 10 10 10 10 $Shield 17 Pins
    0 0 10 9 9 9 10 $Shield 17 Pins
    0 10 9 9 9 9 10 $Shield 17 Pins
    10 9 9 9 9 9 10 $Shield 17 Pins
    10 9 9 9 9 10 0 $Shield 17 Pins
    10 9 9 9 10 0 0 $Shield 17 Pins
    10 10 10 10 0 0 0
205 3 -7.7600000000 -427 -428 -429 430 -431 -432
    imp:n=1 u=110 lat=2 fill=-1:1 -1:1 0:0
    110 110 110
    110 10 110
    110 110 110
305 4 -0.867784327 -327 -328 -329 330 -331 -332
    imp:n=1 u=109 lat=2 fill=-1:1 -1:1 0:0
    109 109 109
    109 110 109
    109 109 109

c
c Core Map Layout $ Assembly Layout
120 4 -0.867784327 -27 -28 -29 30 -31 -32 $ 12 = Coolant
    imp:n=1 u=12 lat=2 fill=0:13 -6:6 0:0 $ 109 = Shield
    0 0 0 0 0 0 0 0 0 0 12 12 $ 600= Reflector
    0 0 0 0 0 0 0 0 0 600 109 12 12 $ 100 = Zone 1 Assembly

```

```

0 0 0 0 0 0 0 300 600 600 109 12 12          $ 300 = Zone 2 Assembly
0 0 0 0 0 0 800 300 300 600 600 109 12 12    $ 800 = Primary CRD
0 0 0 0 100 100 300 300 300 600 600 109 12 12 $ 850 = Secondary CRD
0 0 100 100 100 100 300 300 600 600 109 12 12
950 100 100 850 100 300 800 300 600 600 109 12 12 12 $ 12 = Coolant
0 100 100 100 100 300 300 600 600 109 12 12 12 12 $ 109 = Shield
0 0 100 100 300 300 300 600 600 109 12 12 12 12 $ 600= Reflector
0 0 0 800 300 300 600 600 109 12 12 12 12 12 $ 100 = Zone 1 Assembly
0 0 0 0 300 600 600 109 12 12 12 12 12 12 $ 300 = Zone 2 Assembly
0 0 0 0 0 600 109 12 12 12 12 12 12 12 $ 800 = Primary CRD
0 0 0 0 0 0 12 12 12 12 12 12 12 12 $ 850 = Secondary CRD
130 0 61 62 -63 -64 -65 404 -409 $ Core
      imp:n=1      fill=12      $ Core

```

c

c Nozzle Map Layout

```

150 4 -0.867784327 -95          u=20 imp:n=1 $ mat 4 = Na
151 3 -7.760000000 95          u=20 imp:n=1 $ mat 3 = SS
152 3 -7.760000000 -27 -28 -29 30 -31 -32 $ mat 3 = SS
      imp:n=1 u=21      lat=2 fill=0:13 -6:6 0:0 $ Nozzle
0 0 0 0 0 0 0 0 0 0 21 21 21          $ Nozzle
0 0 0 0 0 0 0 0 0 0 20 20 21 21
0 0 0 0 0 0 0 0 20 20 20 20 21 21
0 0 0 0 0 0 20 20 20 20 20 20 21 21          $ 21 = SS
0 0 0 0 20 20 20 20 20 20 20 21 21          $ 20 = SS/Na
0 0 20 20 20 20 20 20 20 20 20 20 21 21
20 20 20 20 20 20 20 20 20 20 21 21 21
0 20 20 20 20 20 20 20 20 21 21 21 21          $ Nozzle
0 0 20 20 20 20 20 20 20 21 21 21 21          $ Nozzle
0 0 0 20 20 20 20 20 21 21 21 21 21          $ Nozzle
0 0 0 0 20 20 20 20 21 21 21 21 21          $ Nozzle
0 0 0 0 0 20 20 21 21 21 21 21 21 21          $ Nozzle
0 0 0 0 0 0 21 21 21 21 21 21 21 21
153 0 61 62 -63 -64 -65 403 -404 $ SS annulus
      fill=21      imp:n=1      $ SS annulus

```

c

c Bottom Plenum Map Layout

```

154 4 -0.867784327 -95          u=25 imp:n=1 $ SS annulus
155 3 -7.760000000 95 -96      u=25 imp:n=1 $ SS annulus
156 4 -0.867784327 96          u=25 imp:n=1 $ SS annulus
157 4 -0.867784327 -27 -28 -29 30 -31 -32 $ SS annulus
      imp:n=1 u=26      lat=2 fill=0:13 -6:6 0:0 $ SS annulus
0 0 0 0 0 0 0 0 0 0 26 26 26
0 0 0 0 0 0 0 0 0 0 25 25 26 26          $ 26 - Na
0 0 0 0 0 0 0 0 25 25 25 25 26 26          $ 25 - SS annulus
0 0 0 0 0 0 25 25 25 25 25 25 26 26
0 0 0 0 25 25 25 25 25 25 25 25 26 26          $ SS annulus
0 0 25 25 25 25 25 25 25 25 25 25 26 26          $ SS annulus
25 25 25 25 25 25 25 25 25 25 25 26 26 26          $ SS annulus
0 25 25 25 25 25 25 25 25 25 25 26 26 26          $ SS annulus
0 0 25 25 25 25 25 25 25 25 26 26 26 26          $ SS annulus
0 0 0 25 25 25 25 25 26 26 26 26 26 26          $ SS annulus
0 0 0 0 0 25 25 26 26 26 26 26 26 26          $ SS annulus
0 0 0 0 0 0 26 26 26 26 26 26 26 26          $ SS annulus
158 0 61 62 -63 -64 -65 402 -403 $ bottom plate
      fill=26      imp:n=1

```

c

c Boundary Definitions

```

401 3 -7.760000000 61 62 -501 401 -402      imp:n=1 $ bottom Grid Plate
402 4 -0.867784327 (61 62 63 -501 402 -411):

```

```

(61 62 64 -501 402 -411) : (61 62 65 -501 402 -411)    imp:n=1 $ Behind Core
403 41 -0.832068885 61 62 -63 -64 -65
                                409 -411    imp:n=1 $ Upper Handeling Sockett/ Duct Standoff
404 4 -0.867784327 61 62 -503 400 -401    imp:n=1 $relect-low(Sodium)
405 3 -7.760000000 501 -502 61 62 401 -411 imp:n=1 $ core barrel (HT9)
406 4 -0.867784327 502 -503 61 62 401 -408 imp:n=1 $ reflector (Bottom Na ref
to top of gas plentum)
408 4 -0.867784327 502 -503 61 62 408 -411 imp:n=1 $ reflector
407 3 -7.760000000 503 -504 61 62 400 -411 imp:n=1 $ vessel wall
1000 0 -61:-62: 504:-400:411    imp:n=0 $ outside
c end of cell specification

```

```

c
c surface specification
c

```

c trn card constants for equations

1	cz	0.278425				\$ Fuel 1 - driver radius
2	cz	0.3215				\$ Fuel 2 - driver gap outer radius
3	cz	0.3775				\$ Fuel 3 - driver outer clad radius
11	cz	0.278425				\$ Fuel 1 - blanket fuel radius
12	cz	0.3215				\$ Fuel 2 - blanket gap outer radius
13	cz	0.3775				\$ Fuel 3 - blanket outer clad radius
4	cz	0.7705				\$ Reflector 4 - radius
5	cz	1.2765				\$ Shield - radius
6	cz	1.4185				\$ Shield 6 Gap Outer Radius
7	cz	1.6685				\$ Shield 7
8	cz	2.344				\$ CRD 8 - Guide Tube Inner Radius
9	cz	2.387075				\$ CRD 9 - Guide Tube IR + Fuel Gap
Thickness						
10	cz	2.443075				\$ CRD 10 - GT IR + Fuel G.T.+C.T.
95	cz	5.1				\$ hole Nozzle Hole
96	cz	5.6				\$ wall Nozzle Wall
21	px	0.44545				\$ plane 1 Driver Unit Cell Side
22	px	-0.44545				\$ plane 2 Driver Unit Cell Side
23	p	0.257180677	0.44545	0	0.229122266	\$ plane 3 Driver Unit Cell Side
24	p	-0.257180677	-0.44545	0	0.229122266	\$ plane 4 Driver Unit Cell Side
25	p	-0.257180677	0.44545	0	0.229122266	\$ plane 5 Driver Unit Cell Side
26	p	0.257180677	-0.44545	0	0.229122266	\$ plane 6 Driver Unit Cell Side
210	px	0.44545				\$ plane 1 Blanket Fuel Unit Cell Side
220	px	-0.44545				\$ plane 2 Blanket Fuel Unit Cell Side
230	p	0.257180677	0.44545	0	0.229122266	\$ plane 3 Blanket Fuel Unit
CellSide						
240	p	-0.257180677	-0.44545	0	0.229122266	\$ plane 4 Blanket Fuel Unit Cell
Side						
250	p	-0.257180677	0.44545	0	0.229122266	\$ plane 5 Blanket Fuel Unit Cell
Side						
260	p	0.257180677	-0.44545	0	0.229122266	\$ plane 6 Blanket Fuel Unit
CellSide						
35	px	0.7712705				\$ plane 1 Reflector Unit Cell Side
36	px	-0.7712705				\$ plane 2 Reflector Unit Cell Side
37	p	0.445293231	0.7712705	0	0.686883066	\$ plane 3 Reflector Unit Cell
Side						
38	p	-0.445293231	-0.7712705	0	0.686883066	\$ plane 4 Reflector Unit Cell
Side						
39	p	-0.445293231	0.7712705	0	0.686883066	\$ plane 5 Reflector Unit Cell
Side						
40	p	0.445293231	-0.7712705	0	0.686883066	\$ plane 6 Reflector Unit Cell
Side						
900	px	2.411976				\$ plane 1 Guide Tube Unit Cell
901	px	-2.411976				\$ plane 2 Guide Tube Unit Cell

902	p	1.392554993	2.411976	0	6.717618443	\$ plane 3 Guide Tube Unit Cell
903	p	-1.392554993	-2.411976	0	6.717618443	\$ plane 4 Guide Tube Unit Cell
904	p	-1.392554993	2.411976	0	6.717618443	\$ plane 5 Guide Tube Unit Cell
905	p	1.392554993	-2.411976	0	6.717618443	\$ plane 6 Guide Tube Unit Cell
41	px	1.6701685				\$ plane 1 Shield Unit Cell Side
42	px	-1.6701685				\$ plane 2 Shield Unit Cell Side
43	p	0.964272233	1.6701685	0	3.220994218	\$ plane 3 Shield Unit Cell Side
44	p	-0.964272233	-1.6701685	0	3.220994218	\$ plane 4 Shield Unit Cell Side
45	p	-0.964272233	1.6701685	0	3.220994218	\$ plane 5 Shield Unit Cell Side
46	p	0.964272233	-1.6701685	0	3.220994218	\$ plane 6 Shield Unit Cell Side
27	p	8.071	4.659794023	0	75.21839511	\$ plane 1 Assembly Boundry
28	p	-8.071	-4.659794023	0	75.21839511	\$ plane 2 Assembly Boundry
29	py	8.071				\$ plane 3 Assembly Boundry
30	py	-8.071				\$ plane 4 Assembly Boundry
31	p	-8.071	4.659794023	0	75.21839511	\$ plane 5 Assembly Boundry
32	p	8.071	-4.659794023	0	75.21839511	\$ plane 6 Assembly Boundry
327	p	7.883938513	4.551794023	0	71.77212839	\$ plane 1 Duct Outer Boundry
328	p	-7.883938513	-4.551794023	0	71.77212839	\$ plane 2 Duct Outer Boundry
329	py	7.883938513				\$ plane 3 Duct Outer Boundry
330	py	-7.883938513				\$ plane 4 Duct Outer Boundry
331	p	-7.883938513	4.551794023	0	71.77212839	\$ plane 5 Duct Outer Boundry
332	p	7.883938513	-4.551794023	0	71.77212839	\$ plane 6 Duct Outer Boundry
427	p	7.542724504	4.354794023	0	65.69402317	\$ plane 1 Duct Inner Boundry
428	p	-7.542724504	-4.354794023	0	65.69402317	\$ plane 2 Duct Inner Boundry
429	py	7.542724504				\$ plane 3 Duct Inner Boundry
430	py	-7.542724504				\$ plane 4 Duct Inner Boundry
431	p	-7.542724504	4.354794023	0	65.69402317	\$ plane 5 Duct Inner Boundry
432	p	7.542724504	-4.354794023	0	65.69402317	\$ plane 6 Duct Inner Boundry
627	p	7.196314342	4.154794023	0	59.79840763	\$ plane 1 Duct Outer Boundry
628	p	-7.196314342	-4.154794023	0	59.79840763	\$ plane 2 Duct Outer Boundry
629	py	7.196314342				\$ plane 3 Duct Outer Boundry
630	py	-7.196314342				\$ plane 4 Duct Outer Boundry
631	p	-7.196314342	4.154794023	0	59.79840763	\$ plane 5 Duct Outer Boundry
632	p	7.196314342	-4.154794023	0	59.79840763	\$ plane 6 Duct Outer Boundry
727	p	6.855100333	3.957794023	0	54.26215025	\$ plane 1 Duct Inner Boundry
728	p	-6.855100333	-3.957794023	0	54.26215025	\$ plane 2 Duct Inner Boundry
729	py	6.855100333				\$ plane 3 Duct Inner Boundry
730	py	-6.855100333				\$ plane 4 Duct Inner Boundry
731	p	-6.855100333	3.957794023	0	54.26215025	\$ plane 5 Duct Inner Boundry
732	p	6.855100333	-3.957794023	0	54.26215025	\$ plane 6 Duct Inner Boundry
*61	p	68.82477089	-39.736	0	0	\$ symmetry 1 hh= 163
*62	py	0				\$ symmetry 2 rx= 188.2162
63	px	163				\$ core outer rbari= 167.8685
64	p	94.10809388	163	0	30679.2386	\$ plane 1 rx= 194.2378
65	p	169.4273375	97.81891892	0	33146.39798	\$ plane 2 1.4
400	pz	88.9				\$ bottom boundary 100
401	pz	188.9				\$ lower plate - bottom 15.24
402	pz	204.14				\$Bottom Nozzel 91.44
403	pz	295.58				\$ Bottom Nosepiece 35.56 88.9
404	pz	331.14				\$ Bottom Lower sheild Pin 124.46
405	pz	455.6				\$ core bottom 81.28
407	pz	536.88				\$ core top (TRU) 124.46
408	pz	661.34				\$ gas top (He) 2.54
409	pz	663.88				\$ pin top (HT9) 78.74
410	pz	742.62				\$ Duct Standoff (Only Na in 30.48
411	pz	773.1				\$ Handeling Socket (HT9)
413	pz	541.9				\$ CRD height 86.3 100.00
5.02ANARCHY		541.9				
414	pz	541.9				\$ CRD height 5.02ANARCHY
541.9						

```

415 pz 455.6 $ CRD height 5.02ANARCHY
541.9
501 cz 173.8684918 $ Barrel in
502 cz 175.8684918 $ Barrel out
503 cz 245.8684918 $ Vessel In
504 cz 258.3684918 $ Vessel Out
c end of surface specification

c
c data specification
c
c problem type
mode n
c
c cell and surface parameters
c
c source specification
c
c 9. kcode criticality source card
c nsrck rkk ikz kct msrk knrm
kcode 4600 1 250 500
c prdmp 500 500 500
c
c 10. ksrc source point for kcode calculation
c xl yl zl... location for initial source point
c ksrc 13.51 7.386 500 28.775 4.573 510
c 27.848 16.17 480 42.35 7.3 490
c 18.4 22.64 520 27.426 33.13 500
c material specification
c
c 1. mm material card roeZr= 6.5 roeU= 19.1 roeCM 13.511 roeNp 20.4 roe AM
13.6
c fuel meat Pu/Ma/Zr (Zone (10wt%Zr) roe= 15.979 atom% at_fr*Mi weight% wt_fr
final wt%Mi 15.57% roe= 13.29035206
m1 92235.37c -0.0014886 $ fuel u-235 - - 0.200% 0.002 0.1489%
235 18.286.334E-06 0.001300645
92238.37c -0.7428114 $ fuel u-238 - - 99.800% 0.998 74.2811%
238 0.0031211 0.640841031
94238.37c -0.003394599 $ fuel Pu238 - - 2.180% 0.022 0.3395%
238 1.426E-05 0.002928602
94239.37c -0.073715752 $ fuel Pu-239 - - 47.340% 0.473 7.3716%
239 0.0003084 0.063330236
94240.37c -0.035534293 $ fuel Pu240 - - 22.820% 0.228 3.5534%
243 0.0001462 0.030025491
94241.37c -0.013111251 $ fuel Pu241 - - 8.420% 0.084 1.3111%
241 5.44E-05 0.011170582
94242.37c -0.010650945 $ fuel Pu242 - - 6.840% 0.068 1.0651%
242 4.401E-05 0.009036942
93237.37c -0.007349775 $ fuel Np237 - - 4.720% 0.047 0.7350%
237 3.101E-05 0.00636758
95241.37c -0.008735644 $ fuel Am241 - - 5.610% 0.056 0.8736%
241 3.625E-05 0.007442632
95243.37c -0.002429163 $ fuel Am243 - - 1.560% 0.016 0.2429%
243 9.997E-06 0.002052575
96244.37c -0.000716292 $ fuel Cm244 - - 0.460% 0.005 0.0716%
244 2.936E-06 0.000602766
96245.37c -6.22862E-05 $ fuel Cm245 - - 0.040% 0.000 0.0062%
245 2.542E-07 5.22005E-05
40090.37c -0.050707196 $ fuel Zr90 51.45% 0.46305 50.707% 0.507
5.0707% 90 0.0051450.0005634 0.115684665

```

40091.37c	-0.011180879	\$ fuel Zr91	11.22%	0.102102	11.181%	0.112				
1.1181% 91	0.0011220.0001229	0.025228026								
40092.37c	-0.017278007	\$ fuel Zr92	17.15%	0.15778	17.278%	0.173				
1.7278% 92	0.0017150.0001878	0.038561555								
40094.37c	-0.01789037	\$ fuel Zr94	17.38%	0.163372	17.890%	0.179				
1.7890% 94	0.0017380.0001903	0.039078707								
40096.37c	-0.002943547	\$ fuel Zr96	2.80%	0.02688	2.944%	0.029				
0.2944% 96	0.000283.066E-05	0.006295764								
c fuel meat Pu/Ma	(10wt%Zr)	roe=	15.982	atom%	at_fr*Mi	weight% wt_fr				
final wt%Mi	19.46%	Element U	Pu Am Cm Np Zr	Zone1	Zone2					
m10	92235.37c	-0.001410776	\$ fuel u-235	-	-	0.200% 0.002 0.1411%				
235	25.04	Density(g/cc	19.05	19.8	13.6	13.511	20.4	6.5	15.98	15.98
	92238.37c	-0.703977459	\$ fuel u-238	-	-	99.800%	0.998	70.3977%		
238										
	94238.37c	-0.004242961	\$ fuel Pu238	-	-	2.180%	0.022	0.4243%		
238										
	94239.37c	-0.092138423	\$ fuel Pu-239	-	-	47.340%	0.473	9.2138%		
239										
	94240.37c	-0.044414846	\$ fuel Pu240	-	-	22.820%	0.228	4.4415%		
243										
	94241.37c	-0.016387949	\$ fuel Pu241	-	-	8.420%	0.084	1.6388%		
241										
	94242.37c	-0.013312776	\$ fuel Pu242	-	-	6.840%	0.068	1.3313%		
242										
	93237.37c	-0.009186594	\$ fuel Np237	-	-	4.720%	0.047	0.9187%		
237										
	95241.37c	-0.010918812	\$ fuel Am241	-	-	5.610%	0.056	1.0919%		
241										
	95243.37c	-0.003036247	\$ fuel Am243	-	-	1.560%	0.016	0.3036%		
243										
	96244.37c	-0.000895304	\$ fuel Cm244	-	-	0.460%	0.005	0.0895%		
244										
	96245.37c	-7.78525E-05	\$ fuel Cm245	-	-	0.040%	0.000	0.0078%		
245										
	40090.37c	-0.050707196	\$ fuel Zr90	51.45%	0.46305	50.707%	0.507			
5.0707% 90										
	40091.37c	-0.011180879	\$ fuel Zr91	11.22%	0.102102	11.181%	0.112			
1.1181% 91										
	40092.37c	-0.017278007	\$ fuel Zr92	17.15%	0.15778	17.278%	0.173			
1.7278% 92										
	40094.37c	-0.01789037	\$ fuel Zr94	17.38%	0.163372	17.890%	0.179			
1.7890% 94										
	40096.37c	-0.002943547	\$ fuel Zr96	2.80%	0.02688	2.944%	0.029			
0.2944% 96										
m2	11023.36c	1	\$ Na Bond							
m3	26054.36c	-0.04908772		\$ HT9 -Fe		Refernce	INL/EXT-07-13592			
	26056.36c	-0.776263048								
	26057.36c	-0.01861948								
	26058.36c	-0.002369752								
	24050.36c	-0.00525745								
	24052.36c	-0.10138469								
	24053.36c	-0.01149621								
	24054.36c	-0.00286165								
	42092.36c	-0.00154336								
	42094.36c	-0.000962								
	42095.36c	-0.00165568								
	42096.36c	-0.00173472								
	42097.36c	-0.0009932								
	42098.36c	-0.00250952								
	42100.36c	-0.00100152								

	25055.36c	-0.0057	
	28058.36c	-0.003471927	
	28060.36c	-0.001337883	
	28061.36c	-0.00005814	
	28062.36c	-0.000185334	
	28064.36c	-0.000046716	
	74182.36c	-0.001193933	
	74183.36c	-0.000644724	
	74184.36c	-0.001380457	
	74186.36c	-0.001280887	
	23000.36c	-0.0028	
	6000.36c	-0.002	
	14028.36c	-0.0015677	
	14029.36c	-0.0000797	
	14030.36c	-0.0000526	
	7014.36c	-0.00027	
	15031.36c	-0.00016	
	16032.36c	-0.00003	
m4	11023.33c	1	\$ cold Na coolant
m41	11023.34c	1	\$ cold Na coolant
m40	11023.35c	1	\$ hot Na coolant
m5	2004.35c	1	\$ helium
m8	5010.35c	0.48	\$ CRD-b10 Enriched 60%
	5011.35c	0.32	\$ CRD-b11
	6000.35c	0.2	\$ CRD-c
m9	5010.35c	0.1592	\$ CRD-b10 Natural 19.90%
	5011.35c	0.6408	\$ CRD-b11
	6000.35c	0.2	\$ CRD-c
m15	5010.35c	0.1592	\$ shl-b10 Natural 19.90%
	5011.35c	0.6408	\$ shl-b11
	6000.35c	0.2	\$ shl-c

c void

c energy and thermal treatment specification

c

c 1. phys energy physics cutoff cards

c emax emcnf

phys:n 20 0.0

c

c 3. tmp free-gas thermal temperature card

c t1n t2n...n=index of time,t1n=temp for cell 1 at time n

#	tmp1	\$	kb= 8.61734E-05 ev/k		
1	7.755602E-08	\$ Mev	T= 900 K	Fuel	
2	5.411687E-08	\$ Mev	T= 628 K		
3	6.893869E-08	\$ Mev	T= 800 K		
4	6.893869E-08	\$ Mev	T= 800 K	4	628K
5	6.893869E-08	\$ Mev	T= 800 K	40	705.5K
6	6.893869E-08	\$ Mev	T= 800 K	41	783K
7	6.079530E-08	\$ Mev	T= 706 K		
10	7.755602E-08	\$ Mev	T= 900 K	Fuel	
11	5.411687E-08	\$ Mev	T= 628 K		
12	6.893869E-08	\$ Mev	T= 800 K		
13	6.893869E-08	\$ Mev	T= 800 K		
14	6.893869E-08	\$ Mev	T= 800 K		
15	6.893869E-08	\$ Mev	T= 800 K		
16	6.079530E-08	\$ Mev	T= 706 K		
17	6.032135E-08	\$ Mev	T= 700 K		
18	6.079530E-08	\$ Mev	T= 706 K		
20	6.032135E-08	\$ Mev	T= 700 K		
21	6.032135E-08	\$ Mev	T= 700 K		
22	6.032135E-08	\$ Mev	T= 700 K		

23	6.079530E-08	\$ Mev	T= 706 K
44	6.032135E-08	\$ Mev	T= 700 K
45	6.032135E-08	\$ Mev	T= 700 K
46	6.032135E-08	\$ Mev	T= 700 K
47	6.032135E-08	\$ Mev	T= 700 K
48	6.079530E-08	\$ Mev	T= 706 K
101	6.079530E-08	\$ Mev	T= 706 K
102	6.079530E-08	\$ Mev	T= 706 K
103	6.079530E-08	\$ Mev	T= 706 K
106	6.032135E-08	\$ Mev	T= 700 K
107	6.032135E-08	\$ Mev	T= 700 K
120	6.032135E-08	\$ Mev	T= 700 K
130	6.032135E-08	\$ Mev	T= 700 K
150	6.032135E-08	\$ Mev	T= 700 K
151	6.032135E-08	\$ Mev	T= 700 K
152	6.032135E-08	\$ Mev	T= 700 K
153	6.032135E-08	\$ Mev	T= 700 K
154	6.032135E-08	\$ Mev	T= 700 K
155	6.032135E-08	\$ Mev	T= 700 K
156	6.032135E-08	\$ Mev	T= 700 K
157	6.032135E-08	\$ Mev	T= 700 K
158	6.032135E-08	\$ Mev	T= 700 K
401	6.032135E-08	\$ Mev	T= 700 K
402	6.032135E-08	\$ Mev	T= 700 K
403	6.032135E-08	\$ Mev	T= 700 K
404	6.032135E-08	\$ Mev	T= 700 K
405	6.032135E-08	\$ Mev	T= 700 K
406	6.032135E-08	\$ Mev	T= 700 K
407	6.032135E-08	\$ Mev	T= 700 K
408	6.032135E-08	\$ Mev	T= 700 K
1000	6.032135E-08	\$ Mev	T= 700 K
201	6.032135E-08	\$ Mev	T= 700 K
202	6.032135E-08	\$ Mev	T= 700 K
203	6.032135E-08	\$ Mev	T= 700 K
204	6.032135E-08	\$ Mev	T= 700 K
205	6.032135E-08	\$ Mev	T= 700 K
301	6.032135E-08	\$ Mev	T= 700 K
302	6.032135E-08	\$ Mev	T= 700 K
303	6.032135E-08	\$ Mev	T= 700 K
304	6.032135E-08	\$ Mev	T= 700 K
305	6.032135E-08	\$ Mev	T= 700 K
50	6.079530E-08	\$ Mev	T= 706 K
51	6.747374E-08	\$ Mev	T= 783 K
52	6.079530E-08	\$ Mev	T= 706 K
53	6.747374E-08	\$ Mev	T= 783 K
c 54	6.079530E-08	\$ Mev	T= 706 K
c 55	6.079530E-08	\$ Mev	T= 706 K
c 56	6.079530E-08	\$ Mev	T= 706 K
604	6.032135E-08	\$ Mev	T= 700 K
704	6.032135E-08	\$ Mev	T= 700 K
804	6.032135E-08	\$ Mev	T= 700 K
805	6.032135E-08	\$ Mev	T= 700 K
160	6.032135E-08	\$ Mev	T= 700 K
614	6.032135E-08	\$ Mev	T= 700 K
714	6.032135E-08	\$ Mev	T= 700 K
814	6.032135E-08	\$ Mev	T= 700 K
815	6.032135E-08	\$ Mev	T= 700 K
214	6.032135E-08	\$ Mev	T= 700 K
314	6.032135E-08	\$ Mev	T= 700 K
944	6.032135E-08	\$ Mev	T= 700 K

```

945 6.032135E-08 $ Mev T= 700 K
946 6.032135E-08 $ Mev T= 700 K
947 6.032135E-08 $ Mev T= 700 K
948 6.079530E-08 $ Mev T= 706 K
c 956 6.032135E-08 $ Mev T= 700 K
c
  thtme 0
c  problem cutoff cards
c
c  user data array
c
c  periferal cards
c imp:n=1 u=12 lat=2 fill=0:-6:6 0:00
c   0  1  2  3  4  5  6  7  8  9  10  11  12  13
c -6  0  0  0  0  0  0  0  0  0  0  0  12  12
c -5  0  0  0  0  0  0  0  0  0  600 109 12 12
c -4  0  0  0  0  0  0  0 300 600 600 109 12 12
c -3  0  0  0  0  0 800 300 300 600 600 109 12 12
c -2  0  0  0  0 100 100 300 300 300 600 600 109 12 12
c -1  0  0 100 100 100 100 300 300 600 600 109 12 12 12
c  0 850 100 100 850 100 300 800 300 600 600 109 12 12 12
c  1  0 100 100 100 100 300 300 600 600 109 12 12 12 12
c  2  0  0 100 100 300 300 300 600 600 109 12 12 12 12
c  3  0  0  0 800 300 300 600 600 109 12 12 12 12 12
c  4  0  0  0  0 300 600 600 109 12 12 12 12 12 12
c  5  0  0  0  0  0 600 109 12 12 12 12 12 12 12
c  6  0  0  0  0  0  0 12 12 12 12 12 12 12 12
c f4:n          $ FluxTally over fuel rods in Zone 1
c (1<120[61])
c (1<120[62])
c (1<120[73])
c (1<120[74])
c (1<120[75])
c (1<120[76])
c (1<120[86])
c (1<120[87])
c (1<120[89])
c (1<120[100])
c (1<120[101])
c (1<120[102])
c (1<120[103])
c (1<120[115])
c (1<120[116])
c fc4 Flux Tallys in Zone 1      15.57% Enriched
c f14:n          $ Flux Tally over fuel rods in Zone 2
c (10<120[37])
c (10<120[50])
c (10<120[51])
c (10<120[63])
c (10<120[64])
c (10<120[65])
c (10<120[77])
c (10<120[78])
c (10<120[90])
c (10<120[92])
c (10<120[104])
c (10<120[105])
c (10<120[117])
c (10<120[118])
c (10<120[119])

```

```

c (10<120[131])
c (10<120[132])
c (10<120[145])
c fc14 Flux Tallys in Zone 2      19.46% Enriched
c f24:n
c ( 17 <[ 10 -5 0 ] )
c ( 17 <[ 9 -4 0 ] )
c ( 17 <[ 10 -4 0 ] )
c ( 17 <[ 9 -3 0 ] )
c ( 17 <[ 10 -3 0 ] )
c ( 17 <[ 9 -2 0 ] )
c ( 17 <[ 10 -2 0 ] )
c ( 17 <[ 8 -1 0 ] )
c ( 17 <[ 9 -1 0 ] )
c ( 17 <[ 8 0 0 ] )
c ( 17 <[ 9 0 0 ] )
c ( 17 <[ 7 1 0 ] )
c ( 17 <[ 8 1 0 ] )
c ( 17 <[ 7 2 0 ] )
c ( 17 <[ 8 2 0 ] )
c ( 17 <[ 6 3 0 ] )
c ( 17 <[ 7 3 0 ] )
c ( 17 <[ 5 4 0 ] )
c ( 17 <[ 6 4 0 ] )
c ( 17 <[ 5 5 0 ] )
c fc24 Flux Tallys in Zone 2      Reflectors
f57:n      $ Heating Tally over fuel rods in Zone 1
(1<120[61])
(1<120[62])
(1<120[73])
(1<120[74])
(1<120[75])
(1<120[76])
(1<120[86])
(1<120[87])
(1<120[89])
(1<120[100])
(1<120[101])
(1<120[102])
(1<120[103])
(1<120[115])
(1<120[116])
(10<120[37])
(10<120[50])
(10<120[51])
(10<120[63])
(10<120[64])
(10<120[65])
(10<120[77])
(10<120[78])
(10<120[90])
(10<120[92])
(10<120[104])
(10<120[105])
(10<120[117])
(10<120[118])
(10<120[119])
(10<120[131])
(10<120[132])
(10<120[145])

```

```

fc57 Heating Tallys
c      -10  -9  -8  -7  -6  -5  -4  -3  -2  -1  0  1  2  3  4  5
6      7  8  9  10
c-10   0  0  0  0  0  0  0  0  0  0  1  1  1  1  1  1
1      1  1  1  1  1
c-9    0  0  0  0  0  0  0  0  0  1  2  2  2  2  2  2  2
2      2  2  1
c-8    0  0  0  0  0  0  0  1  2  2  2  2  2  2  2  2
2      2  2  1
c-7    0  0  0  0  0  0  1  2  2  2  2  2  2  2  2  2
2      2  2  1
c-6    0  0  0  0  0  1  2  2  2  2  2  2  2  2  2  2
2      2  2  1
c-5    0  0  0  0  1  2  2  2  2  2  2  2  2  2  2  2
2      2  2  1
c-4    0  0  0  1  2  2  2  2  2  2  2  2  2  2  2  2
2      2  2  1
c-3    0  0  0  1  2  2  2  2  2  2  2  2  2  2  2  2
2      2  2  1
c-2    0  0  1  2  2  2  2  2  2  2  2  2  2  2  2  2
2      2  2  1
c-1    0  1  2  2  2  2  2  2  2  2  2  2  2  2  2  2
2      2  2  1
c0     1  2  2  2  2  2  2  2  2  2  2  2  2  2  2  2
2      2  2  1
c1     1  2  2  2  2  2  2  2  2  2  2  2  2  2  2  2
2      2  1  0
c2     1  2  2  2  2  2  2  2  2  2  2  2  2  2  2  2
2      1  0  0
c3     1  2  2  2  2  2  2  2  2  2  2  2  2  2  2  2
1      0  0  0
c4     1  2  2  2  2  2  2  2  2  2  2  2  2  2  2  1
0      0  0  0
c5     1  2  2  2  2  2  2  2  2  2  2  2  2  2  1  0
0      0  0  0
c6     1  2  2  2  2  2  2  2  2  2  2  2  2  1  0  0
0      0  0  0
c7     1  2  2  2  2  2  2  2  2  2  2  2  1  0  0  0
0      0  0  0
c8     1  2  2  2  2  2  2  2  2  2  2  1  0  0  0  0
0      0  0  0
c9     1  2  2  2  2  2  2  2  2  2  1  0  0  0  0  0
0      0  0  0
c10    1  1  1  1  1  1  1  1  1  1  1  0  0  0  0  0
0      0  0  0  0
c
c
c
c
c
print -60 -85 -130 -126 -128
c
c MCODE INPUT
c1 69736.9 fftfc.lib 900 0.999 1 50 $ Burn Mat 1, 13 assemblies * 271 Pins per
Assembly * vol/pin, FFTFC ORIGEN lib, 900K, Tally 50
c10 91194.4 fftfc.lib 900 0.999 1 80 $ Burn Mat 10, 17 assemblies * 271 Pins per
Assembly * vol/pin, FFTFC ORIGEN lib, 900K, Tally 80
c mce /mcnprun
c mcxs /home/CODES/mcode/mcnpxs.sum
c orge /home/CODES/origen22/origen22

```



```

c orgl /home/CODES/origen22/libs decay.lib gxuo2brm.lib
c mcs      2      labrs      $ Use the source file labrs
c tal      1      1
c          10     10
c nor      2      0
c cor      0
c pow     166666666.7      $ The total power of the 1/6 model core is 1000e6/6
watts
c DEP      D      1      1      $ Run a full power and recalculate flux at the following
days
c          10     1
c          30     1
c          60     1
c          100    1
c          150    1
c          200    1
c          250    1
c          300    1
c          365    1
c mci      -1      $ Print all MCODE INPUTS ?
c sta
c end      $ RUN
          $ END

```

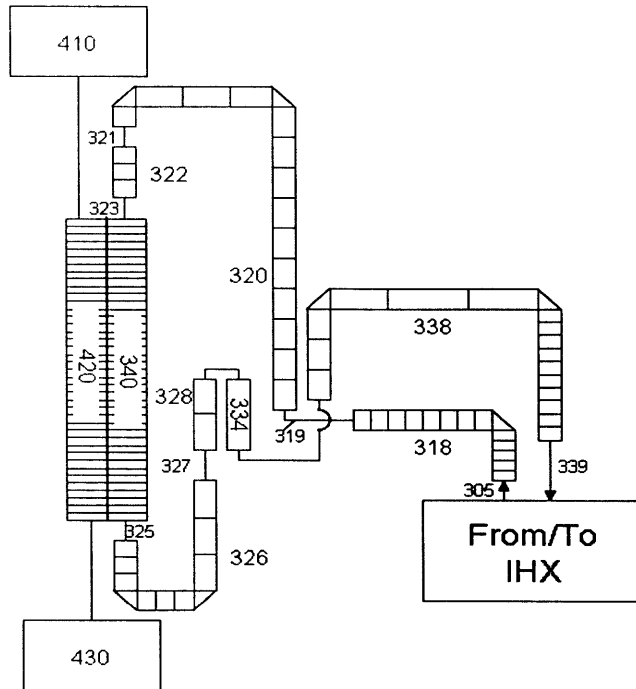



FIGURE B-0-2: RELAP5 MODEL OF THE ABR-1000 INTERMEDIATE HEAT TRANSPORT SYSTEM.

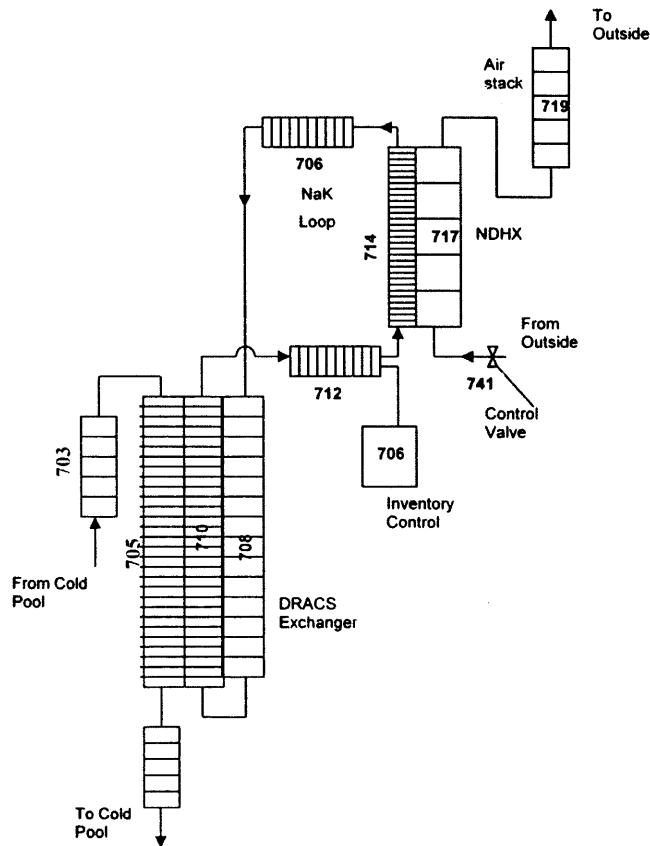


FIGURE B-0-3: RELAP5 MODEL OF THE ABR-1000 DECAY HEAT REMOVAL SYSTEM.

```

= Primary Heat Transport System for ABR 1000 ULOF – METAL FUEL
* Created from information found in ANL 1000 Design Report
* (See file ABR1000.xls for geometric considerations, assumptions, and
* Calculations)
* CURIE POINT EFFECTIVENESS - ULOF - Metal
* Last updated April 30, 2010
* J. D. DeWitte, M.R Denman, M.J Memmott
*****
* Distribution Parameters
*****
* Flow Halving Time:0.000000
* Doppler 300.000000 -0.366056
* 600.000000 -2.928274
* 900.000000 -5.223893
* 1064.385820 -6.420841
* 1125.000000 -6.862193
* 1275.000000 -7.479196
* Sodium 0.001524
* CRE -0.003342 CRDLE -0.471077
*****
* run setup
*****
0000100 restart transnt
0000101 run
0000102 si si
0000103 -1
0000105 1.0 2.0 1.e6
0000107 1 1 1
*****
* Matt D Added Card
*****
0000200 0 1
*****
0000201 100.000000 1.0e-7 0.005 00019 17 6000 60000
*
*
*****
* minor edit variables *
*****
$ Var. Parameter
301 mflowj 201010000 *Core Mass Flow Rate
302 cntrlvar 8800 *DRACS Power
303 pmpvel 262 *Primary Pump Velocity
304 tempf 2010000 *Core Inlet Temperature
305 tempf 4010000 *Core Outlet Temperature
306 cntrlvar 8150 *Max Coolant Temp
308 rktpow 0 *Reactor Power
309 tempf 150140000 *Hot Channel Outlet Temperature
310 cntrlvar 10 *Max Clad Temp
311 cntrlvar 11 *Max Fuel Temp
312 cntrlvar 8210 * Core Radial Expansion
313 cntrlvar 8211 * CRDLE
314 cntrlvar 8212 *Structural Expansion
315 cntrlvar 8213 * Axial Expansion
316 rkreact 0 * Reactivity
317 tempf 150160000 *Hot Channel Top Outlet Temperature
318 tempf 110160000 *Control Rod Top Outlet Temperature
*
*
* Thermal Conductivity

```

```

20100300 tbl/fctn 1 1
20100301 310.93 14.143
20100302 533.15 17.632
20100303 699.82 20.249
20100304 810.93 21.994
20100305 1088.71 26.355
20100306 4088.71 26.355
* Heat Capacity
20100351 310.93 3.690e6
20100352 533.15 4.256e6
20100353 699.82 4.407e6
20100354 810.93 4.513e6
20100355 1088.71 4.913e6
20100356 4088.71 4.913e6
*
*
*
20582000 RADexp sum 1.0 -2.616082 1
20582001 0.0 -0.003342 tempf 004010000
*
20582010 CRDLexp sum 1.0 -7.009479 1
20582011 0.0 1.0 cntrlvar 8205
*
20582050 CRDLcalc sum 1.0 -7.009479 1
20582051 0.0 -0.471077 cntrlvar 8204
*
*****
* Control Vars to Plot reactivity for each effect listed above
*****
*
20582100 radexp sum 1.0 0.0 1
20582101 2.616082 -0.003342 tempf 004010000
*
20582110 CRDLexp sum 1.0 0.0 1
20582111 7.009479 1.0 cntrlvar 8205
*
20582140 NORMPOW sum 1.0 0.0 1
20582141 0.0 0.00000001 rktpow 0
*
20582150 NORMFLOW sum 1.0 0.0 1
20582151 0.0 0.000196 mflowj 201010000
*
20582160 POWFLOW div 1.0 0.0 1
20582161 cntrlvar 8215 cntrlvar 8214
*
*****
* Transient trips
*****
*
20600000 expanded
20605010 time 0 ge null 0 3. 1 *DRACS Valve Trip
20602620 time 0 ge null 0 3. 1 *Pump Trip
20609990 time 0 ge null 0 3. 1 *Decay Power initiation
*20601000 time 0 ge null 0 3. 1 *UTOP initiation
*20606660 rktpow 0 ge null 0 1.19e9 1 *SCRAM on Power
*20606670 tempf 4010000 ge null 0 830. 1 *SCRAM on Temp
*20606680 cntrlvar 8216 ge null 0 1.3 1 *SCRAM on Temp
20605030 tempf 110160000 gt null 0 811.849504 1 *Curie Point Actuation
*
*****

```

* Reactivity Insertion Table

```

*
*
*
20299100 reac-t 503
20299101 0.0 0.0
20299102 1.5 0.0
20299103 2.0 -0.15
20299104 2.5 -1.0215
20299105 3.0 -3.9
20299106 3.5 -6.7
20299107 100000. -6.7
20299200 reac-t 0
20299201 0.0 0.0
20299202 1.0 0.0
20299203 3.0 -6.0
20299204 100000. -6.0
20299300 reac-t 0
20299301 0.0 0.0
20299302 1.0 0.0
20299303 3.0 -6.0
20299304 100000. -6.0

```

* Pump Coastdown Tables

** For each of these EM pumps, 2 pumps are combined in series for a total of 4 p

```

*hydro name type
2600000 pmp1ent snglvol
2600101 0.676071 1.6 0.0 0.0 90. 1.6 4.5e-5 0.2 0000000
2600200 0 202801.3 549470. 5255980. 0.

```

```

*hydro name type
2700000 pmp1ent snglvol
2700101 0.676071 1.6 0.0 0.0 90. 1.6 4.5e-5 0.2 0000000
2700200 0 198729.3 549470. 5255394. 0.

```

*For the pumps sized in the ANL Report, the area is wrong! For pumps of that
*a velocity of 400m/s through the pump duct is achieved. AS a result, a new are
*reflects the appropriate pressure drop of the system is achieved by adjusting t
*until the pressure drop matches the pump area. An alternative to this is maint
*area which gives a velocity of ~ 4m/s, and adjusting the ks to give an approp
*In this model, Kwere approximated sudden entrance/exit, and the area was
*until an adequate pressure drop/flow rate was achieved.
*(Actual calculated area is 0.006154, adjusted is 0.405255)

```

*hydro name type
2620000 empump1 pump
2620101 .405255 1.6 0.0 0.0 -90. -1.6 0000000
2620108 260010000 0.0 .5 .1 00000000 * these Ks are based upon a flanged 180 re
2620109 264000000 0.0 1. .5 00000000
2620200 0 569575. 550428. 5279694. 0.
2620201 0 7.26608 8.03966 0. * 2556.006

```

```

2620202 0 7.26696 7.26696 0. * 2556.006
*****
*****
* Brinham pump, 1 phase, no 2 phase, no tourqe table used,time dependant pump velocity index, trip
on 262, reverse flow allowed
2620301 0 -1 -3 -1 0 262 1 $ This is for variable pumping** mrd 4/11
*****
*****
*2620301 0 -1 -3 -1 0 262 0 $ This is for pump table (gradual startup)
*2620302 251.32 1.0 2.96 91.02 18421.227 160.0 851.35 0. .1 21.53 21.53 0. 0. *t
2620302 251.32 1. 2.96 91.02 18421.227 160.0 851.35 0. .1 21.53 21.53 0. 0. *to
*2626100 0
*2626101 0.0 0.0
*2626102 0.1 251.32
*head curve, region 1
2621100 1 1 0.0 .45263 *extrapolated value*
2621101 .11904762 .46315789
2621102 .15873016 .47368421
2621103 .23809524 .51578947
2621104 .31746032 .55263158
2621105 .39682540 .60526316
2621106 .47619048 .67105263
2621107 .55555556 .73684211
2621108 .63492063 .81578947
2621109 .71428571 .90789474
2621110 .79365079 1.0
2621111 .87301587 1.10526316
2621112 .95238095 1.14473684
2621113 1. 1.
*torque curve, region 1
2621200 2 1 0.0 .51087174 *extrapolated value*
2621201 .11904762 0.51522074
2621202 .15873016 0.52191192
2621203 .23809524 0.53278508
2621204 .31746032 0.58790078
2621205 .39682540 0.61423844
2621206 .47619048 0.66071828
2621207 .55555556 0.68588425
2621208 .63492063 0.77036280
2621209 .71428571 0.87528978
2621210 .79365079 0.91817838
2621211 .87301587 1.01924103
2621212 .95238095 1.07018303
2621213 1. 1.
*head curve, region 2
2621300 1 2 .89 .00016955 *extrapolated value*
2621301 .9 .05328947 *extrapolated value*
2621302 .91636364 .25412649
2621303 .93333333 .48140351
2621304 .96923077 .84052320
*torque curve, region 2
2621400 2 2 .86 .001851911 *extrapolated value*
2621401 .89 .290312645 *extrapolated value*
2621402 .9 .479506579 *extrapolated value*
2621403 .91636364 .539000268
2621404 .93333333 .626555263
2621405 .96923077 .877865891
*head curve, region 8 *extrapolated values*
2621501 1 8 -1.0 .880611
2621502 0.0 .880611

```

```

*torque curve, region 8 *extrapolated values*
2621601 2 8 -1.0 .846348
2621602 0.0 .846348
*head curve, region 3
2621700 1 3 -1.0 0.45263
2621701 0.0 0.45263
*torque curve, region 3
2621800 2 3 -1.0 0.51087174
2621801 0.0 0.51087174
*
*For Some Strange Reason, region 4 is needed durring startup, so here is a guess
*
*head curve, region 4 *extrapolated values*
2621900 1 4 -1.0 0.200
2621901 0.0 .200
*torque curve, region 4 *extrapolated values*
2622000 2 4 -1.0 0.220
2622001 0.0 .220
*****mrd
4/11/09*****
*****
***
* 4 primary pumps break, no coastdown
2626101 -1.0 253.0 $ time =0, full flow
2626102 0.5 253.0
2626103 5.000000 253.000000
2626104 14.000000 0.000000
2626105 23.000000 0.000000
2626106 32.000000 0.000000
2626107 41.000000 0.000000
2626108 50.000000 0.000000
2626109 1000.0 0.1
*
*****
***
*
*hydro name type
2720000 empump1 pump
2720101 .405255 1.6 0.0 0.0 -90. -1.6 0000000
2720108 270010000 0.0 .5 .1 00000000 * these Ks are based upon a flanged 18 upo
2720109 274000000 0.0 1. .5 00000000
2720200 0 567583. 550431. 5279639. 0.
2720201 0 7.25373 8.02682 0. * 2551.66
2720202 0 7.25461 7.25461 0. * 2551.66
*****
*****
* Brinham pump, 1 phase, no 2 phase, no tourqe table used,time dependant pump velocity index, trip
on 262, reverse flow allowed
2720301 0 -1 -3 -1 0 262 1 $ This is for variable pumping*
*****
*****
*2720301 0 -1 -3 -1 0 262 0 $ This is for pump table (gradual startup) $
*2720302 251.32 1.0 2.96 91.02 18421.227 160.0 851.35 0. .1 21.53 21.53 0. 0. *
2720302 251.32 1. 2.96 91.02 18421.227 160.0 851.35 0. .1 21.53 21.53 0. 0. *t
*2726100 0
*2726101 0.0 0.0
*2726102 0.1 251.32
*head curve, region 1
2721100 1 1 0.0 .45263 *extrapolated value*
2721101 .11904762 .46315789

```


2721102 .15873016 .47368421
 2721103 .23809524 .51578947
 2721104 .31746032 .55263158
 2721105 .39682540 .60526316
 2721106 .47619048 .67105263
 2721107 .55555556 .73684211
 2721108 .63492063 .81578947
 2721109 .71428571 .90789474
 2721110 .79365079 1.0
 2721111 .87301587 1.10526316
 2721112 .95238095 1.14473684
 2721113 1. 1.
 *torque curve, region 1
 2721200 2 1 0.0 .51087174 *extrapolated value*
 2721201 .11904762 0.51522074
 2721202 .15873016 0.52191192
 2721203 .23809524 0.53278508
 2721204 .31746032 0.58790078
 2721205 .39682540 0.61423844
 2721206 .47619048 0.66071828
 2721207 .55555556 0.68588425
 2721208 .63492063 0.77036280
 2721209 .71428571 0.87528978
 2721210 .79365079 0.91817838
 2721211 .87301587 1.01924103
 2721212 .95238095 1.07018303
 2721213 1. 1.
 *head curve, region 2
 2721300 1 2 .89 .00016955 *extrapolated value*
 2721301 .9 .05328947 *extrapolated value*
 2721302 .91636364 .25412649
 2721303 .93333333 .48140351
 2721304 .96923077 .84052320
 *torque curve, region 2
 2721400 2 2 .86 .001851911 *extrapolated value*
 2721401 .89 .290312645 *extrapolated value*
 2721402 .9 .479506579 *extrapolated value*
 2721403 .91636364 .539000268
 2721404 .93333333 .626555263
 2721405 .96923077 .877865891
 *head curve, region 8 *extrapolated values*
 2721501 1 8 -1.0 .880611
 2721502 0.0 .880611
 *torque curve, region 8 *extrapolated values*
 2721601 2 8 -1.0 .846348
 2721602 0.0 .846348
 *head curve, region 3
 2721700 1 3 -1.0 0.45263
 2721701 0.0 0.45263
 *torque curve, region 3
 2721800 2 3 -1.0 0.51087174
 2721801 0.0 0.51087174
 *
 *
 *For Some Strange Reason, region 4 is needed durring startup, so here is a guess
 *
 *head curve, region 4 *extrapolated values*
 2721900 1 4 -1.0 0.200
 2721901 0.0 .600
 *torque curve, region 4 *extrapolated values*

2722000 2 4 -1.0 0.220
2722001 0.0 .220

*
*

*****mrd

4/11/09*****

* 2 primary pumps break, no coastdown

2726102 0.5 253.0
2726103 1.0 253.0
2726104 1.5 253.0
2726105 2.0 253.0
2726106 2.5 253.0
2726107 3.0 253.0
2726108 1000.0 253.0

*

*

\$=====

* decay power based on Eugenes calculations for the new core

20210600 power 999 1.0 1.0

* time p/po

20210601 -1.0 0.0
20210602 0.0E+00 7.00E-02
20210603 1.0E+00 5.52E-02
20210604 1.5E+00 5.37E-02
20210605 2.0E+00 5.24E-02
20210606 4.0E+00 4.88E-02
20210607 6.0E+00 4.65E-02
20210608 8.0E+00 4.48E-02
20210609 1.0E+01 4.35E-02
20210610 1.5E+01 4.12E-02
20210611 2.0E+01 3.96E-02
20210612 4.0E+01 3.57E-02
20210613 6.0E+01 3.35E-02
20210614 8.0E+01 3.19E-02
20210615 1.0E+02 3.07E-02
20210616 1.5E+02 2.86E-02
20210617 2.0E+02 2.73E-02
20210618 4.0E+02 2.42E-02
20210619 6.0E+02 2.25E-02
20210620 8.0E+02 2.12E-02
20210621 1.0E+03 2.01E-02
20210622 1.5E+03 1.82E-02
20210623 2.0E+03 1.68E-02
20210624 4.0E+03 1.37E-02
20210625 6.0E+03 1.23E-02
20210626 8.0E+03 1.14E-02
20210627 1.0E+04 1.08E-02
20210628 1.5E+04 9.92E-03
20210629 2.0E+04 9.35E-03
20210630 4.0E+04 8.08E-03
20210631 6.0E+04 7.35E-03
20210632 8.0E+04 6.85E-03
20210633 1.0E+05 6.47E-03
20210634 1.5E+05 5.79E-03

```

20210635 2.0E+05 5.32E-03
20210636 4.0E+05 4.24E-03
20210637 6.0E+05 3.67E-03
20210638 8.0E+05 3.32E-03
20210639 1.0E+06 3.08E-03
20210640 1.5E+06 2.71E-03
20210641 2.0E+06 2.48E-03
20210642 4.0E+06 1.98E-03
20210643 6.0E+06 1.72E-03
20210644 8.0E+06 1.54E-03
20210645 1.0E+07 1.40E-03
20210646 1.5E+07 1.14E-03
20210647 2.0E+07 9.61E-04
20210648 4.0E+07 5.92E-04
20210649 6.0E+07 4.35E-04
20210650 8.0E+07 3.55E-04
20210651 1.0E+08 3.10E-04
20210652 1.5E+08 2.58E-04
20210653 2.0E+08 2.38E-04
20210654 4.0E+08 2.07E-04
20210655 6.0E+08 1.89E-04
20210656 8.0E+08 1.73E-04
20210657 1.0E+09 1.60E-04
20210658 1.5E+09 1.35E-04
20210659 2.0E+09 1.17E-04
20210660 4.0E+09 7.85E-05
20210661 6.0E+09 5.97E-05
20210662 8.0E+09 4.82E-05
20210663 1.0E+10 4.05E-05
*****
* Utilization of Fast Reactor Decay Power Curve
*****
*
20502000 rctrp tripunit 1.0 0.0 1
20502001 999
*
20502010 invrctrp tripunit 1.0 1.0 1
20502011 -999
*
20502020 tabdecy function 1000.e6 700000000. 0 0
20502021 time 0 106
*
20502030 codedcyP mult 1.0 70000000.0 1
20502031 cntrlvar 201 rkgapow 0
*
20502040 fastdcyP mult 1.0 70000000. 1
20502041 cntrlvar 200 cntrlvar 202
*
20502050 DPchoose stdfctn 1.0 70000000. 1
20502051 max cntrlvar 203 cntrlvar 204
*
20502100 TotPow sum 1.0 996000000. 1
20502101 0.0 1.0 cntrlvar 205 1.0 rkfpow 0
*
*
*=====
===
* Reactor Kinetics - To be inserted once steady state is reached -
*=====
===

```

```

*
30000000 point separabl
*
*   fp-decay power  rinit  beta/lambda  fp-y  u239-y  G-factor
30000001 gamma  1000.e6  -1.0e-60  9305.556  1.0  1.0e-60  0
*
*   Mod.-Dens Reactivity ($) - Density effects included in vol. temp. feed
30000501 0000.00  0.000000
30000502 1000.00  0.000000
*
30000011 18200 *radial expansion $ $ $This was input by MJM on 11-04-08$ $ $
30000012 18201 *CRDL expansion feedback $alpha = 1.9e-5/C, Lo = 10m, reac = .49$/cm
30000013 18202 *Structural expansion $This is positive feedback for vessel expansion
30000014 18203 *axial expansion $ this is for expansion of clad and assembly walls
30000015 991 *This is the control rod ejection reactivity insertion (input by MJM on 2/2/09)
*30000016 992 *This is the control rod ejection reactivity insertion (input by MJM on 2/2/09)
*30000017 993 *This is the control rod ejection reactivity insertion (input by MJM on 2/2/09)
*
* Doppler Reactivity + Fuel Expansion/Density Feedback (-0.006 $/C)
*   Fuel-Temp Reactivity($) (F.C. = -0.0013 $/C +- 30 percent)
* Doppler T (K) vs alpha, sigma (c/C) EOC Numbers
* 450   -0.3205  +-20percent * sigma taken from ANL-IFR-80
* 750   -0.1587  +-20percent
* 1050  -0.0912  +-20percent
* 1200  -0.085   +-30percent *****NOTE, this is a conservative made up number...MCNP Data
does not go beyond 1050oC.
*           Higher uncertienties are thus used
*
30000601 300.000000 -0.366056
30000602 600.000000 -2.928274
30000603 900.000000 -5.223893
30000604 1064.385820 -6.420841
30000605 1125.000000 -6.862193
30000606 1275.000000 -7.479196
*
* Sodium Temperature/Density Feedback (+0.0011 $/C)
*
* Inner Driver
*   hydro-vol# inc weight  temp-coeff
30000701 111050000 0 1.0 7.774437e-005
30000702 111060000 0 1.0 1.046313e-004
30000703 111070000 0 1.0 1.141196e-004
30000704 111080000 0 1.0 1.046313e-004
30000705 111090000 0 1.0 7.774437e-005
*
* Outer Driver
*   hydro-vol# inc weight  temp-coeff
30000706 123050000 0 1.0 8.485349e-005
30000707 123060000 0 1.0 1.141991e-004
30000708 123070000 0 1.0 1.245549e-004
30000709 123080000 0 1.0 1.141991e-004
30000710 123090000 0 1.0 8.485349e-005
*
* Hot Driver
*   hydro-vol# inc weight  temp-coeff
30000711 150050000 0 1.0 8.485349e-005
30000712 150060000 0 1.0 1.141991e-004
30000713 150070000 0 1.0 1.245549e-004
30000714 150080000 0 1.0 1.141991e-004

```

```

30000715 150090000 0 1.0 8.485349e-005
*
* Fuel Density/Temperature Feedback & Doppler Weights
*
* Hot Channel
*   ht-str# inc weight  fuel-temp-coeff
30000801 1502001 0 0.001148 -0.00
30000802 1502002 0 0.001547 -0.00
30000803 1502003 0 0.001686 -0.00
30000804 1502004 0 0.001547 -0.00
30000805 1502005 0 0.001148 -0.00
*
* Inner Driver
*   ht-str# inc weight  fuel-temp-coeff
30000816 1112001 0 0.077075 -0.00
30000817 1112002 0 0.103739 -0.00
30000818 1112003 0 0.113137 -0.00
30000819 1112004 0 0.103739 -0.00
30000820 1112005 0 0.077075 -0.00
*
* Outer Driver
*   ht-str# inc weight  fuel-temp-coeff
30000831 1232001 0 0.084119 -0.00
30000832 1232002 0 0.113221 -0.00
30000833 1232003 0 0.123478 -0.00
30000834 1232004 0 0.113221 -0.00
30000835 1232005 0 0.084119 -0.00
*
. *end of file
coeff
30000816 1112001 0 0.077075 -0.00
30000817 1112002 0 0.103739 -0.00
30000818 1112003 0 0.113137 -0.00
30000819

```

```

= Primary Heat Transport System for ABR 1000 UTOP – METAL FUEL
* Created from information found in ANL 1000 Design Report
* (See file ABR1000.xls for geometric considerations, assumptions, and
* Calculations)
* Last updated Jan 12, 2011
* J. D. DeWitte, M.R Denman, M.J Memmott
*****
* Distribution Paramters
*****
* Total Reactivity: 0.900000 Time: 5.454545
* Doppler 300.000000 1.587977
*   600.000000 -2.020858
*   900.000000 -4.961925
*   1064.385820 -6.420841
*   1125.000000 -6.958789
*   1275.000000 -7.763241
* Sodium 0.000827
* CRE -0.004213 CRDLE -0.536672
* weight 0.062500
*****
* run setup
*****
0000100 restart transnt
0000101 run
0000102 si si
0000103 -1
0000105 1.0 2.0 1.e6
0000107 1 1 1
*****
* Matt D Added Card
*****
0000200 0 1
*****
0000201 105.454545 1.0e-6 0.007 00019 17 6000 60000
0000202 300.000000 1.0e-6 0.007 00019 200 6000 60000
*
*
*****
* minor edit variables *
*****
$ Var. Parameter
301 mflowj 201010000 *Core Mass Flow Rate
302 cntrlvar 8800 *DRACS Power
303 pmpvel 262 *Primary Pump Velocity
304 tempf 2010000 *Core Inlet Temperature
305 tempf 4010000 *Core Outlet Temperature
306 cntrlvar 8150 *Max Coolant Temp
308 rktpow 0 *Reactor Power
309 tempf 150140000 *Hot Channel Outlet Temperature
310 cntrlvar 10 *Max Clad Temp
311 cntrlvar 11 *Max Fuel Temp
312 cntrlvar 8210 * Core Radial Expansion
313 cntrlvar 8211 * CRDLE
314 cntrlvar 8212 *Strucural Expansion
315 cntrlvar 8213 * Axial Expansion
316 rkreat 0 * Reactivity
317 tempf 150160000 *Hot Channel Top Outlet Temperature
318 tempf 110160000 *Control Rod Top Outlet Temperature
*
*

```

* Thermal Conductivity

20100300 tbl/fctn 1 1
20100301 310.93 14.143
20100302 533.15 17.632
20100303 699.82 20.249
20100304 810.93 21.994
20100305 1088.71 26.355
20100306 4088.71 26.355

* Heat Capacity

20100351 310.93 3.690e6
20100352 533.15 4.256e6
20100353 699.82 4.407e6
20100354 810.93 4.513e6
20100355 1088.71 4.913e6
20100356 4088.71 4.913e6

*
*
*

20582000 RADexp sum 1.0 -3.297461 1
20582001 0.0 -0.004213 tempf 004010000

*
20582010 CRDLexp sum 1.0 -7.985521 1
20582011 0.0 1.0 cntrlvar 8205

*
20582050 CRDLcalc sum 1.0 -7.985521 1
20582051 0.0 -0.536672 cntrlvar 8204

*

* Control Vars to Plot reactivity for each effect listed above

*

20582100 radexp sum 1.0 0.0 1
20582101 3.297461 -0.004213 tempf 004010000

*

20582110 CRDLexp sum 1.0 0.0 1
20582111 7.985521 1.0 cntrlvar 8205

*

* Transient trips

*

20600000 expanded
20605010 time 0 ge null 0 800000. 1 *DRACS Valve Trip
20602620 tempf 2010000 ge null 0 808. 1 *Pump Trip
20609990 time 0 ge null 0 3. 1 *Decay Power initiation
20601000 time 0 ge null 0 3. 1 *UTOP Initiation
20605030 tempf 110160000 gt null 0 803.111942 1 *Curie Point Actuation

*

*

* Reactivity Insertion Table

*

*

*

*

20299000 reac-t 100
20299001 0.0 0.0
20299002 5.454545 0.900000
20299003 100000.0 0.900000
20299100 reac-t 503

```

20299101  0.0  0.0
20299102  0.1 -0.01
20299103  0.5 -0.15
20299104  1.0 -1.0215
20299105  1.5 -3.9
20299106  2.0 -6.7
20299107  2.5 -6.7
20299108 100000. -6.7

```

```

*
*
*
*-----
* SG Structure 1
*-----
*
*
* The SG is simplified to provide the right inventory of steam and sodium
* while still providing the right heat transfer without knowing the actual
* design. Thus, the SAMult was adjusted until these factors matched.
*
*

```

```

*HiStr axialN radialMP Geom ss LBcoor
13401000 50 5 1 1 .01
* location format (1= Intrvl#,RightCoord, 2= MeshIntrvl,Intrvl#)
13401100 0 1
* intrvl# RightCoor
13401101 4 .0159
* Compos# Intrvl#
13401201 003 4
* Srce Intrvl#
13401301 0. 4
* ITF
13401400 0
* T(K) mshpnt#
13401401 761.15 5
* BCVol Incr BCType SACode SAMult HS#
13401501 0 0. 0. 0. 344. 50
13401601 410500000 -10000 1 1 344.000 50
* PStype Pf DMH DMHM HS#
13401701 0 0. 0. 0. 50
* words (0=9,1=12)
13401900 1
* Dhe LeHf leHr Lgsf Lgsr Kfwd Krev Fboil nclf P/d ff #
13401901 0.0 100. 100. 0. 0. 0. 0. 1.0 0. 1.1 1.35 50

```

* Pump Coastdown Tables

** For each of these EM pumps, 2 pumps are combined in series for a total of 4 p

*

*hydro name type

```

2600000 pmp1ent snglvol
2600101 0.676071 1.6 0.0 0.0 90. 1.6 4.5e-5 0.2 0000000
2600200 0 202801.3 549470. 5255980. 0.

```

*

*

*hydro name type

```

2700000 pmp1ent snglvol
2700101 0.676071 1.6 0.0 0.0 90. 1.6 4.5e-5 0.2 0000000
2700200 0 198729.3 549470. 5255394. 0.

```



```

*
*
*
*For the pumps sized in the Argon Report, the area is wrong! For pumps of that
*a velocity of 400m/s through the pump duct is achieved. AS a result, a new are
*reflects the appropriate pressure drop of the system is achieved by adjusting t
*until the pressure drop matches the pump area. An alternative to this is maint
*area which gives a velocity of ~ 4m/s, and adjusting the ks to give an appropr
*In this model, Kwere approximated sudden entrance/exit, and the area was
*until an adequate pressure drop/flow rate was achieved.
*(Actual calculated area is 0.006154, adjusted is 0.405255)
*
*hydro name type
2620000 empump1 pump
2620101 .405255 1.6 0.0 0.0 -90. -1.6 0000000
2620108 260010000 0.0 .5 .1 00000000 * these Ks are based upon a flanged 180 re
2620109 264000000 0.0 1. .5 00000000
2620200 0 569575. 550428. 5279694. 0.
2620201 0 7.26608 8.03966 0. * 2556.006
2620202 0 7.26696 7.26696 0. * 2556.006
*****
*****
* Brinham pump, 1 phase, no 2 phase, no tourqe table used,time dependant pump velocity index, trip
on 262, reverse flow allowed
2620301 -1 -1 -3 -1 -1 262 1 $ This is for variable pumping** mrd 4/11
*****
*****
2620302 251.32 1. 2.96 91.02 18421.227 160.0 851.35 0. .1 21.53 21.53 0. 0. *to
*
*hydro name type
2720000 empump1 pump
2720101 .405255 1.6 0.0 0.0 -90. -1.6 0000000
2720108 270010000 0.0 .5 .1 00000000 * these Ks are based upon a flanged 18 upo
2720109 274000000 0.0 1. .5 00000000
2720200 0 567583. 550431. 5279639. 0.
2720201 0 7.25373 8.02682 0. * 2551.66
2720202 0 7.25461 7.25461 0. * 2551.66
*****
*****
* Brinham pump, 1 phase, no 2 phase, no tourqe table used,time dependant pump velocity index, trip
on 262, reverse flow allowed
2720301 -1 -1 -3 -1 -1 262 1 $ This is for variable pumping*
*****
*****
2720302 251.32 1. 2.96 91.02 18421.227 160.0 851.35 0. .1 21.53 21.53 0. 0. *t
=====
=====
* Reactor Kinetics - To be inserted once steady state is reached -
*=====
=====
*
*
30000000 point separabl
*
* fp-decay power rinit beta/lambda fp-y u239-y G-factor
30000001 gamma 1000.e6 -1.0e-60 9305.556 1.0 1.0e-60 0
*
* Mod.-Dens Reactivity ($) - Density effects included in vol. temp. feed
30000501 0000.00 0.000000
30000502 1000.00 0.000000
*

```

30000011 18200 *radial expansion \$ \$ \$This was input by MJM on 11-04-08\$ \$ \$
 30000012 18201 *CRDL expansion feedback \$alpha = 1.9e-5/C, Lo = 10m, reac = .49\$/cm
 30000013 18202 *Structural expansion \$This is positive feedback for vessel expansion
 30000014 18203 *axial expansion \$ this is for expansion of clad and assembly walls
 30000015 990 *This is the control rod ejection reactivity insertion (input by MJM on 2/2/09)
 *
 * Doppler Reactivity + Fuel Expansion/Density Feedback (-0.006 \$/C)
 * Fuel-Temp Reactivity(\$ (F.C. = -0.0013 \$/C +- 30 percent)
 * Doppler T (K) vs alpha, sigma (c/C) EOC Numbers
 * 450 -0.3205 +-20percent * sigma taken from ANL-IFR-80
 * 750 -0.1587 +-20percent
 * 1050 -0.0912 +-20percent
 * 1200 -0.085 +-30percent *****NOTE, this is a conservative made up number...MCNP Data
 does not go beyond 1050oC.
 * Higher uncertienties are thus used
 *
 30000601 300.000000 1.587977
 30000602 600.000000 -2.020858
 30000603 900.000000 -4.961925
 30000604 1064.385820 -6.420841
 30000605 1125.000000 -6.958789
 30000606 1275.000000 -7.763241
 *
 * Sodium Temperature/Density Feedback (+0.0011 \$/C)
 *
 * Inner Driver
 * hydro-vol# inc weight temp-coeff
 30000701 111050000 0 1.0 4.217627e-005
 30000702 111060000 0 1.0 5.676243e-005
 30000703 111070000 0 1.0 6.190980e-005
 30000704 111080000 0 1.0 5.676243e-005
 30000705 111090000 0 1.0 4.217627e-005
 *
 * Outer Driver
 * hydro-vol# inc weight temp-coeff
 30000706 123050000 0 1.0 4.603296e-005
 30000707 123060000 0 1.0 6.195292e-005
 30000708 123070000 0 1.0 6.757097e-005
 30000709 123080000 0 1.0 6.195292e-005
 30000710 123090000 0 1.0 4.603296e-005
 *
 * Hot Driver
 * hydro-vol# inc weight temp-coeff
 30000711 150050000 0 1.0 4.603296e-005
 30000712 150060000 0 1.0 6.195292e-005
 30000713 150070000 0 1.0 6.757097e-005
 30000714 150080000 0 1.0 6.195292e-005
 30000715 150090000 0 1.0 4.603296e-005
 *
 * Fuel Density/Temperature Feedback & Doppler Weights
 *
 * Hot Channel
 * ht-str# inc weight fuel-temp-coeff
 30000801 1502001 0 0.001148 -0.00
 30000802 1502002 0 0.001547 -0.00
 30000803 1502003 0 0.001686 -0.00
 30000804 1502004 0 0.001547 -0.00
 30000805 1502005 0 0.001148 -0.00
 *

```
* Inner Driver
*   ht-str# inc weight  fuel-temp-coeff
30000816 1112001 0 0.077075 -0.00
30000817 1112002 0 0.103739 -0.00
30000818 1112003 0 0.113137 -0.00
30000819 1112004 0 0.103739 -0.00
30000820 1112005 0 0.077075 -0.00
*
* Outer Driver
*   ht-str# inc weight  fuel-temp-coeff
30000831 1232001 0 0.084119 -0.00
30000832 1232002 0 0.113221 -0.00
30000833 1232003 0 0.123478 -0.00
30000834 1232004 0 0.113221 -0.00
30000835 1232005 0 0.084119 -0.00
*
.*end of file
```

Appendix C – Matlab Wrapper

This Appendix contains the wrapper code suite as coded by author. The flowpath of the code suite is shown in the figure below.

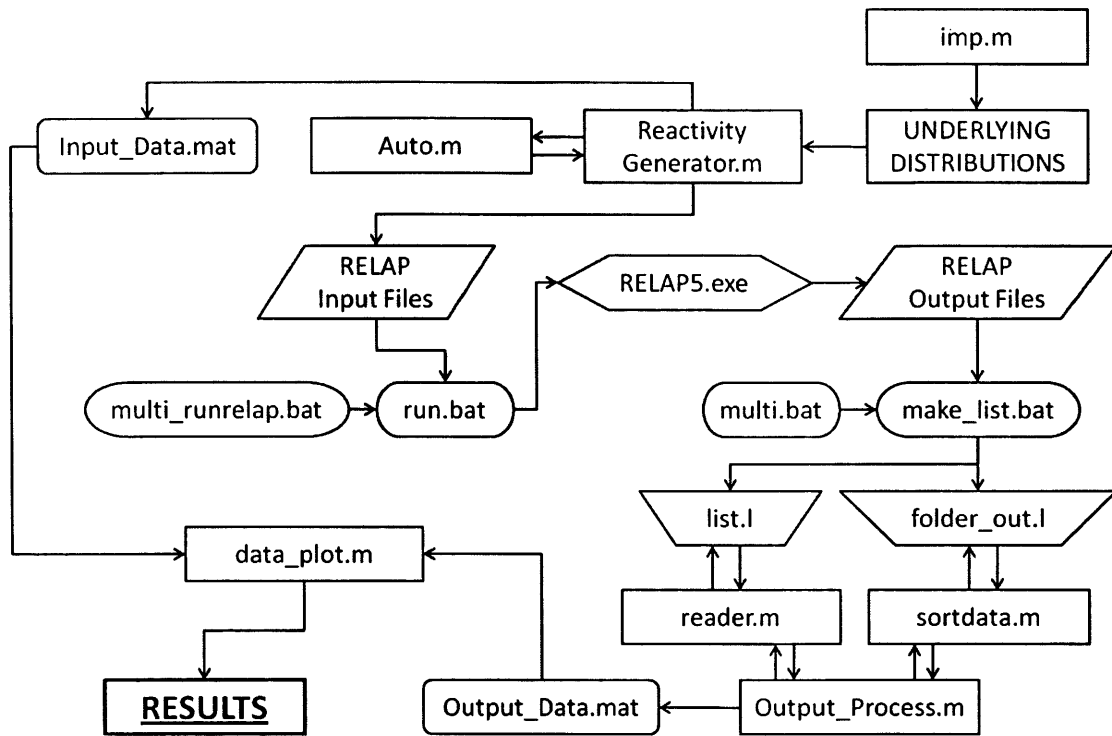


FIGURE C-0-1: MATLAB WRAPPER CODE SUITE FLOW PATH.

For more information, please refer to the Matlab Manual.

imp.m

```

function [num,wgt]=imp(random)
if random<=0.5
    num=0.0+rand*5/100;
    wgt=.1;
elseif random<=0.8
    num=0.05+rand*45/100;
    wgt=1.5;
else
    num=0.5+rand*50/100;
    wgt=2.5;
end
  
```

Reactivity_Generator.m – Metal Core ULOF

```

% Loss of Flow Input Generator
clear all
% close all
In_folder_name='C:/Jake_SASS/ULOF_803_8/In'; % The Folders must be made before running
Ou_folder_name='C:/Jake_SASS/ULOF_803_8/Ou'; % The Folders must be made before running
folders=5;

CP_SET=803.15;
CP_UNC=5;

%%%%%%%%%%%%%%%%%%%%%%%%%%%%%%%%%%%%%%%%%%%%%%%%%%%%%%%%%%%%%%%%%%%%%%%%
%% Generates the Paramters Used In the UTOP Uncertanty Study
%%%%%%%%%%%%%%%%%%%%%%%%%%%%%%%%%%%%%%%%%%%%%%%%%%%%%%%%%%%%%%%%%%%%%%%%
runs=100; %number of inputs to be created
inputs=1; %if inputs=1 then the inputs will print, else they will not
plots=1; %if inputs=1 then the inputs will print, else they will not

%%%%%%%%%%%%%%%%%%%%%%%%%%%%%%%%%%%%%%%%%%%%%%%%%%%%%%%%%%%%%%%%%%%%%%%%
%% Should the parameter be (mean), (random), or (2sigma off, in a bad way)
%% 1=mean, 2=rand 3="2 sig"
doppler=2; %%% Doppler
expansion=2; %%% Expansion
sodiumdensity=2; %%% Na Density
CRExpansion=2; %%% CRE
CRDLExpansion=2; %%% CRDLE
CPL=2; %%% Curie Point Latch

if (doppler~=2 && (expansion~=2 && (sodiumdensity~=2 && (CRExpansion~=2 && (CRDLExpansion~=2
&& CPL~=2))))
    random_sel=0;
else
    random_sel=1;
end

reactivity(1)=.7;
reactivity(2)=.9;
for iii=1:folders
    %%%%%%%%%%%%%%%%%%%%%%%%%%%%%%%%%%%%%%%%%%%%%%%%%%%%%%%%%%%%%%%%%%%%%%%%%
    %% Reactivity Values
    %%%%%%%%%%%%%%%%%%%%%%%%%%%%%%%%%%%%%%%%%%%%%%%%%%%%%%%%%%%%%%%%%%%%%%%%%
    if reactivity(1)~=0
        for i=1:runs
            %[rnd,wgt(1,i)]=imp(rand);
            react(i)=reactivity(1)+(reactivity(2)-reactivity(1))*rand; %%Reactivity value between $0.7 to $0.9
            wgt(1,i)=1.0;
            rate=0.165; %% $/s
            time(i)=react(i)/rate; %% s
        end
    else
        for i=1:runs
            react(i)=reactivity(2); %%Reactivity value between $0.7 to $0.9
            rate=0.165; %% $/s
            time(i)=react(i)/rate; %% s
        end
    end
end

bound(1)=.3;
bound(2)=.9;

```

```

drho=(bound(2)-bound(1))/12;
x=bound(1):drho:bound(2);

%%%%%%%%%Plot
if plots==1 % Only if plots=1, at top of file
    subplot(4,2,1)
    hist(react,x);
    title('Reactivity Insertion Distribution')
    xlabel('Reactivity Inserted ($)')
    ylabel('Number of Samples')
end

%%%%%%%%%
%%% Doppler
%%%%%%%%%

%%%%%%%%%
%%%%%%%%% Calc Reference Doppler Temp

%%%%%%%%%
temp150=[819.629,888.248,937.336,961.404,956.226]; % Temperatures in 150
weight150=[0.001148,0.001547,0.001686,0.001547,0.001148]; % Dop weight in 150

ave150=0;
for i=1:5
    ave150=ave150+temp150(i)*weight150(i); % Average Temp in 150
end
temp111=[798.65,862.28,909.86,935.63,935.26];
weight111=[0.077075,0.103739,0.3113137,0.103739,0.077075];

ave111=0;
for i=1:5
    ave111=ave111+temp111(i)*weight111(i);
end
temp123=[789.8,850.8,897.7,924.5,926.9];
weight123=[0.084119,0.113221,0.123478,0.1113221,0.084119];

ave123=0;
for i=1:5
    ave123=ave123+temp123(i)*weight123(i);
end

avetot=ave150+ave111+ave123;
averho=-5.04+(5.04-7.56)/(1200-900)*(avetot-900);

temp(1)=300;
temp(2)=600;
temp(3)=900;
temp(4)=avetot;
temp(5)=1125;
temp(6)=1275;

Axial=-0.006;
sigaxial=-Axial*.3;

```

```
%%%%%%%%%%%%%%%%%%%%%%%%%%%%%%%%%%%%%%%%%%%%%%%%%%%%%%%%%%%%%%%%%%%%%%%%
%%%%%%%%%%%%%%%%%%%%%%%%%%%%%%%%%%%%%%%%%%%%%%%%%%%%%%%%%%%%%%%%%%%%%%%%
```

```
Alphas ($/k)
```

```
%%%%%%%%%%%%%%%%%%%%%%%%%%%%%%%%%%%%%%%%%%%%%%%%%%%%%%%%%%%%%%%%%%%%%%%%
%%%%%%%%%%%%%%%%%%%%%%%%%%%%%%%%%%%%%%%%%%%%%%%%%%%%%%%%%%%%%%%%%%%%%%%%
```

```
if doppler==1
```

```
for ii=1:runs
```

```
alpha(1)=-.3205e-2; % 20% std
alpha(2)=-.1587e-2; % 20% std
alpha(3)=-0.0912e-2; % 20% std
alpha(4)=-.085e-2; % 30% std - Not calculated
```

```
if expansion==1
```

```
ax(ii)=Axial;
alpha=alpha+ax(ii);
```

```
elseif expansion==2
```

```
ax(ii)=norminv(ranexp,Axial,sigaxial);
alpha=alpha+ax(ii); % 30% std - Axial Expansion
```

```
else
```

```
ax(ii)=axial+2*sigaxial;
alpha=alpha+ax(ii);
```

```
end
```

```
dop(ii)=alpha(3);
```

```
rho(4,ii)=averho;
```

```
rho(3,ii)=averho-alpha(3)*(avetot-900);
```

```
rho(2,ii)=rho(3,ii)-alpha(2)*(900-600);
```

```
rho(1,ii)=rho(2,ii)-alpha(1)*(600-300);
```

```
rho(5,ii)=rho(3,ii)-alpha(3)*(900-1125);
```

```
rho(6,ii)=rho(4,ii)-alpha(4)*(1125-1275);
```

```
end
```

```
elseif doppler==2
```

```
for ii=1:runs
```

```
[rnd,wgt(2,ii)]=imp(rand);
```

```
randop=(1-rnd); % All doppler values draw from the same Z value
```

```
[rnd,wgt(3,ii)]=imp(rand);
```

```
ranexp=(1-rnd); % Z for axial expansion
```

```
alpha(1)=norminv(randop,-.3205e-2,.3205e-2*.2); % 20% std
```

```
alpha(2)=norminv(randop,-.1587e-2,.1587e-2*.2); % 20% std
```

```
alpha(3)=norminv(randop,-0.0912e-2,0.0912e-2*.2); % 20% std
```

```
alpha(4)=norminv(randop,-.085e-2,.085e-2*.3); % 30% std - Not calculated
```

```
if expansion==1
```

```
ax(ii)=Axial;
alpha=alpha+ax(ii);
```

```
elseif expansion==2
```

```
ax(ii)=norminv(ranexp,Axial,sigaxial);
alpha=alpha+ax(ii); % 30% std - Axial Expansion
```

```
else
```

```
ax(ii)=axial+2*sigaxial;
alpha=alpha+ax(ii);
```

```
end
```

```
dop(ii)=alpha(3);
```

```
rho(4,ii)=averho;
```

```
rho(3,ii)=averho-alpha(3)*(avetot-900);
```

```
rho(2,ii)=rho(3,ii)-alpha(2)*(900-600);
```

```
rho(1,ii)=rho(2,ii)-alpha(1)*(600-300);
```

```
rho(5,ii)=rho(3,ii)-alpha(3)*(900-1125);
```

```
rho(6,ii)=rho(4,ii)-alpha(4)*(1125-1275);
```

```
end
```

```
else
```

```

for ii=1:runs
alpha(1)=-.3205e-2+2*.3205e-2*.2; % 20% std
alpha(2)=-.1587e-2+2.1587e-2*.2; % 20% std
alpha(3)=-0.0912e-2+2*0.0912e-2*.2; % 20% std
alpha(4)=-.085e-2+2*.085e-2*.3; % 30% std - Not calculated
if expansion==1
ax(ii)=Axial;
alpha=alpha+ax(ii);
elseif expansion==2
ax(ii)=norminv(ranexp,Axial,sigaxial);
alpha=alpha+ax(ii); % 30% std - Axial Expansion
else
ax(ii)=Axial+2*sigaxial;
alpha=alpha+ax(ii);
end
dop(ii)=alpha(3);
rho(4,ii)=averho;
rho(3,ii)=averho-alpha(3)*(avetot-900);
rho(2,ii)=rho(3,ii)-alpha(2)*(900-600);
rho(1,ii)=rho(2,ii)-alpha(1)*(600-300);
rho(5,ii)=rho(3,ii)-alpha(3)*(900-1125);
rho(6,ii)=rho(4,ii)-alpha(4)*(1125-1275);
end
end

if plots==1 % Only if plots=1, at top of file
subplot(3,2,[5 6])
plot(temp,rho,'*-')
title('Doppler and Axial Expansion Distribution')
xlabel('Temperature (K)')
ylabel('Reactivity ($)')
end

%%%%%%%%%%%%%%
%% Sodium Density
%%%%%%%%%%%%%%
for ii=1:runs
if sodiumdensity==1; % use mean values
%%%%%%%%%%%%%%
%% Region 111
%%%%%%%%%%%%%%
j=1;
a=2.0533068e-2; % Buckling type term
mean(j)=1.2445e-4*.12/.17; % Convert from Pu (Matt M.) to TRU core (Matt D.)
sig(j)=mean(j)*.16; % 20% std
peak111=mean(j);
n=10;
for i=1:5
sod111(i,ii)=peak111*cos(a*(50-n)); % Create sodium density distributon
n=n+20;
end

%%%%%%%%%%%%%%
%% Region 123
%%%%%%%%%%%%%%
j=2;
mean(j)=1.3583e-04*.12/.17;
sig(j)=mean(j)*.16; % 20% std
peak123=mean(j);

```



```

n=10;
for i=1:5
    sod123(i,ii)=peak123*cos(a*(50-n));
    n=n+20;
end

%%%%%%%%%%
%%% Region 150
%%%%%%%%%%
j=3;
mean(j)=1.3583e-04*.12/.17;
sig(j)=mean(j)*.16; % 20% std
peak150=mean(j);
n=10;
for i=1:5
    sod150(i,ii)=peak150*cos(a*(50-n));
    n=n+20;
end

elseif sodiumdensity==2; % random values
%%%%%%%%%%
%%% Region 111
%%%%%%%%%%
j=1;
a=2.0533068e-2; % Buckeling type term
mean(j)=1.2445e-4*.12/.17; % Convert from Pu (Matt M.) to TRU core (Matt D.)
sig(j)=mean(j)*.16; % 20% std

[rd,wgt(4,ii)]=imp(rand);

peak111=norminv((1-rd),mean(j),sig(j));
n=10;
for i=1:5
    sod111(i,ii)=peak111*cos(a*(50-n)); % Create sodium density distributon
    n=n+20;
end

%%%%%%%%%%
%%% Region 123
%%%%%%%%%%
j=2;
mean(j)=1.3583e-04*.12/.17;
sig(j)=mean(j)*.16; % 20% std

peak123=norminv((1-rd),mean(j),sig(j));
n=10;
for i=1:5
    sod123(i,ii)=peak123*cos(a*(50-n));
    n=n+20;
end

%%%%%%%%%%
%%% Region 150
%%%%%%%%%%
j=3;
mean(j)=1.3583e-04*.12/.17;
sig(j)=mean(j)*.16; % 20% std

peak150=norminv((1-rd),mean(j),sig(j));
n=10;

```

```

for i=1:5
    sod150(i,ii)=peak150*cos(a*(50-n));
    n=n+20;
end
else % 2 sig values
    %%%%%%%%%%
    %%% Region 111
    %%%%%%%%%%
    j=1;
    a=2.0533068e-2; % Buckling type term
    mean(j)=1.2445e-4*.12/.17; % Convert from Pu (Matt M.) to TRU core (Matt D.)
    sig(j)=mean(j)*.16; % 20% std
    peak111=mean(j)+2*sig(j);
    n=10;
    for i=1:5
        sod111(i,ii)=peak111*cos(a*(50-n)); % Create sodium density distribuiton
        n=n+20;
    end

    %%%%%%%%%%
    %%% Region 123
    %%%%%%%%%%
    j=2;
    mean(j)=1.3583e-04*.12/.17;
    sig(j)=mean(j)*.16; % 20% std
    peak123=mean(j)+2*sig(j);
    n=10;
    for i=1:5
        sod123(i,ii)=peak123*cos(a*(50-n));
        n=n+20;
    end

    %%%%%%%%%%
    %%% Region 150
    %%%%%%%%%%
    j=3;
    mean(j)=1.3583e-04*.12/.17;
    sig(j)=mean(j)*.16; % 20% std
    peak150=mean(j)+2*sig(j);
    n=10;
    for i=1:5
        sod150(i,ii)=peak150*cos(a*(50-n));
        n=n+20;
    end
end
clear mean sig

sod(ii)=sum(sod150(:,ii))+sum(sod123(:,ii))+sum(sod111(:,ii)); % add all of the regional sodium density
coeff.
end

bound(1)=mean(sod)-3*std(sod);
bound(2)=mean(sod)+3*std(sod);
dsod=(bound(2)-bound(1))/10;
x=bound(1):dsod:bound(2);

%%%%%%%%%Plot
if plots==1 % Only if plots=1, at top of file
    subplot(3,2,1)
    hist(sod,x);

```

```

title('Sodium Density Coefficient Distribution')
xlabel('Sodium Density Coefficient ($/K)')
ylabel('Number of Samples')
end
%%%%%%%%%%%%%%%%%%%%%%%%%%%%%%%%%%%%%%%%%%%%%%%%%%%%%%%%%%%%%%%%%%%%%%%%
%% Radial Expansion
%%%%%%%%%%%%%%%%%%%%%%%%%%%%%%%%%%%%%%%%%%%%%%%%%%%%%%%%%%%%%%%%%%%%%%%%

%% Coolant Temperature = 782.7311401 K

averad=-0.0039;
sigrad=-averad*.2; % 20% std
if CRExpansion==1
    for i=1:runs
        cre(1,i)=averad; % Reactivity Coefficient

        cre(2,i)=cre(1,i)*782.7311401; % Constant Term
    end
elseif CRExpansion==2
    for i=1:runs
        [rnd,wgt(5,i)]=imp(rand);

        cre(1,i)=nonminv((1-rnd),averad,sigrad); % Reactivity Coefficient

        cre(2,i)=cre(1,i)*782.7311401; % Constant Term
    end
else
    for i=1:runs
        cre(1,i)=averad+2*sigrad; % Reactivity Coefficient

        cre(2,i)=cre(1,i)*782.7311401; % Constant Term
    end
end

bound(1)=mean(cre(1,:))-3*std(cre(1,:));
bound(2)=mean(cre(1,:))+3*std(cre(1,:));
dcre=(bound(2)-bound(1))/10;
x=bound(1):dcre:bound(2);

if plots==1 % Only if plots=1, at top of file
    subplot(3,2,2)
    hist(cre(1,:),x);
    title('Core Radial Expansion Coefficient Distribution')
    xlabel('CRE Coefficient ($/K)')
    ylabel('Number of Samples')
end
%%%%%%%%%%%%%%%%%%%%%%%%%%%%%%%%%%%%%%%%%%%%%%%%%%%%%%%%%%%%%%%%%%%%%%%%
%% CRDLE
%%%%%%%%%%%%%%%%%%%%%%%%%%%%%%%%%%%%%%%%%%%%%%%%%%%%%%%%%%%%%%%%%%%%%%%%

avecrdle=-0.49;
sigcrdle=-avecrdle*.2; % 5% std
if CRDLExpansion==1
    for i=1:runs
        crdle(1,i)=avecrdle; % Reactivity Coefficient

        crdle(2,i)=-crdle(1,i)*14.8797; % Constant Term
    end
elseif CRDLExpansion==2

```

```

for i=1:runs
    [rnd,wgt(6,i)]=imp(rand);

    crdle(1,i)=norminv((1-rnd),avecrdle,sigcrdle); % Reactivity Coefficient

    crdle(2,i)=-crdle(1,i)*14.8797;    % Constant Term
end
else
for i=1:runs
    crdle(1,i)=avecrdle+2*sigcrdle; % Reactivity Coefficient

    crdle(2,i)=-crdle(1,i)*14.8797;    % Constant Term
end
end

bound(1)=mean(crdle(1,:))-3*std(crdle(1,:));
bound(2)=mean(crdle(1,:))+3*std(crdle(1,:));
dcrdle=(bound(2)-bound(1))/10;
x=bound(1):dcrdle:bound(2);

if plots==1 % Only if plots=1, at top of file
    subplot(3,2,3)
    hist(crdle(1,:),x);
    title('Control Rod Drive Line Expansion Coefficient Distribution')
    xlabel('CRDLE Coefficient ($/K)')
    ylabel('Number of Samples')
end

%%%%%%%%%%%%%%
%% Curie Point
%%%%%%%%%%%%%%

CP_avg=CP_SET;
CP_sig=CP_UNC;
if CPL==1
for i=1:runs
    CP(1,i)=CP_avg; % Curie Point Temperature
end
elseif CPL==2
for i=1:runs
    [rnd,wgt(7,i)]=imp(rand);
    CP(1,i)=norminv((1-rnd),CP_avg,CP_sig); % Curie Point Temperature
end
else
for i=1:runs
    CP(1,i)=CP_avg+2*CP_sig; % Curie Point Temperature
end
end

bound(1)=mean(CP(1,:))-3*std(CP(1,:));
bound(2)=mean(CP(1,:))+3*std(CP(1,:));
dCP=(bound(2)-bound(1))/10;
x=bound(1):dCP:bound(2);

if plots==1 % Only if plots=1, at top of file
    subplot(3,2,4)
    hist(CP(1,:),x);
    title('Curie Point Temperature Distribution')

```

```

xlabel('Temperature (K)')
ylabel('Number of Samples')
end

%%%%
%% Write Inputs
%%%%
if inputs==1 % Only if inputs=1, at top of file
    name1=sprintf('%s%d/output.1',Ou_folder_name,iii);
    fid=fopen(name1,'w');
    fprintf(fid,'Run #, React ($), Axial, Dop, Sod, CRE, CRDLE, Curie Point\n');
    for i=1:runs
        sod(i)=sum(sod150(:,i))+sum(sod123(:,i))+sum(sod111(:,i));
        fprintf(fid,'%f %f %f %f %f %f %f %f\n',i,react(i),ax(i),dop(i),sod(i),cre(1,i),crdle(1,i),CP(1,i));
    end

    for i=1:runs
        name=sprintf('%s%d/run%03.0f.i',In_folder_name,iii,i);
        if random_sel==1
            wgtt(i)=wgt(1,i).*wgt(2,i).*wgt(3,i).*wgt(4,i).*wgt(5,i).*wgt(6,i).*wgt(7,i);
        else
            wgtt(i)=1;
        end
        Auto(name,react(i),time(i),temp,rho(:,i),sod111(:,i),sod123(:,i),sod150(:,i),cre(:,i),crdle(:,i),CP(i),wgtt)
    end

    fclose('all');
    if iii > 1
        load data
    end
    Par.react(iii,:)=react';
    Par.ax(iii,:)=ax';
    Par.dop(iii,:)=dop';
    Par.sod(iii,:)=sod';
    Par.cre(iii,:)=cre(1,:);
    Par.crdle(iii,:)=crdle(1,:);
    Par.CP(iii,:)=CP(1,:);
    Par.wgt(iii,:)=wgtt';
    save data Par
end

%% test weighting
if random_sel == 1
    wgttot(1,:)=wgt(1,:).*wgt(2,:).*wgt(3,:).*wgt(4,:).*wgt(5,:).*wgt(6,:).*wgt(7,:);
    sum(wgttot);
end

end

```

Auto.m – Metal Core ULOF

```

function xyz=auto(name,react,time,temp,rho,sod111,sod123,sod150,cre,crdle,CP,wgt)

tau=3.0;
% Example Code for Printing Progress to the Command Window

%%%%%%%%%%%%%%%%%%%%%%%%%%%%%%%%%%%%%%%%%%%%%%%%%%%%%%%%%%%%%%%%%%%%%%%%
%%%%%%%%%%%%%%%%%%%%%%%%%%%%%%%%%%%%%%%%%%%%%%%%%%%%%%%%%%%%%%%%%%%%%%%%
%%%%%%%%%%%%%%%%%%%%%%%%%%%%%%%%%%%%%%%%%%%%%%%%%%%%%%%%%%%%%%%%%%%%%%%%
% Print
%%%%%%%%%%%%%%%%%%%%%%%%%%%%%%%%%%%%%%%%%%%%%%%%%%%%%%%%%%%%%%%%%%%%%%%%
%%%%%%%%%%%%%%%%%%%%%%%%%%%%%%%%%%%%%%%%%%%%%%%%%%%%%%%%%%%%%%%%%%%%%%%%
expansion=1; % 1 if expansion is updated
runtime=900; % # of seconds of runtime
ramptime=100;

fid=fopen(name,'w');
fprintf(fid,'% Primary Heat Transport System for ABR 1000 \n');
fprintf(fid,'% Created from information found in ANL 1000 Design Report\n');
fprintf(fid,'% (See file ABR1000.xls for geometric considerations, assumptions, and \n');
fprintf(fid,'% Calculations) \n');
fprintf(fid,'% CURIE POINT EFFECTIVENESS - ULOF - Metal \n');
fprintf(fid,'% Last updated April 30, 2010 \n');
fprintf(fid,'% J. D. DeWitte, M.R Denman, M.J Memmott \n');

fprintf(fid,'*****
\n');
fprintf(fid,'% Distribution Parameters \n');
fprintf(fid,'*****
\n');
fprintf(fid,'% Flow Halving Time:%f \n',tau);
fprintf(fid,'% Doppler %f %f \n',temp(1),rho(1));
fprintf(fid,'% %f %f \n',temp(2),rho(2));
fprintf(fid,'% %f %f \n',temp(3),rho(3));
fprintf(fid,'% %f %f \n',temp(4),rho(4));
fprintf(fid,'% %f %f \n',temp(5),rho(5));
fprintf(fid,'% %f %f \n',temp(6),rho(6));
sod=sum(sod150(:))+sum(sod123(:))+sum(sod111(:));
fprintf(fid,'% Sodium %f\n',sod);
fprintf(fid,'% CRE %f CRDLE %f\n',cre(1),crdle(1));
% fprintf(fid,'% weight %f \n',wgt);

fprintf(fid,'*****
\n');
fprintf(fid,'% run setup \n');
fprintf(fid,'*****
\n');
fprintf(fid,'0000100 restart transnt \n');
fprintf(fid,'0000101 run\n');
fprintf(fid,'0000102 si si \n');
fprintf(fid,'0000103 -1\n');
fprintf(fid,'0000105 1.0 2.0 1.e6 \n');
fprintf(fid,'0000107 1 1 1 \n');
fprintf(fid,'*****
\n');
fprintf(fid,'% Matt D Added Card\n');
fprintf(fid,'*****
\n');
fprintf(fid,'0000200 0 1\n');

```

```
fprintf(fid,'*****\n');
n');
% fprintf(fid,'0000201 %f 1.0e-7 0.007 00019 17 6000 60000\n',0.5); %diagnostic run
fprintf(fid,'0000201 %f 1.0e-7 0.005 00019 17 6000 60000\n',ramptime);
% fprintf(fid,'0000202 %f 1.0e-7 0.007 00019 200 6000 60000\n',runtime);
```

```
fprintf(fid,'*\n');
fprintf(fid,'*\n');
```

```
fprintf(fid,'*****\n');
fprintf(fid,'*          minor edit variables          *\n');
fprintf(fid,'*****\n');
fprintf(fid,'$ Var. Parameter \n');
fprintf(fid,'301 mflowj 201010000 *Core Mass Flow Rate\n');
fprintf(fid,'302 cntrlvar 8800 *DRACS Power\n');
fprintf(fid,'303 pmpvel 262 *Primary Pump Velocity\n');
fprintf(fid,'304 tempf 2010000 *Core Inlet Temperature\n');
fprintf(fid,'305 tempf 4010000 *Core Outlet Temperature\n');
fprintf(fid,'306 cntrlvar 8150 *Max Coolant Temp \n');
fprintf(fid,'308 rktpow 0 *Reactor Power\n');
fprintf(fid,'309 tempf 150140000 *Hot Channel Outlet Temperature\n');
fprintf(fid,'310 cntrlvar 10 *Max Clad Temp\n');
fprintf(fid,'311 cntrlvar 11 *Max Fuel Temp\n');
fprintf(fid,'312 cntrlvar 8210 * Core Radial Expansion\n');
fprintf(fid,'313 cntrlvar 8211 * CRDLE \n');
fprintf(fid,'314 cntrlvar 8212 *Strucural Expansion\n');
fprintf(fid,'315 cntrlvar 8213 * Axial Expansion \n');
fprintf(fid,'316 rkreact 0 * Reactivity\n');
fprintf(fid,'317 tempf 150160000 *Hot Channel Top Outlet Temperature\n');
fprintf(fid,'318 tempf 110160000 *Control Rod Top Outlet Temperature\n');
```

```
fprintf(fid,'*\n');
fprintf(fid,'*\n');
```

```
fprintf(fid,'* Thermal Conductivity \n');
fprintf(fid,'20100300 tbl/fctn 1 1\n');
fprintf(fid,'20100301 310.93 14.143\n');
fprintf(fid,'20100302 533.15 17.632\n');
fprintf(fid,'20100303 699.82 20.249\n');
fprintf(fid,'20100304 810.93 21.994\n');
fprintf(fid,'20100305 1088.71 26.355\n');
fprintf(fid,'20100306 4088.71 26.355\n');
fprintf(fid,'* Heat Capacity \n');
fprintf(fid,'20100351 310.93 3.690e6\n');
fprintf(fid,'20100352 533.15 4.256e6\n');
fprintf(fid,'20100353 699.82 4.407e6\n');
fprintf(fid,'20100354 810.93 4.513e6\n');
fprintf(fid,'20100355 1088.71 4.913e6\n');
fprintf(fid,'20100356 4088.71 4.913e6\n');
fprintf(fid,'*\n');
fprintf(fid,'*\n');
%%%%%%%%%%
%%%%%%%%%% UPDATE CRE and CRDLE
%%%%%%%%%%
%%%%%%%%%%
```

```

if expansion==1
  fprintf(fid, '*\n');
  fprintf(fid, '20582000 RADexp sum 1.0 %f 1\n', cre(2));
  fprintf(fid, '20582001 0.0 %f tempf 004010000\n', cre(1));
  fprintf(fid, '*\n');
  fprintf(fid, '20582010 CRDLexp sum 1.0 %f 1\n', -crdle(2));
  fprintf(fid, '20582011 0.0 1.0 cntrlvar 8205\n');
  fprintf(fid, '*\n');
  fprintf(fid, '20582050 CRDLcalc sum 1.0 %f 1\n', -crdle(2));
  fprintf(fid, '20582051 0.0 %f cntrlvar 8204\n', crdle(1));
  fprintf(fid, '*\n');

  fprintf(fid, '*****\n');
  fprintf(fid, '* Control Vars to Plot reactivity for each effect listed above\n');

  fprintf(fid, '*****\n');
  fprintf(fid, '*\n');
  fprintf(fid, '20582100 radexp sum 1.0 0.0 1\n');
  fprintf(fid, '20582101 %f %f tempf 004010000\n', -1*cre(2), cre(1));
  fprintf(fid, '*\n');
  fprintf(fid, '20582110 CRDLexp sum 1.0 0.0 1\n');
  fprintf(fid, '20582111 %f 1.0 cntrlvar 8205\n', crdle(2));
  fprintf(fid, '*\n');

  fprintf(fid, '20582140 NORMPOW sum 1.0 0.0 1\n');
  fprintf(fid, '20582141 0.0 0.00000001 rktpow 0\n');
  fprintf(fid, '*\n');
  fprintf(fid, '20582150 NORMFLOW sum 1.0 0.0 1\n');
  fprintf(fid, '20582151 0.0 0.000196 mflowj 201010000\n');
  fprintf(fid, '*\n');

  fprintf(fid, '20582160 POWFLOW div 1.0 0.0 1\n');
  fprintf(fid, '20582161 cntrlvar 8215 cntrlvar 8214\n');
  fprintf(fid, '*\n');

end

%%%%%%%%%% Transient Trips
%%%%%%%%%%
fprintf(fid, '*****\n');
fprintf(fid, '* Transient trips\n');
fprintf(fid, '*****\n');
fprintf(fid, '*\n');
fprintf(fid, '20600000 expanded\n');
fprintf(fid, '20605010 time 0 ge null 0 3. 1 *DRACS Valve Trip\n');
fprintf(fid, '20602620 time 0 ge null 0 3. 1 *Pump Trip\n');
fprintf(fid, '20609990 time 0 ge null 0 3. 1 *Decay Power initiation \n');
fprintf(fid, '20601000 time 0 ge null 0 3. 1 *UTOP initiation \n');
fprintf(fid, '20606660 rktpow 0 ge null 0 1.19e9 1 *SCRAM on Power \n');
fprintf(fid, '20606670 tempf 4010000 ge null 0 830. 1 *SCRAM on Temp \n');
fprintf(fid, '20606680 cntrlvar 8216 ge null 0 1.3 1 *SCRAM on Temp \n');
fprintf(fid, '20605030 tempf 4010000 gt null 0 %f 1 *Curie Point Actuation \n', CP(1));

```



```

%fprintf(fid,'20605030 tempf 110160000 gt null 0 %f1 *Curie Point Actuation \n',CP(1))
%fprintf(fid,'20605030 mflowj 201010000 gt null 0 %f1 *Curie Point Actuation \n',CP(1))
fprintf(fid,'*\n')

fprintf(fid,'*****
)\n')
fprintf(fid,'* Reactivity Insertion Table\n')
fprintf(fid,'*****
\n')
fprintf(fid,'*\n')
fprintf(fid,'*\n')
fprintf(fid,'*\n')
fprintf(fid,'20299100 reac-t 503\n')
fprintf(fid,'20299101 0.0 0.0\n')
fprintf(fid,'20299102 1.5 0.0\n')
fprintf(fid,'20299103 2.0 -0.15\n')
fprintf(fid,'20299104 2.5 -1.0215\n')
fprintf(fid,'20299105 3.0 -3.9\n')
fprintf(fid,'20299106 3.5 -6.7\n')
fprintf(fid,'20299107 100000. -6.7\n')
fprintf(fid,'20299200 reac-t 0\n')
fprintf(fid,'20299201 0.0 0.0\n')
fprintf(fid,'20299202 1.0 0.0\n')
fprintf(fid,'20299203 3.0 -6.0\n')
fprintf(fid,'20299204 100000. -6.0\n')
fprintf(fid,'20299300 reac-t 0\n')
fprintf(fid,'20299301 0.0 0.0\n')
fprintf(fid,'20299302 1.0 0.0\n')
fprintf(fid,'20299303 3.0 -6.0\n')
fprintf(fid,'20299304 100000. -6.0\n')
fprintf(fid,'*\n')
fprintf(fid,'*\n')
fprintf(fid,'*\n')
fprintf(fid,'*****
\n')
fprintf(fid,'* Pump Coastdown Tables\n')
fprintf(fid,'*****
\n')
fprintf(fid,'** For each of these EM pumps, 2 pumps are combined in series for a total of 4 p\n')
fprintf(fid,'*\n')
fprintf(fid,'*hydro name type\n')
fprintf(fid,'2600000 pmp1ent snglvol\n')
fprintf(fid,'2600101 0.676071 1.6 0.0 0.0 90. 1.6 4.5e-5 0.2 0000000\n')
fprintf(fid,'2600200 0 202801.3 549470. 5255980. 0.\n')
fprintf(fid,'*\n')
fprintf(fid,'*\n')
fprintf(fid,'*hydro name type\n')
fprintf(fid,'2700000 pmp1ent snglvol\n')
fprintf(fid,'2700101 0.676071 1.6 0.0 0.0 90. 1.6 4.5e-5 0.2 0000000\n')
fprintf(fid,'2700200 0 198729.3 549470. 5255394. 0.\n')
fprintf(fid,'*\n')
fprintf(fid,'*\n')
fprintf(fid,'*\n')
fprintf(fid,'*For the pumps sized in the ANL Report, the area is wrong! For pumps of that\n')
fprintf(fid,'*a velocity of 400m/s through the pump duct is achieved. AS a result, a new are\n')
fprintf(fid,'*reflects the appropriate pressure drop of the system is achieved by adjusting t\n')
fprintf(fid,'*until the pressure drop matches the pump area. An alternative to this is maint\n')
fprintf(fid,'*area which gives a velocity of ~ 4m/s, and adjusting the ks to give an appropr\n')
fprintf(fid,'*In this model, Kwere approximated sudden entrance/exit, and the area was\n')
fprintf(fid,'*until an adequate pressure drop/flow rate was achieved.\n')

```

```

fprintf(fid, '* (Actual calculated area is 0.006154, adjusted is 0.405255)\n')
fprintf(fid, '*\n')
fprintf(fid, '*hydro name type\n')
fprintf(fid, '262000 empump1 pump\n')
fprintf(fid, '2620101 .405255 1.6 0.0 0.0 -90. -1.6 0000000\n')
fprintf(fid, '2620108 260010000 0.0 .5 .1 00000000 * these Ks are based upon a flanged 180 re\n')
fprintf(fid, '2620109 264000000 0.0 1. .5 00000000\n')
fprintf(fid, '2620200 0 569575. 550428. 5279694. 0.\n')
fprintf(fid, '2620201 0 7.26608 8.03966 0. * 2556.006\n')
fprintf(fid, '2620202 0 7.26696 7.26696 0. * 2556.006\n')
fprintf(fid, '*****\n')
fprintf(fid, '* Brinham pump, 1 phase, no 2 phase, no tourqe table used,time dependant pump velocity index, trip on 262, reverse flow allowed \n')
fprintf(fid, '2620301 0 -1 -3 -1 0 262 1 $ This is for variable pumping** mrd 4/11\n')
fprintf(fid, '*****\n')
fprintf(fid, '*2620301 0 -1 -3 -1 0 262 0 $ This is for pump table (gradual startup)\n')
fprintf(fid, '*2620302 251.32 1.0 2.96 91.02 18421.227 160.0 851.35 0. .1 21.53 21.53 0. 0. *t\n')
fprintf(fid, '2620302 251.32 1. 2.96 91.02 18421.227 160.0 851.35 0. .1 21.53 21.53 0. 0. *to\n')
fprintf(fid, '*2626100 0\n')
fprintf(fid, '*2626101 0.0 0.0\n')
fprintf(fid, '*2626102 0.1 251.32\n')
fprintf(fid, '*head curve, region 1\n')
fprintf(fid, '2621100 1 1 0.0 .45263 *extrapolated value*\n')
fprintf(fid, '2621101 .11904762 .46315789\n')
fprintf(fid, '2621102 .15873016 .47368421\n')
fprintf(fid, '2621103 .23809524 .51578947\n')
fprintf(fid, '2621104 .31746032 .55263158\n')
fprintf(fid, '2621105 .39682540 .60526316\n')
fprintf(fid, '2621106 .47619048 .67105263\n')
fprintf(fid, '2621107 .55555556 .73684211\n')
fprintf(fid, '2621108 .63492063 .81578947\n')
fprintf(fid, '2621109 .71428571 .90789474\n')
fprintf(fid, '2621110 .79365079 1.0\n')
fprintf(fid, '2621111 .87301587 1.10526316\n')
fprintf(fid, '2621112 .95238095 1.14473684\n')
fprintf(fid, '2621113 1. 1.\n')
fprintf(fid, '*torque curve, region 1\n')
fprintf(fid, '2621200 2 1 0.0 .51087174 *extrapolated value*\n')
fprintf(fid, '2621201 .11904762 0.51522074\n')
fprintf(fid, '2621202 .15873016 0.52191192\n')
fprintf(fid, '2621203 .23809524 0.53278508\n')
fprintf(fid, '2621204 .31746032 0.58790078\n')
fprintf(fid, '2621205 .39682540 0.61423844\n')
fprintf(fid, '2621206 .47619048 0.66071828\n')
fprintf(fid, '2621207 .55555556 0.68588425\n')
fprintf(fid, '2621208 .63492063 0.77036280\n')
fprintf(fid, '2621209 .71428571 0.87528978\n')
fprintf(fid, '2621210 .79365079 0.91817838\n')
fprintf(fid, '2621211 .87301587 1.01924103\n')
fprintf(fid, '2621212 .95238095 1.07018303\n')
fprintf(fid, '2621213 1. 1.\n')
fprintf(fid, '*head curve, region 2\n')
fprintf(fid, '2621300 1 2 .89 .00016955 *extrapolated value*\n')
fprintf(fid, '2621301 .9 .05328947 *extrapolated value*\n')
fprintf(fid, '2621302 .91636364 .25412649\n')
fprintf(fid, '2621303 .93333333 .48140351\n')
fprintf(fid, '2621304 .96923077 .84052320\n')
fprintf(fid, '*torque curve, region 2\n')

```

```

fprintf(fid,'2621400 2 2 .86 .001851911 *extrapolated value*\n')
fprintf(fid,'2621401 .89 .290312645 *extrapolated value*\n')
fprintf(fid,'2621402 .9 .479506579 *extrapolated value*\n')
fprintf(fid,'2621403 .91636364 .539000268\n')
fprintf(fid,'2621404 .93333333 .626555263\n')
fprintf(fid,'2621405 .96923077 .877865891\n')
fprintf(fid,'*head curve, region 8 *extrapolated values*\n')
fprintf(fid,'2621501 1 8 -1.0 .880611\n')
fprintf(fid,'2621502 0.0 .880611\n')
fprintf(fid,'*torque curve, region 8 *extrapolated values*\n')
fprintf(fid,'2621601 2 8 -1.0 .846348\n')
fprintf(fid,'2621602 0.0 .846348\n')
fprintf(fid,'*head curve, region 3\n')
fprintf(fid,'2621700 1 3 -1.0 0.45263\n')
fprintf(fid,'2621701 0.0 0.45263\n')
fprintf(fid,'*torque curve, region 3\n')
fprintf(fid,'2621800 2 3 -1.0 0.51087174\n')
fprintf(fid,'2621801 0.0 0.51087174\n')
fprintf(fid,'*\n')
fprintf(fid,'*For Some Strange Reason, region 4 is needed during startup, so here is a guess\n')
fprintf(fid,'*\n')
fprintf(fid,'*head curve, region 4 *extrapolated values*\n')
fprintf(fid,'2621900 1 4 -1.0 0.200\n')
fprintf(fid,'2621901 0.0 .200\n')
fprintf(fid,'*torque curve, region 4 *extrapolated values*\n')
fprintf(fid,'2622000 2 4 -1.0 0.220\n')
fprintf(fid,'2622001 0.0 .220\n')
fprintf(fid,'*****mrd
4/11/09*****\n')
fprintf(fid,'*****
*****\n')
%% tau second halving time
m(1)=253;
t=linspace(5,50,6);
for i=2:6
    m(i)=m(1)/(1+1/tau*(t(i)-5));
end

%%%%%%%%%%
fprintf(fid,'* 4 primary pumps break, no coastdown\n')
%%%%%%%%%%
fprintf(fid,'2626101 -1.0 253.0 $ time =0, full flow\n')
fprintf(fid,' 2626102 0.5 253.0\n')
fprintf(fid,' 2626103 %f %f\n',t(1),m(1))
fprintf(fid,' 2626104 %f %f\n',t(2),m(2))
fprintf(fid,' 2626105 %f %f\n',t(3),m(3))
fprintf(fid,' 2626106 %f %f\n',t(4),m(4))
fprintf(fid,' 2626107 %f %f\n',t(5),m(5))
fprintf(fid,' 2626108 %f %f\n',t(6),m(6))
fprintf(fid,' 2626109 1000.0 0.1\n')
%%%%%%%%%%
fprintf(fid,'*\n')
fprintf(fid,'*****
*****\n')
fprintf(fid,'*\n')
fprintf(fid,'*hydro name type\n')

```

```

fprintf(fid,'2720000 empump1 pump\n')
fprintf(fid,'2720101 .405255 1.6 0.0 0.0 -90. -1.6 0000000\n')
fprintf(fid,'2720108 270010000 0.0 .5 .1 00000000 * these Ks are based upon a flanged 18 upo\n')
fprintf(fid,'2720109 274000000 0.0 1. .5 00000000\n')
fprintf(fid,'2720200 0 567583. 550431. 5279639. 0.\n')
fprintf(fid,'2720201 0 7.25373 8.02682 0. * 2551.66\n')
fprintf(fid,'2720202 0 7.25461 7.25461 0. * 2551.66\n')
fprintf(fid,
*****\n')
fprintf(fid,* Brinham pump, 1 phase, no 2 phase, no tourqe table used,time dependant pump velocity index, trip
on 262, reverse flow allowed \n')
fprintf(fid,'2720301 0 -1 -3 -1 0 262 1 $ This is for variable pumping*\n')
fprintf(fid,
*****\n')
fprintf(fid,*2720301 0 -1 -3 -1 0 262 0 $ This is for pump table (gradual startup) $\n')
fprintf(fid,*2720302 251.32 1.0 2.96 91.02 18421.227 160.0 851.35 0. .1 21.53 21.53 0. 0. *\n')
fprintf(fid,'2720302 251.32 1. 2.96 91.02 18421.227 160.0 851.35 0. .1 21.53 21.53 0. 0. *t\n')
fprintf(fid,*2726100 0\n')
fprintf(fid,*2726101 0.0 0.0\n')
fprintf(fid,*2726102 0.1 251.32\n')
fprintf(fid,*head curve, region 1\n')
fprintf(fid,'2721100 1 1 0.0 .45263 *extrapolated value*\n')
fprintf(fid,'2721101 .11904762 .46315789\n')
fprintf(fid,'2721102 .15873016 .47368421\n')
fprintf(fid,'2721103 .23809524 .51578947\n')
fprintf(fid,'2721104 .31746032 .55263158\n')
fprintf(fid,'2721105 .39682540 .60526316\n')
fprintf(fid,'2721106 .47619048 .67105263\n')
fprintf(fid,'2721107 .55555556 .73684211\n')
fprintf(fid,'2721108 .63492063 .81578947\n')
fprintf(fid,'2721109 .71428571 .90789474\n')
fprintf(fid,'2721110 .79365079 1.0\n')
fprintf(fid,'2721111 .87301587 1.10526316\n')
fprintf(fid,'2721112 .95238095 1.14473684\n')
fprintf(fid,'2721113 1. 1.\n')
fprintf(fid,*torque curve, region 1\n')
fprintf(fid,'2721200 2 1 0.0 .51087174 *extrapolated value*\n')
fprintf(fid,'2721201 .11904762 0.51522074\n')
fprintf(fid,'2721202 .15873016 0.52191192\n')
fprintf(fid,'2721203 .23809524 0.53278508\n')
fprintf(fid,'2721204 .31746032 0.58790078\n')
fprintf(fid,'2721205 .39682540 0.61423844\n')
fprintf(fid,'2721206 .47619048 0.66071828\n')
fprintf(fid,'2721207 .55555556 0.68588425\n')
fprintf(fid,'2721208 .63492063 0.77036280\n')
fprintf(fid,'2721209 .71428571 0.87528978\n')
fprintf(fid,'2721210 .79365079 0.91817838\n')
fprintf(fid,'2721211 .87301587 1.01924103\n')
fprintf(fid,'2721212 .95238095 1.07018303\n')
fprintf(fid,'2721213 1. 1.\n')
fprintf(fid,*head curve, region 2\n')
fprintf(fid,'2721300 1 2 .89 .00016955 *extrapolated value*\n')
fprintf(fid,'2721301 .9 .05328947 *extrapolated value*\n')
fprintf(fid,'2721302 .91636364 .25412649\n')
fprintf(fid,'2721303 .93333333 .48140351\n')
fprintf(fid,'2721304 .96923077 .84052320\n')
fprintf(fid,*torque curve, region 2\n')
fprintf(fid,'2721400 2 2 .86 .001851911 *extrapolated value*\n')
fprintf(fid,'2721401 .89 .290312645 *extrapolated value*\n')
fprintf(fid,'2721402 .9 .479506579 *extrapolated value*\n')

```

```

fprintf(fid,'2721403 .91636364 .539000268\n')
fprintf(fid,'2721404 .93333333 .626555263\n')
fprintf(fid,'2721405 .96923077 .877865891\n')
fprintf(fid,'*head curve, region 8 *extrapolated values*\n')
fprintf(fid,'2721501 1 8 -1.0 .880611\n')
fprintf(fid,'2721502 0.0 .880611\n')
fprintf(fid,'*torque curve, region 8 *extrapolated values*\n')
fprintf(fid,'2721601 2 8 -1.0 .846348\n')
fprintf(fid,'2721602 0.0 .846348\n')
fprintf(fid,'*head curve, region 3\n')
fprintf(fid,'2721700 1 3 -1.0 0.45263\n')
fprintf(fid,'2721701 0.0 0.45263\n')
fprintf(fid,'*torque curve, region 3\n')
fprintf(fid,'2721800 2 3 -1.0 0.51087174\n')
fprintf(fid,'2721801 0.0 0.51087174\n')
fprintf(fid,'*\n')
fprintf(fid,'*\n')
fprintf(fid,'*For Some Strange Reason, region 4 is needed durring startup, so here is a guess\n')
fprintf(fid,'*\n')
fprintf(fid,'*head curve, region 4 *extrapolated values*\n')
fprintf(fid,'2721900 1 4 -1.0 0.200\n')
fprintf(fid,'2721901 0.0 .600\n')
fprintf(fid,'*torque curve, region 4 *extrapolated values*\n')
fprintf(fid,'2722000 2 4 -1.0 0.220\n')
fprintf(fid,'2722001 0.0 .220\n')
fprintf(fid,'*\n')
fprintf(fid,'*\n')
%%
fprintf(fid,'*****mrd
4/11/09*****\n')
fprintf(fid,'*****\n')
fprintf(fid,'* 2 primary pumps break, no coastdown\n')
%%%%%%%%%%%%%%
fprintf(fid,'2726101 -1.0 253.0 $ time =0, full flow\n')
fprintf(fid,' 2726102 0.5 253.0\n')
fprintf(fid,' 2726103 1.0 253.0\n')
fprintf(fid,' 2726104 1.5 253.0\n')
fprintf(fid,' 2726105 2.0 253.0\n')
fprintf(fid,' 2726106 2.5 253.0\n')
fprintf(fid,' 2726107 3.0 253.0\n')
fprintf(fid,' 2726108 1000.0 253.0\n')
%%%%%%%%%%%%%%
fprintf(fid,'*\n')
fprintf(fid,'*****\n')
fprintf(fid,'*\n')
fprintf(fid,'$=====
n')
fprintf(fid,'*-----*\n')
fprintf(fid,'* decay power based on Eugene calculations for the new core\n')
fprintf(fid,'*-----*\n')
fprintf(fid,'20210600 power 999 1.0 1.0\n')
fprintf(fid,' time p/po\n')
fprintf(fid,'20210601 -1.0 0.0\n')
fprintf(fid,'20210602 0.0E+00 7.00E-02\n')
fprintf(fid,'20210603 1.0E+00 5.52E-02\n')
fprintf(fid,'20210604 1.5E+00 5.37E-02\n')
fprintf(fid,'20210605 2.0E+00 5.24E-02\n')
fprintf(fid,'20210606 4.0E+00 4.88E-02\n')

```

```

fprintf(fid,'20210607 6.0E+00 4.65E-02\n')
fprintf(fid,'20210608 8.0E+00 4.48E-02\n')
fprintf(fid,'20210609 1.0E+01 4.35E-02\n')
fprintf(fid,'20210610 1.5E+01 4.12E-02\n')
fprintf(fid,'20210611 2.0E+01 3.96E-02\n')
fprintf(fid,'20210612 4.0E+01 3.57E-02\n')
fprintf(fid,'20210613 6.0E+01 3.35E-02\n')
fprintf(fid,'20210614 8.0E+01 3.19E-02\n')
fprintf(fid,'20210615 1.0E+02 3.07E-02\n')
fprintf(fid,'20210616 1.5E+02 2.86E-02\n')
fprintf(fid,'20210617 2.0E+02 2.73E-02\n')
fprintf(fid,'20210618 4.0E+02 2.42E-02\n')
fprintf(fid,'20210619 6.0E+02 2.25E-02\n')
fprintf(fid,'20210620 8.0E+02 2.12E-02\n')
fprintf(fid,'20210621 1.0E+03 2.01E-02\n')
fprintf(fid,'20210622 1.5E+03 1.82E-02\n')
fprintf(fid,'20210623 2.0E+03 1.68E-02\n')
fprintf(fid,'20210624 4.0E+03 1.37E-02\n')
fprintf(fid,'20210625 6.0E+03 1.23E-02\n')
fprintf(fid,'20210626 8.0E+03 1.14E-02\n')
fprintf(fid,'20210627 1.0E+04 1.08E-02\n')
fprintf(fid,'20210628 1.5E+04 9.92E-03\n')
fprintf(fid,'20210629 2.0E+04 9.35E-03\n')
fprintf(fid,'20210630 4.0E+04 8.08E-03\n')
fprintf(fid,'20210631 6.0E+04 7.35E-03\n')
fprintf(fid,'20210632 8.0E+04 6.85E-03\n')
fprintf(fid,'20210633 1.0E+05 6.47E-03\n')
fprintf(fid,'20210634 1.5E+05 5.79E-03\n')
fprintf(fid,'20210635 2.0E+05 5.32E-03\n')
fprintf(fid,'20210636 4.0E+05 4.24E-03\n')
fprintf(fid,'20210637 6.0E+05 3.67E-03\n')
fprintf(fid,'20210638 8.0E+05 3.32E-03\n')
fprintf(fid,'20210639 1.0E+06 3.08E-03\n')
fprintf(fid,'20210640 1.5E+06 2.71E-03\n')
fprintf(fid,'20210641 2.0E+06 2.48E-03\n')
fprintf(fid,'20210642 4.0E+06 1.98E-03\n')
fprintf(fid,'20210643 6.0E+06 1.72E-03\n')
fprintf(fid,'20210644 8.0E+06 1.54E-03\n')
fprintf(fid,'20210645 1.0E+07 1.40E-03\n')
fprintf(fid,'20210646 1.5E+07 1.14E-03\n')
fprintf(fid,'20210647 2.0E+07 9.61E-04\n')
fprintf(fid,'20210648 4.0E+07 5.92E-04\n')
fprintf(fid,'20210649 6.0E+07 4.35E-04\n')
fprintf(fid,'20210650 8.0E+07 3.55E-04\n')
fprintf(fid,'20210651 1.0E+08 3.10E-04\n')
fprintf(fid,'20210652 1.5E+08 2.58E-04\n')
fprintf(fid,'20210653 2.0E+08 2.38E-04\n')
fprintf(fid,'20210654 4.0E+08 2.07E-04\n')
fprintf(fid,'20210655 6.0E+08 1.89E-04\n')
fprintf(fid,'20210656 8.0E+08 1.73E-04\n')
fprintf(fid,'20210657 1.0E+09 1.60E-04\n')
fprintf(fid,'20210658 1.5E+09 1.35E-04\n')
fprintf(fid,'20210659 2.0E+09 1.17E-04\n')
fprintf(fid,'20210660 4.0E+09 7.85E-05\n')
fprintf(fid,'20210661 6.0E+09 5.97E-05\n')
fprintf(fid,'20210662 8.0E+09 4.82E-05\n')
fprintf(fid,'20210663 1.0E+10 4.05E-05\n')
fprintf(fid,'*****\n')
fprintf(fid,'* Utilization of Fast Reactor Decay Power Curve\n')

```

```

fprintf(fid,'*****\n')
fprintf(fid,'*\n')
fprintf(fid,'20502000 rctrp tripunit 1.0 0.0 1\n')
fprintf(fid,'20502001 999\n')
fprintf(fid,'*\n')
fprintf(fid,'20502010 invrctrp tripunit 1.0 1.0 1\n')
fprintf(fid,'20502011 -999\n')
fprintf(fid,'*\n')
fprintf(fid,'20502020 tabdecy function 1000.e6 700000000. 0 0\n')
fprintf(fid,'20502021 time 0 106\n')
fprintf(fid,'*\n')
fprintf(fid,'20502030 codedcyP mult 1.0 70000000.0 1\n')
fprintf(fid,'20502031 cntrlvar 201 rkgapow 0\n')
fprintf(fid,'*\n')
fprintf(fid,'20502040 fastdcyP mult 1.0 70000000. 1\n')
fprintf(fid,'20502041 cntrlvar 200 cntrlvar 202\n')
fprintf(fid,'*\n')
fprintf(fid,'20502050 DPchoose stdfctn 1.0 70000000. 1\n')
fprintf(fid,'20502051 max cntrlvar 203 cntrlvar 204\n')
fprintf(fid,'*\n')
fprintf(fid,'20502100 TotPow sum 1.0 996000000. 1\n')
fprintf(fid,'20502101 0.0 1.0 cntrlvar 205 1.0 rkfipow 0\n')
fprintf(fid,'*\n')
fprintf(fid,'*\n')
fprintf(fid,'*=====\n')
=====\n')
fprintf(fid,'* Reactor Kinetics - To be inserted once steady state is reached -\n')
fprintf(fid,'*=====\n')
=====\n')
fprintf(fid,'*\n')
fprintf(fid,'30000000 point separabl\n')
fprintf(fid,'*\n')
fprintf(fid,'* fp-decay power rinit beta/lambda fp-y u239-y G-factor\n')
fprintf(fid,'30000001 gamma 1000.e6 -1.0e-60 9305.556 1.0 1.0e-60 0\n')
fprintf(fid,'*\n')
fprintf(fid,'* Mod.-Dens Reactivity ($) - Density effects included in vol. temp. feed\n')
fprintf(fid,'30000501 0000.00 0.000000\n')
fprintf(fid,'30000502 1000.00 0.000000\n')
fprintf(fid,'*\n')
%%%%%%%%%% Expansion Feedbacks
%%%%%%%%%%
fprintf(fid,'30000011 18200 *radial expansion $ $ $This was input by MJM on 11-04-08$ $ \n');
fprintf(fid,'30000012 18201 *CRDL expansion feedback $alpha = 1.9e-5/C, Lo = 10m, reac = .49$/cm\n');
fprintf(fid,'30000013 18202 *Structural expansion $This is positive feedback for vessel expansion\n');
fprintf(fid,'30000014 18203 *axial expansion $ this is for expansion of clad and assembly walls\n');
fprintf(fid,'30000015 991 *This is the control rod ejection reactivity insertion (input by MJM on 2/2/09)\n');
fprintf(fid,'*30000016 992 *This is the control rod ejection reactivity insertion (input by MJM on 2/2/09)\n');
fprintf(fid,'*30000017 993 *This is the control rod ejection reactivity insertion (input by MJM on 2/2/09)\n');
fprintf(fid,'*\n');
%%%%%%%%%% Fuel Feedbacks
%%%%%%%%%%
fprintf(fid,'* Doppler Reactivity + Fuel Expansion/Density Feedback (-0.006 $/C)\n');

```

```

fprintf(fid,* Fuel-Temp Reactivity($ (F.C. = -0.0013 $/C +- 30 percent)\n');
fprintf(fid,* Doppler T (K) vs alpha, sigma (c/C) EOC Numbers\n');
fprintf(fid,* 450 -0.3205 +-20percent * sigma taken from ANL-IFR-80\n');
fprintf(fid,* 750 -0.1587 +-20percent\n');
fprintf(fid,* 1050 -0.0912 +-20percent\n');
fprintf(fid,* 1200 -0.085 +-30percent *****NOTE, this is a conservative made up number...MCNP
Data does not go beyond 1050oC.\n');
fprintf(fid,* Higher uncertienties are thus used\n');
fprintf(fid,*\n');
fprintf(fid,'30000601 %f %f \n',temp(1),rho(1));
fprintf(fid,'30000602 %f %f \n',temp(2),rho(2));
fprintf(fid,'30000603 %f %f \n',temp(3),rho(3));
fprintf(fid,'30000604 %f %f \n',temp(4),rho(4));
fprintf(fid,'30000605 %f %f \n',temp(5),rho(5));
fprintf(fid,'30000606 %f %f \n',temp(6),rho(6));
fprintf(fid,\n');
fprintf(fid,*\n');
%%%%%%%%%% Sodium Density
%%%%%%%%%% Sodium Temperature/Density Feedback (+0.0011 $/C)\n');
fprintf(fid,*\n');
fprintf(fid,* Inner Driver\n');
fprintf(fid,* hydro-vol# inc weight temp-coeff\n');
fprintf(fid,'30000701 111050000 0 1.0 %d\n',sod111(1));
fprintf(fid,'30000702 111060000 0 1.0 %d\n',sod111(2));
fprintf(fid,'30000703 111070000 0 1.0 %d\n',sod111(3));
fprintf(fid,'30000704 111080000 0 1.0 %d\n',sod111(4));
fprintf(fid,'30000705 111090000 0 1.0 %d\n',sod111(5));
fprintf(fid,*\n');
fprintf(fid,* Outer Driver\n');
fprintf(fid,* hydro-vol# inc weight temp-coeff\n');
fprintf(fid,'30000706 123050000 0 1.0 %d\n',sod123(1));
fprintf(fid,'30000707 123060000 0 1.0 %d\n',sod123(2));
fprintf(fid,'30000708 123070000 0 1.0 %d\n',sod123(3));
fprintf(fid,'30000709 123080000 0 1.0 %d\n',sod123(4));
fprintf(fid,'30000710 123090000 0 1.0 %d\n',sod123(5));
fprintf(fid,*\n');
fprintf(fid,* Hot Driver\n');
fprintf(fid,* hydro-vol# inc weight temp-coeff\n');
fprintf(fid,'30000711 150050000 0 1.0 %d\n',sod150(1));
fprintf(fid,'30000712 150060000 0 1.0 %d\n',sod150(2));
fprintf(fid,'30000713 150070000 0 1.0 %d\n',sod150(3));
fprintf(fid,'30000714 150080000 0 1.0 %d\n',sod150(4));
fprintf(fid,'30000715 150090000 0 1.0 %d\n',sod150(5));
fprintf(fid,*\n');
fprintf(fid,* Fuel Density/Temperature Feedback & Doppler Weights\n');
fprintf(fid,*\n');
fprintf(fid,* Hot Channel\n');
fprintf(fid,* ht-str# inc weight fuel-temp-coeff\n');
fprintf(fid,'30000801 1502001 0 0.001148 -0.00\n');
fprintf(fid,'30000802 1502002 0 0.001547 -0.00\n');
fprintf(fid,'30000803 1502003 0 0.001686 -0.00\n');
fprintf(fid,'30000804 1502004 0 0.001547 -0.00\n');
fprintf(fid,'30000805 1502005 0 0.001148 -0.00\n');
fprintf(fid,*\n');
fprintf(fid,* Inner Driver\n');
fprintf(fid,* ht-str# inc weight fuel-temp-coeff\n');

```



```
fprintf(fid,'30000816 1112001 0 0.077075 -0.00\n');
fprintf(fid,'30000817 1112002 0 0.103739 -0.00\n');
fprintf(fid,'30000818 1112003 0 0.113137 -0.00\n');
fprintf(fid,'30000819 1112004 0 0.103739 -0.00\n');
fprintf(fid,'30000820 1112005 0 0.077075 -0.00\n');
fprintf(fid,'*\n');
fprintf(fid,'* Outer Driver\n');
fprintf(fid,'*      ht-str# inc weight  fuel-temp-coeff\n');
fprintf(fid,'30000831 1232001 0 0.084119 -0.00\n');
fprintf(fid,'30000832 1232002 0 0.113221 -0.00\n');
fprintf(fid,'30000833 1232003 0 0.123478 -0.00\n');
fprintf(fid,'30000834 1232004 0 0.113221 -0.00\n');
fprintf(fid,'30000835 1232005 0 0.084119 -0.00\n');
fprintf(fid,'*\n');
fprintf(fid,'*end of file\n');
fclose('all');
```

multi_runrelap.bat.m

```
set relapdir= C:\r5\r3d236ie\relap
set mydir= %CD%
set rundir=C:\Jake_SASS\restart
set inputdir=C:\Jake_SASS\ULOF_803_3\In1

del %inputdir%\*.

copy %inputdir%\*.i %inputdir%\*.

for /F %%a IN ('dir /b %inputdir%\*.') do CALL run %%a

pause
```

run.bat

```
set inputfile=%1

del %inputfile%.o
del %inputfile%.r

copy %rundir%\ABR1000ssM.r %inputfile%.r

cd %relapdir%
relap5 -i %inputdir%\%inputfile%.i -o %mydir%\%inputfile%.o -r %mydir%\%inputfile%.r -m
%rundir%\tpfna2> %mydir%\%inputfile%.out
cd %mydir%
del %inputfile%.r
```

multi.bat

```
REM This is the main file
SET INDEX_FILE=list.l
del %INDEX_FILE%

del folder_out.l

dir /B /AD * > folder_out.l

SET FOLDER_FILE=folder_out.l
SET HOME_DIR=%CD%

FOR /F %%A IN (%FOLDER_FILE%) DO CALL make_list %%A

pause
```

make_list.bat

```
cd %1
set OUTPUTS=all_outs.1

copy output.o output.1

del output.o

del %OUTPUTS%

dir /B *.o > %OUTPUTS%

FOR /F %%A IN (%OUTPUTS%) DO ECHO %CD%\%%A >> %HOME_DIR%/list.1

REM FOR /F %%A IN (%OUTPUTS%) DO ECHO %CD%\%%A >> %HOME_DIR%/list.1

pause

cd ..
```

Output_Process.m

```
numfiles=1;

cd C:\Jake_SASS\ULOF_803_0
runcounter=0;
for i=1:numfiles
    left=numfiles-i;
    % list=sprintf('list%d.!',i);
    list=sprintf('list.!',i);
    ARRAY=sortdata(list,left);
    [nn] = size(ARRAY,2);
    start=runcounter+1;
    runcounter=runcounter+nn;
    reactbin3(start:runcounter)=ARRAY;
end

ARRAY=reactbin3;

save ULOF_803_0_Metal ARRAY
clear all
load ULOF_803_0_Metal

%cd C:\RELAP
%pause

%cd C:\Jake_SASS\ULOF_800\Damage

%Object_builder_burnup
```

sortdata.m

```
function [ARRAY]=sortdata(list,nn)

close all

fid = fopen(list, 'r'); %opens file with list of ouput fiels to read
i=0;
while feof(fid) == 0
    i=i+1;
    tline = fgetl(fid); %reads line
    if i==1
        files=tline;
    else
        files=strvcat(files,tline); % adds extra files to list
    end
end
fclose(fid);

clear i

[m,n]=size(files);

% Print Verification of ouput list to Screen
fprintf(1,'\n');
fprintf(1,'Output Files In List\n');
fprintf(1,'\n');
for i=1:m
    fprintf(1,'%s\n',files(i,:)); % Prints ith file name
end
fprintf(1,'\n');
fprintf(1,'End of Output Files In List\n');
fprintf(1,'\n');

clear i time
time=0;
for i=1:m
    tic;
    ARRAY(i).VALUE=reader(files(i,:));
    time=time+toc;
    ave_time=time/i;
    left=(m-i)*(nn+1);
    time_remaining=(left)*ave_time;
    fprintf(1,'%d files remain: Finished %s with ~ %6.2f min remaining\n',left,files(i,:),time_remaining/60);
end

%%%%%%%%%%%%%%%%%%%%%%%%%%%%%%%%%%%%%%%%%%%%%%%%%%%%%%%%%%%%%%%%%%%%%%%%
% nn = number of time steps
%%%%%%%%%%%%%%%%%%%%%%%%%%%%%%%%%%%%%%%%%%%%%%%%%%%%%%%%%%%%%%%%%%%%%%%%

save Output_Data ARRAY

plotter
```

reader.m

```
function apend = reader(filename)
% Search for number of string matches per line.
% For RELAP Files, literal should be MINOR EDIT in capital Letters
% This file is for 15 outputs. If outputs are between 10 and 18, then vary
% Outputs accordingly. If 9 or below, comment out 4 lines which indicate so
% And change the 10 in first to #M.E. +1

outputs=17;

literal='MINOR EDIT';

fid = fopen(filename, 'rt');
y = 0;
while feof(fid) == 0
    tline = fgetl(fid);           %Moves to the next line and copies it in tline
    matches = findstr(tline, literal); %Is tline what you were looking for?
    num = length(matches);       %How many times did what you were looking for
                                   %appear in the line?
    if num > 0                   %Did you get a hit?
        y = y + num;            %How many hits do we have?

        for i=1:4
            skip=fgets(fid);     %Skip 4 lines after target word
        end

        first=fscanf(fid,'%e',[10,50]); %reads in first 10 RELAP MINOR EDIT parameters
                                   % , prints out 50 points at a time

        if size(first,2)==50
            n=5;
            if first(1,50)==1
                first(:,50)=[];
                n=4;
            end
        else
            n=4;
            first(:,size(first,2))=[];
        end

        for i=1:n
            skip=fgetl(fid);     %Skips an extra 4 lines
        end

        %reads in second 7 RELAP MINOR EDIT parameters
        % , prints out 50 points at a time
        second=fscanf(fid,'%e',[outputs+2-10,50]);

        if y==1
            apend1=first;       %Starts Matrix 1
            apend2=second;      %Starts Matrix2 (Comment out if less than 10 M.E.)
        else
            apend1=cat(2,apend1,first); %Builds off Matrix 1
            apend2=cat(2,apend2,second); %Builds off Matrix 2 (Comment out if less than 10 M.E.)
        end
    end
end
```

```
end

end

end

apend2(1,:)=[];          % Removes second time column (Comment out if less than 10 M.E.)
apend=cat(1,apend1,apend2);    % Combines Matrix 1 and 2 (Comment out if less than 10 M.E.)
% apend=apend1;          %(Comment in if less than 10 M.E.)

fclose(fid);
```

plotter.m

```
%%%%%%%%%%
% ll = number of files....should equal m
% mm = 1 + number of outputs
% nn = number of time steps
%%%%%%%%%%

ll = size(ARRAY,2);

% % % Pull Time

close all
%% Pull Peak Clad Temperature
figure(1)
for j=1:ll
    time=ARRAY(j).VALUE(1,:);
    pctemp=ARRAY(j).VALUE(10,:)-273.15;
    semilogx(time,pctemp)
    if j ~= ll
        hold on
    else
        hold off
    end
end

title('Peak Clad Temperature vs Time')
xlabel('Time (s)')
ylabel('Peak Clad Temperature ( ^o C)')
axis([1,max(time),0,1])
axis 'auto y'

%% Pull Peak Coolant Outlet Temperature
figure(2)
for j=1:ll
    time=ARRAY(j).VALUE(1,:);
    pcooltemp=ARRAY(j).VALUE(7,:)-273.15;
    semilogx(time,pcooltemp)
    if j ~= ll
        hold on
    else
        hold off
    end
end

title('Peak Coolant Temperature vs Time')
xlabel('Time (s)')
ylabel('Peak Coolant Temperature ( ^o C)')
axis([1,max(time),0,1])
axis 'auto y'

%% Pull Peak Core Outlet Temperature
figure(21)
for j=1:ll
    time=ARRAY(j).VALUE(1,:);
    cooltemp=ARRAY(j).VALUE(6,:)-273.15;
    semilogx(time,cooltemp)
    if j ~= ll
        hold on
    else
```

```

        hold off
    end
end
title('Coolant Outlet Temperature vs Time')
xlabel('Time (s)')
ylabel('Coolant Outlet Temperature ( ^o C)')
axis([1,max(time),0,1])
axis 'auto y'
%% Pull Mass Flow Rate

figure(22)
for j=1:ll
    time=ARRAY(j).VALUE(1,:);
    mflow=ARRAY(j).VALUE(2,:);
    plot(time,mflow)
    if j ~= ll
        hold on
    else
        hold off
    end
end

title('Mass Flow vs Time')
xlabel('Time (s)')
ylabel('Mass Flow (kg/s), and Pump Velocity (rad/s)')
axis([1,max(time),0,1])
axis 'auto y'
%% Pull Peak Fuel Temperature

figure(3)
for j=1:ll
    time=ARRAY(j).VALUE(1,:);
    pftemp=ARRAY(j).VALUE(11,:)-273.15;
    semilogx(time,pftemp)
    if j ~= ll
        hold on
    else
        hold off
    end
end

title('Peak Fuel Temperature vs Time')
xlabel('Time (s)')
ylabel('Peak Fuel Temperature ( ^o C)')
axis([1,max(time),0,1])
axis 'auto y'

%% Power
figure(4)
for j=1:ll
    time=ARRAY(j).VALUE(1,:);
    pow=ARRAY(j).VALUE(8,:)/1e7;
    loglog(time,pow)
    if j ~= ll
        hold on
    else
        hold off
    end
end
end

```



```

title('% Full Power vs Time')
xlabel('Time (s)')
ylabel('Thermal Power (%)')%% Power
axis([1,max(time),90,1e3])
% axis 'auto y'

%% Reactivity
figure(5)
for j=1:11
    time=ARRAY(j).VALUE(1,:);
    react=ARRAY(j).VALUE(16,:);
    semilogx(time,react)
    if j ~= 11
        hold on
    else
        hold off
    end
end
end

title('Reactivity vs Time')
xlabel('Time (s)')
ylabel('Reactivity ($)')
axis([1,max(time),0,1])
axis 'auto y'

%% Pull CR Assembly Outlet Temperature
figure(1)
for j=1:11
    time=ARRAY(j).VALUE(1,:);
    pctemp=ARRAY(j).VALUE(10,:)-273.15;
    semilogx(time,pctemp)
    if j ~= 11
        hold on
    else
        hold off
    end
end
end

title('Peak Clad Temperature vs Time')
xlabel('Time (s)')
ylabel('Peak Clad Temperature ( ^o C)')
axis([1,max(time),0,1])
axis 'auto y'

```

plotter.m

```
clear all

cd C:\Jake_SASS\ULOF_803_0

load ULOF_803_0_Metal.mat

zzz = size(ARRAY,2);

%time=ARRAY(j).VALUE(1,:);
%corein=ARRAY(j).VALUE(5,;)-273.15;
%coreout=ARRAY(j).VALUE(6,;)-273.15;
%peakfueltemp=ARRAY(j).VALUE(11,;)-273.15;
%peakcladtemp=ARRAY(j).VALUE(10,;)-273.15;
%peakcooltemp=ARRAY(j).VALUE(7,;)-273.15;
%peakfuelout=ARRAY(j).VALUE(17,;)-273.15;
%peakCRout=ARRAY(j).VALUE(18,;)-273.15;
%power=ARRAY(j).VALUE(8,;);
%mdot=ARRAY(j).VALUE(2,;);
%Reactivity=ARRAY(j).VALUE(16,;);

exc=0;
fail(1:zzz)=0;
fail_index=1;

figure(1)
for j=1:zzz
    peakcladtemp=ARRAY(j).VALUE(10,;)-273.15;

    if max(peakcladtemp) > 750
        exc=exc+1;
        fail(j)=1;
        fail_run(fail_index)=j;
        fail_index=fail_index+1;
    end

    time=ARRAY(j).VALUE(1,;);
    semilogx(time,peakcladtemp)
    if j ~= zzz
        hold on
    else
        hold off
    end
end
title('Peak Clad Temperature vs Time')
xlabel('Time (s)')
ylabel('Peak Clad Temperature (C)')
axis([1,max(time),0,1])
axis 'auto y'

%% Failure Calculator
exc
load input_data
m=1;
for k=1:5
    for l=1:100
        wgt(m)=Par.wgt(k,l);
        m=m+1;
    end
end
```

```
    end
end

for n=1:exc
    failwgt(n)=wgt(fail_run(n));
end

failrate=sum(failwgt)/sum(wgt)
reliability=1-failrate
```